

**UNIVERSIDADE FEDERAL DE PELOTAS**  
**Faculdade de Odontologia**  
**Programa de Pós-Graduação em Odontologia**  
**Tese**



**Tese**

**Novo sistema de entrega a base de um hidrogel injetável fotopolimerizável (GelMA) como estratégia de desinfecção endodôntica inteligente (*on-demand*) e regeneração de tecidos orais.**

**Juliana Silva Ribeiro**

Pelotas, 2021

**Juliana Silva Ribeiro**

**Novo sistema de entrega a base de um hidrogel injetável fotopolimerizável (GelMA) como estratégia de desinfecção endodôntica inteligente (*on-demand*) e regeneração de tecidos orais.**

Tese apresentada ao Programa de Pós-Graduação em Odontologia da Faculdade de Odontologia da Universidade Federal de Pelotas, como requisito parcial à obtenção do título de Doutor em Clínica Odontológica, com Ênfase em Endodontia.

Orientador: Rafael Guerra Lund

Coorientador: Evandro Piva

Pelotas, 2021

Juliana Silva Ribeiro

**Novo sistema de entrega a base de um hidrogel injetável fotopolimerizável (GelMA) como estratégia de desinfecção endodôntica inteligente (*on-demand*) e regeneração de tecidos orais.**

Tese apresentada, como requisito parcial, para obtenção do grau de Doutor em Odontologia, Programa de Pós Graduação em Odontologia, Faculdade de Odontologia de Pelotas, Universidade Federal de Pelotas.

Data da defesa: 20/04/2021

**Banca Examinadora:**

Prof. Dr. Rafael Guerra Lund (Orientador)

Doutorem odontologia com área de concentração em Dentística pela Universidade Federal de Pelotas– RS

Prof. Dr. Wellington Luiz De Oliveira da Rosa

Doutor em Materiais Dentários pela Universidade Federal de Pelotas– RS

Prof. Dra. Fabiana Soares Grecca

Doutor em odontologia com área de concentração em Dentística pela Universidade Federal de Pelotas– RS

Prof. Dr. Carlos Enrique Cuevas Suárez

Doutor em Biologia Oral e Biomateriais pela Universidade Federal de Pelotas– RS

Prof. Dr. Eliseu AldrichiMünchow (Suplente)

Doutor em odontologia com área de concentração em Dentística pela Universidade Federal de Pelotas– RS

Prof. Dra. Fernanda Geraldo Pappen (Suplente)

Doutorado em Endodontia pela Universidade Estadual Paulista Júlio de Mesquita Filho - SP

## **Agradecimentos**

A Deus que em sua imensa sabedoria me guiou até aqui, planejou todos os detalhes deste doutorado me fazendo crescer e ser melhor a cada momento.

Ao Alex que foi meu namorado, noivo e agora esposo durante esta etapa do doutorado.

A minha família que sempre me apoiou mesmo sendo caminhos que nunca foram trilhados por eles, mas sempre me incentivaram mesmo que significasse passar muito tempo longe deles.

A minha nova família aqui em Pelotas, formada durante estes 10 anos que passei nesta cidade.

Aos amigos do CDC e do Laboratório da Micro, vocês com certeza fizeram meus dias aqui melhores.

To my friends from the Michigan University, spend one year with you was awesome.

A Universidade Federal de Pelotas que me acolheu aqui em 2010 e até hoje tem me proporcionado muitas oportunidades que com certeza eu aproveitei com todo o meu empenho.

*Não importa o que aconteça, continue a nadar (Walters,  
Graham; Procurando Nemo, 2003)*

### **Notas Preliminares**

O presente trabalho de conclusão de curso foi redigido segundo o Manual de normas UFPel para trabalhos acadêmicos da Universidade Federal de Pelotas de 2019, adotando o Nível de Descrição em Artigo, descrita no referido manual.  
<<https://wp.ufpel.edu.br/sisbi/files/2019/06/Manual.pdf>> Acesso em: <08 de março de 2020>.

O projeto de pesquisa foi qualificado em 05 de fevereiro de 2018 e aprovado pela Banca Examinadora composta pelos Professores Doutores Rafael Guerra Lund, Adriana Fernandes da Silva, Fernanda Geraldo Pappen e Luciana Geanini Pena.

## Resumo

RIBEIRO, Juliana Silva. **Novo sistema de entrega a base de um hidrogel injetável fotopolimerizável (GelMA) como estratégia de desinfecção endodôntica inteligente (*on-demand*) e regeneração de tecidos orais.** 2021.100f. Tese (Doutorado em Odontologia). Programa de Pós-Graduação em Odontologia, Universidade Federal de Pelotas, 2021.

Este estudo teve como objetivo sintetizar, caracterizar e avaliar um novo sistema de entrega de fármacos *on-demand* (sob-demanda) para desinfecção endodôntica na endodontia regenerativa. A síntese do hidrogel de metacrilato de gelatina (GelMA) foi realizada e subsequentemente a clorexidina foi adicionada diretamente ao GelMA ou adicionada através de um sistema de liberação controlada (nanotubos de haloisita) em diferentes concentrações. A análise em Microscopia Eletrônica de Varredura/Espectroscopia por Dispersão (MEV/EDS) caracterizou a morfologia e funcionalização do GelMA. As propriedades dos GelMA avaliadas foram: sorção, degradação, liberação de fármaco, módulo de compressão e citotoxicidade. As propriedades antimicrobianas foram avaliadas por meio do halo de inibição, teste de contato direto e inibição da formação de biofilme bacteriano na superfície dos materiais, por meio da contagem de unidades formadoras de colônia (CFU) e visualização de imagens em microscopia confocal (CLSM). A biocompatibilidade e biodegradação *in vivo* foi analisada por meio de um microscópio óptico, pela presença de estruturas luminosas contendo sangue vermelho e células inflamatórias, ao mesmo tempo em que se avaliou a biodegradação do hidrogel, após o preenchimento de pequenas bolsas subcutâneas. As análises estatísticas foram realizadas de acordo com cada análise, considerando-se  $p < 0.05$  como estatisticamente significante. Resultados: O GelMA modificado com nanotubos de haloisita carregado com clorexidina (CHX) mostrou adequadas propriedades mecânicas, taxa de degradação, liberação sustentada de CHX para ablação de infecção e boa biocompatibilidade. O GelMA modificado mostrou respostas inflamatórias localizadas mínimas, apoiando sua capacidade para aplicações de entrega de drogas. Além disso, a incorporação de nanotubos carregados com CHX reduziu as propriedades mecânicas, aumentou a razão sorção e diminui a taxa de degradação dos hidrogéis. É importante ressaltar que a presença de nanotubos carregados com CHX inibe o crescimento bacteriano com toxicidade celular mínima. Alíquotas contendo antibióticos levaram a uma redução na viabilidade de SHEDs, mas não foram consideradas tóxicas. Considerando a caracterização inicial proporcionada neste estudo é possível afirmar que desenvolvemos uma nova estratégia de entrega de drogas *on-demand* para terapia endodôntica regenerativa através da modificação de um hidrogel GelMA carregados de agentes antimicrobianos.

Palavras-chave: Hidrogel. Antimicrobiano. Endodontia regenerativa. Sistema de liberação controlada. Infecção.

## **Abstract**

RIBEIRO, Juliana Silva. **Novel delivery system based on a photopolymerizable injectable hydrogel (GelMA) as a strategy for intelligent endodontic disinfection (on-demand) and regeneration of oral tissues.** 2021. 100f. Thesis (Ph.D.in Dentistry). Graduate Program in Dentistry, Federal University of Pelotas, 2021.

This study aimed to synthesize, characterize and evaluate a new on-demand drug delivery system for endodontic disinfection in regenerative endodontics. The synthesis of the gelatin methacrylate hydrogel (GelMA) was carried out and subsequently different potentially antimicrobial particles were added. The analysis in Scanning Electron Microscopy / Dispersion Spectroscopy (SEM / EDS) characterized the morphology and functionalization of GelMA. The properties of the GelMA evaluated were: sorption, degradation, drug release, compression module, and cytotoxicity. The antimicrobial properties were evaluated through the inhibition halo, direct contact test, and inhibition of the formation of bacterial biofilm on the surface of the materials, through the counting of colony-forming units (CFU) and visualization of images in confocal microscopy. The biocompatibility and biodegradation in vivo were analyzed using an optical microscope, for the presence of luminous structures containing red blood and inflammatory cells, at the same time that the biodegradation of the hydrogel was evaluated, after filling small subcutaneous pockets. Statistical analyzes were performed according to each analysis, considering  $p < 0.05$  as statistically significant. Results: GelMA modified with chlorhexidine-loaded halloysite nanotubes (CHX) showed adequate mechanical properties, degradation rate sustained release of CHX for ablation of infection, and good biocompatibility. The modified GelMA showed minimal localized inflammatory responses, supporting its ability for drug delivery applications. Besides, the incorporation of nanotubes loaded with CHX reduced the mechanical properties, increased the sorption ratio, and decreased the degradation rate of the hydrogels. It is important to note that the presence of CHX-loaded nanotubes inhibits bacterial growth with minimal cellular toxicity. Aliquots containing antibiotics led to a reduction in the viability of SHEDs but were not considered toxic. Considering the initial characterization provided in this study, it is possible to affirm that we have developed a new strategy for delivering on-demand drugs for regenerative endodontic therapy through the modification of a GelMA hydrogel loaded with antimicrobial agents.

**Keywords:** Hydrogel. Antimicrobial. Regenerative endodontics. Controlled release system. Infection.

## **1 INTRODUÇÃO**

A cárie dentária é a doença crônica mais comum entre crianças e adultos jovens de 6 a 19 anos no mundo(CENTER FOR HEALTH STATISTICS, 2015). Etiologicamente falando, a cárie é uma doença multifatorial açúcar dependente que, se não tratada adequadamente, pode levar à necrose do tecido pulpar, levando consequente a demanda de tratamento através da terapia endodôntica(ERAMO et al., 2018). Da mesma forma, as lesões dentárias traumáticas podem levar a necrose pulpar, essas lesões ocorrem com freqüência em crianças e adultos jovens, segundo a International Association of Dental Traumatology, 25% de todas as crianças em idade escolar sofrem traumas dentários e 33% dos adultos sofreram traumas na dentição permanente, sendo a maior parte das lesões ocorrendo antes dos 19 anos. Adicionalmente, dados da American Association of Endodontists, revelam que aproximadamente 16 milhões de pacientes são submetidos a tratamento de canal radicular a cada ano em um procedimento que tradicionalmente é limitado a pulpectomia e endodontia(EKLUND, 2010).

O manejo da necrose pulpar em dentes permanentes em estágio derizogênese incompleta é desafiador devido à interrupção abrupta do desenvolvimento da raiz resultando em paredes dentinária finas, ápices aberto e aumento do risco de fratura cervical impossibilitando um tratamento endodôntico tradicional (TORABINEJAD et al., 2017; WIDBILLER et al., 2018). Nestes casos, o tratamento de dentes com necrose pulpar em estágio de rizogênese incompleta é realizado através da apicificação usando técnicas de aplicação demateriais hidróxido de cálcio (HC)ou agregado de trióxido mineral (MTA) para induzir formação de barreira de tecido calcificado (HARLAMB; S.C., 2016).

Apesar desses materiais serem considerados o tratamento de primeira opção para estes casos, existem vários problemas relacionados ao uso destes na apicificação: o longo tempo necessário para completar o processo de apicogênese; o número de seções necessárias para completar o fechamento, o papel da infecção e a resistência à fratura dos dentes após a aplicação a longo prazo de formulações a base de hidróxido de cálcio (WITHERSPOON et al., 2008). Apesar do MTA apresentar a capacidade de induzir formação de cementoide ou outro tecido duro (TORABINEJAD et al., 2014)(HARLAMB; S.C., 2016; SACHDEVA et al., 2015; STAMBOLSKY et al., 2016), ele não é capaz de induzir o desenvolvimento completo da raiz (comprimento e espessura), o que compromete a integridade mecânica a longo prazo do dente (DIOGENES; RUPAREL, 2017; NAZZAL et al., 2018). Essa condição está associada a uma maior predisposição para falhas do tratamento devido a fraturas e consequentemente diminuição da sobrevida dentária (DIOGENES; RUPAREL, 2017; NAZZAL et al., 2018).

Nesse sentido, torna-se estratégico os esforços para desenvolvimento de procedimentos endodônticos regenerativos (REPs), como revascularização e revitalização do tecido pulpar em dentes necróticos imaturos com periodontite apical (AP). Esse tipo de terapia poderia permitir o reforço das paredes do canal radicular e, às vezes, a continuação do seu desenvolvimento, abrindo assim novas possibilidades terapêuticas neste campo (KIM et al., 2018; MURRAY et al., 2007; WHITING et al., 2018).

A engenharia de tecidos surgiu como um campo encarregado de fornecer uma possibilidade clínica para a regeneração de tecidos e órgãos (CONDE et al., 2017). Três elementos principais constituem a base para a engenharia de tecidos, nomeadamente células estaminais, moléculas de sinalização bioativas e os *scaffolds*. Os *scaffolds*, por sua vez, podem ter propriedades estruturais, químicas, mecânicas e biofísicas únicas. Essas propriedades foram exploradas individualmente e em conjunto para garantir a regeneração de tecidos controláveis (BOTTINO et al., 2017).

Nos últimos anos, o desenvolvimento de novas terapias clínicas para a regeneração da polpa dentária, como o método EB (*evocable bleeding*) que trouxe uma promessa para melhorar os resultados do tratamento. No EB, após a adequada desinfecção do canal radicular, uma ampliação do forame apical é realizada para promover sangramento e formar um suporte baseado em fibrina para interagir com células estaminais endógenas e fatores de crescimento (GFs). Esse método, preconiza o uso da pasta tri antimicrobótica (pasta TAP), composta por antibióticos (ciprofloxacina, metronidazol eminociclina) ou pode ser utilizada também a pasta DAP onde não há adição da minociclina.

Pesquisas recentes têm demonstrado que a pasta TAP está associada a inúmeras desvantagens, incluindo, mas não se limitando apenas a questões de biocompatibilidade e sim, devido a preocupações de toxicidade sobre seu uso indiscriminado (DUBEY et al., 2019). O que afetaria negativamente a sobrevivência das células estaminais (BOTTINO et al., 2017; JACOBS et al., 2017). Embora os materiais a base de HC tenham sido apontados como alternativa a pasta TAP, por ter sido utilizado por muito tempo na endodontia como um medicamento de interconsulta, a literatura mostra que o HC pode não ser totalmente eficaz contra *E. faecalis* e *C. albicans*, possuindo um potencial antimicrobiano muito limitado.

Uma vez que a infecção tem sido apontada como o principal motivo para a falha clínica da endodontia, é extremamente importante controlar e / ou erradicar a contaminação bacteriana. Clinicamente falando, a anatomia do canal radicular é altamente complexa e, portanto, a remoção mecânica de restos de tecido, biofilme e dentina infectada nem sempre pode garantir um nicho livre de bactérias. Como resultado, os tecidos infectados podem ser deixados dentro dos canais, onde os microrganismos podem crescer e proliferar.

Coletivamente, os desafios anatômicos, bem como a presença de sinais / sintomas clínicos, apoiam fortemente a indicação de uma terapia de múltiplas consultas e o emprego de medicamentos intracanal.

Como alternativa, alguns estudos têm sugerido o uso do digluconato de clorexidina (BARBOSA-RIBEIRO et al., 2019; MOHAMMADI; SHALAVI, 2012). A clorexidina (CHX) é um anti-séptico de uso comum, amplamente utilizado e que tem propriedades bacteriostáticas e bactericidas contra bactérias gram positivas e negativas (GOMES et al., 2001, 2013b). Especificamente, CHX é um agente anti-séptico, desinfetante, farmacêutico, cosmético e antiplaca. A alta efetividade deste fármaco contra microorganismos é devido à presença de aminas secundárias que podem ser protonadas e, portanto, carregadas positivamente em condições normais de pH (GOMES et al., 2013b). A incorporação de CHX em quantidades diminutas demonstrou atividade antimicrobiana para materiais dentários, como por exemplo o ionômero de vidro, sem afetar significativamente suas propriedades físicas (DUQUE et al., 2017) e capacidade de modular a inflamação periapical(MOHAMMADI, 2008a; RIAZ et al., 2018). Porém, um número crescente de pesquisas tem sugerido a CHX apresenta uma toxicidade dependente da dose(LESSA et al., 2010; NAZZAL et al., 2018); assim, faz-se necessário o desenvolvimento de um sistema de entrega que promova a liberação controlada, de CHX, melhorando sua biocompatibilidade e ação antimicrobiana.

Gelatina metacriloil (GelMA) é um hidrogel fotopolimerizável, biocompatível e biodegradável que se originou da modificação de grupos laterais de gelatina contendo amina (Gel) com grupos metacrilamida e metacrilato(NICHOL et al., 2010a; RAHALI et al., 2017). A gelatina é um polímero natural que pode ser obtido por desnaturação do colágeno. Ela apresenta composição e propriedades biológicas quase idênticas às do colágeno, ao mesmo tempo que retém a ligação celular e os locais de degradação responsivos as metaloproteinases da matriz (MMPs)(MONTEIRO et al., 2018a). Semelhante a outros hidrogéis, ao considerar seu uso como um sistema de liberação de drogas, o GelMA pode ser misturado de forma eficiente com uma ampla gama de aditivos, tais como, nanotubos, nanopartículas, nanofibras, biomoléculas entre outros(PAUL et al., 2016). Suas características físico químicas e mecânicas como taxa de sorção de água, molhabilidade, viscosidade e injetabilidade pode ser facilmente remodelada e ajustada para servir como medicação intracanal, podendo ter forma de apresentação como um hidrogel injetável.

Digno de nota e altamente relevante para o trabalho proposto, durante o desenvolvimento da patologia periapical, principalmente em infecções persistentes tem sido relatado o aumento dos níveis de metaloproteinases de matriz (MMP-1, MMP- 2, MMP-8 e

MMP-9) na área periapical(GOMES; HERRERA, 2018; JAIN; BAHUGUNA, 2015a; PAULA-SILVA; DA SILVA; KAPILA, 2010). Assim, postulamos que GelMA poderia ser sintetizado e funcionalizado com substâncias antimicrobianas como a CHX e agindo como um depósito sob demanda deste antimicrobiano, que seria acionado pela exposição ao hidrogel a altos níveis de MMPs, uma vez que a infecção apical esteja estabelecida.

## **1.1 Objetivos**

### **1.1.1 Geral**

O objetivo da presente tese foi desenvolver um sistema de entrega de drogas sob demanda para aplicação em terapia endodôntica. Este sistema foi composto por um hidrogel injetável, GelMA, biodegradável (responsivo a metaloproteinases da matriz) e biocompatível para entrega de clorexidina intracanal como uma estratégia para resolução das infecções endodônticas.

### **1.1.2 Específicos**

Desenvolver diferentes sistemas de entrega e formulações de GelMA e testar a ação da adição de fármacos nas propriedades:

Morfológicas: Microscopia eletrônica de varredura; Microscopia eletrônica de transmissão.

Físico químicas: Analise de espectroscopia no infravermelho por transformada de Fourier, Ressonância nuclear magnética, sorção, degradação *in vitro*, liberação de droga.

Mecânicas: Modulo de compressão

e biológicas: Teste de difusão em ágar, teste de contato direto, Unidades formadoras de colônias – Biofilme microcosmos e monocultura, teste de citotoxicidade, biocompatibilidade e biodegradação *in vivo*.

## **1.2 Justificativa**

Altas concentrações de fármacos dentro dos canais radiculares, podem levar a resistência microbiana, toxicidade as células periapicais assim como uma reação de hipersensibilidade do paciente. Sendo assim, uma liberação do agente antimicrobiano somente quando há necessidade (sob demanda) é uma alternativa altamente desejável.

## **2. PROJETO DE PESQUISA**

### **Introdução**

A perda de dentes em crianças pequenas, como resultado de lesões escoriais e spr ofundas ou trauma, pode acarretar complicações em doenças relacionadas ao crescimento e desenvolvimento craniomaxilofacial, impactando assim sua relação psicossocial bem-

estar (CEHREL et al., 2011; CEHREL, SARA, AKSOY 2012). Do ponto de vista clínico, o manejo da necrose pulpar em dentes permanentes com o ápice aberto é desafiador devido à interrupção abrupta do desenvolvimento da raiz resultando em paredes dentinárias finas, ausência debatente apical e consequentemente aumento risco de fratura cervical (FARIK et al., 2002; JEERUPHAN et al., 2012).

O hidróxido de cálcio e o agregado de trióxido mineral têm sido amplamente utilizados para tratar dentes permanentes imaturos com polpas necróticas em um esforço para obter um ambiente asséptico e uma barreira apical

calcificada. No entanto, apesar de um longo histórico de uso nos procedimentos de encerramento apical, existem vários problemas relacionados ao uso de hidróxido de cálcio para a apexificação: o longo tempo necessário para que o ápice das raízes feche, o número de seções necessárias para completar o fechamento, a possibilidade de contaminação e a possibilidade de fratura dos dentes devido à aplicação a longo prazo de hidróxido de cálcio (WITHERSPOON et al., 2008).

O material alternativo, ao hidróxido de cálcio é o agregado de trióxido mineral (MTA). O MTA é composto de silicato dicálcico e tricálcico, óxido de bismuto e sulfato de cálcio. Apesar do MTA apresentar a capacidade de induzir formação de tecido duro de cimento quando usado adjacente a osteocidose perirradicular (SHABAHAN et al., 1999; REGAN, GUTMANN and WITHERSPOON 2002; APAYDIN, SHABAHAN and TORABINEJAD 2004), ele não é capaz de induzir o desenvolvimento completo da raiz (comprimento e espessura), o que compromete a integridade mecânica a longo prazo do dente (FARIK et al., 2002; JEERUPHAN et al., 2012). Essa condição está associada a uma maior predisposição para falhas e fraturas de tratamento e diminuição da sobrevida dentária (FARIK et al., 2002; JEERUPHAN et al., 2012).

Procedimentos endodônticos regenerativos (REPs), como revascularização e revitalização do tecido pulpar em dentes necróticos imaturos com

periodontite apical (AP), surgiram para permitir o reforço das paredes do canal radicular e, às vezes, a continuação desse eixo de desenvolvimento, abrindo assim novas possibilidades terapêuticas neste campo (IWAYA, IKAWA and KUBOTA 2001; MURRAY, GARCIA-GODOY and HARGRAVES 2007; HARGRAVES, DIOGENES and TEIXEIRA 2013).

A engenharia de tecidos surgiu com o campo encarregado de fornecer um mapa da possibilidade clínica para a regeneração de tecidos e órgãos (LANGER and VACANTI, 1993). Três elementos principais constituem a base para a engenharia de tecidos, nomeadamente células estaminais, moléculas de sinalização bioativas e os scaffolds. Os scaffolds, por sua vez, podem ter propriedades estruturais, químicas, mecânicas e biofísicas. Essas propriedades podem ser exploradas individualmente em conjunto para garantir a regeneração de tecidos de forma controlável (BOTTINO, PANKAJAKSHAN and NÖR 2017).

Nos últimos anos, o desenvolvimento de novas terapias clínicas para a regeneração da polpa dentária, como o método EB (evocate bleeding) trouxe uma promessa para melhorar os resultados do tratamento. No EB, após a adequada desinfecção do canal radicular, uma ampliação do forame apical é realizada para promover sangramento e formar um suporte baseado em fibrina para atrair células estaminais endógenas e fatores de crescimento (GFs). Tem sido demonstrado que o sangramento intracanal é parte dos tecidos apicais e traz substancial número de células-tronco mesenquimáticas (mesenchymal stem cells-MSCs) no sistema de canais (LOVELACE et al., 2011). Embora um coágulo de sangue (BC) tenha sido tradicionalmente usado como um scaffold, essa técnica apresenta várias limitações, que incluem uma composição indefinida (imprevisibilidade técnica), presença de células simunes, cinética de ruptura desconhecida e que sua geração requer traumatisar os tecidos apicais.

Esse método, proconiza o uso da pasta tri antimicrobótica (ciprofloxacina [CIP], metronidazol [MET] e minociclina [MINO]) ou antimicrobiano duplo (MINOLivre) uma pasta antibiótica muito concentrada para desinfecção.

No entanto, essas pastas, afetam negativamente a sobrevivência das células e staminais (BOTTINO, PANKAJAKSHAN and NÖR 2017). Além disso, a toxicidade, para os tecidos do hospedeiro e células residenciais, desta mistura de antibióticos não é conhecida atualmente. Independentemente dos resultados promissores alcançados pela EB de 57 relatos de caso reportados, apenas 1 mostra a formação de tecido tipo pulpar, ao tratar dentes permanentes imaturos com polpanecrótica, (SHIMIZU et al., 2012). A maioria dos achados histológicos apontou a invaginação de tecido periapical contendo tecido duro de semelhante a um tecido ósseo e tecido de cimento que levou para aumento da espessamento da parede do canal de raiz (MARTIN et al., 2013; BECERRA et al., 2014).

Diante disso, existem esforços contínuos de pesquisa para desenvolver scaffolds para regeneração de tecidos usando materiais sintéticos (GALLER et al., 2011). Esses scaffolds alternativos foram avaliados em modelos animais de endodontia regenerativa, incluindo colágeno (THIBODEAU et al., 2007), plasmárico em plaquetas (ZHU et al., 2012) e gelatina absorvíveis (WANG et al., 2013). No entanto, esses modelos, eles não conseguiram melhorar o conteúdo histológico. Atualmente, apenas esponjas de colágeno reticuladas em solução líquida estão associadas a melhores resultados (YAMAUCHI et al., 2011a; YAMAUCHI et al., 2011b).

A infecção é o principal motivo para a falha clínica da regeneração periodontal. Portanto, é extremamente importante controlar e / ou erradicar a contaminação bacteriana (HAFFAJEE AND SOCRANSKY, 1994; SLOTS, MACDONALD and NOWZARI, 1999). Uma ampla gama de antimicrobianos, incluindo o cloridrato de tetraciclina, MET e amoxicilina, foram incorporados em membranas de polímero (KENAWY et al., 2002; HE, HUANG and HAN, 2009; ZAMANI et al., 2010). Furtos colaboradores relataram assim sínteses de membranas à base de nanocompósito de polícaprolactona (PCL) modificadas com amoxicilina e nanohidroxiapatita para fornecer propriedades antimicrobianas e osteocondutoras, respectivamente (FURTOS et al., 2017).

Vários avanços substanciais nas técnicas de desinfecção que combinam o equilíbrio entre o efeito antimicrobiano e a biocompatibilidade com MSCs são

descritos na literatura (PALMA et al., 2017; DIOGENES and HARGREAVES 2017; BOTTINO, PANKAJAKSHAN and NÖR 2017). Com base nos

efeitos colaterais bem conhecidos, como a resistência à deformação bacteriana, associada ao uso excessivo de antibióticos, e a citotoxicidade destas pastas, agentes alternativos como as nanopartículas de óxido de zinco ( $ZnO$ ), têm sido propostos (MUNCHOW et al., 2015). Uma outra alternativa que tem se mostrado bom sucedido é a síntese de membranas nanofibrosas baseadas em PCL contendo ZnO foi relatada recentemente (MUNCHOW et al., 2015).

A clorexidina (CHX) é um anti-séptico de uso comum, amplamente utilizado e que tem propriedades bacteriostáticas e bactericidas contra bactérias gram positivas e negativas (KAEHN, 2010; KOVTUN et al., 2012). Especificamente, CHX é um agente anti-séptico, desinfetante, farmacêutico, cosmético e antiplaca. A alta efetividade deste fármaco contra microorganismos é devida à presença de aminas secundárias que podem ser protonadas, portanto, carregadas positivamente em condições normais de pH (GREEN, FULGHUM and NORDHAUS 2011). A incorporação de CHX em quantidades diminutas demonstrou atividade antimicrobiana para materiais dentários, como por exemplo o ionômero de vidro, sem afetar significativamente suas propriedades físicas (JEDRYCHOWSKI, CAPUTO, KERPER, 1983).

Os agentes antimicrobianos imobilizados oferecem uma alternativa que elimina a exposição dos pacientes aos agentes ativos, aumentando potencialmente a duração da eficácia antimicrobiana (VASILEV, COOK and GRIESSER 2009; CHARNLEY, TEXTOR and ACIKGOZ 2011). Os agentes podem ser imobilizados em uma grande variedade de materiais, incluindo metais e plásticos, bem como tecidos naturais e artificiais, como os scaffolds obtidos através de eletrospinning especificamente dentro das nanofibras constituintes.

Outro composto que vem sendo utilizado em alguns materiais odontológicos com a função de estimular a regeneração óssea e promover a mineralização do esmalte é o beta tri cálcio fosfato ( $\beta$ -TCP). O  $\beta$ -TCP possuiem sua composição íons cálcio e fósforo que em meio bucal, em contato com a saliva, promove a mineralização dos tecidos. Para que ocorra essa dissolução, é necessário que o CaP esteja subsaturado (em relação à concentração salivar)

e o pH bucal esteja abaixo do pH crítico resultando em aumento na liberação desses íons e ação remineralizante (RODRIGUES et al., 2015). Imatazo et al., (1998) demonstraram que a adição de cloreto de benzalcônio, um amônioquaternário, também tem sido adicionado promovendo sucessivas propriedades desantibacterianas.

Uma alternativa promissora seria desenvolver um material com ação tanto antibacteriana quanto osteoindutora. Diversos estudos já sintetizaram  $\beta$ -TCP e já avaliaram os agentes antimicrobianos a base de prata, clorexidina e salquaternário de amônio; no entanto, nenhum deles avaliou a adição de nanopartículas  $\beta$ -TCP com esses materiais incorporados em um scaffold baseado em nanofibras eletrofiadas conforme se propõe neste projeto.

Dante disso, uma alternativa sugerida é a incorporação de nanopartículas de  $\beta$ -TCP, das quais contêm antimicrobianos, em um scaffold baseado em nanofibras. Uma vez que as nanofibras tridimensionais podem facilmente ser carregadas com antibióticos ou partículas antimicrobianas, e ser combinadas com scaffolds injetáveis, enriquecidos com células-tronco e fatores de crescimento, levando a uma maior probabilidade de se conseguir uma regeneração de poliparentáriamais previsível.

## **Objetivos**

### **Objetivo Geral**

O objetivo deste estudo será de incorporar nanopartículas de  $\beta$ -TCP, das quais contêm antimicrobianos, em um scaffold a base de nanofibras, e avaliar o potencial antibacteriano e de regeneração detectado no pulpa desse material *in vitro* em modelo animal.

### **Objetivos Específicos**

Sintetizar scaffolds nanofibrosos contendo nanopartículas de  $\beta$ -TCP dopadas com clorexidina ou cloreto de benzalcônio;

Avaliar a morfologia e composição das fibras eletrofiadas através de microscopia eletrônica de varredura

(MEV), espectroscopia de raios X de dispersão de energia (EDS), microscopia eletrônica de transmissão (TEM, modelo JEM-

2010, JEOL), e espectroscopia de infravermelho transformada de Fourier (FTIR);

Avaliar propriedades físicas, através do ângulo de contato e resistência à tração, módulo de Young, alongamento a intervalo;

Caracterizar ação antimicrobiana dos scaffold através de testes de difusão em ágar, contato direto e formação de biofilme;

Avaliar a ação biológica através da adesão e proliferação de células tronco pulpar (DPSC) ao scaffold e da capacidade de diferenciação de células tronco da polpa dental (DPSC) semeadas *in vitro* com o modelo de cultivo dentário;

Avaliar a capacidade de respostas do tecido ósseo frente aos scaffold sem modelo animal com ratos.

## **Metodologia**

### **Dopagem das nanopartículas de $\beta$ TCP com agentes antimicrobianos**

Para a dopagem do  $\beta$ -TCP com os diferentes agentes antimicrobianos, será adotado um método de imersão. O  $\beta$ -TCP, já calcinado, será adicionado à solução e previamente preparadas a uma concentração final de 20% de clorexidina ou 20% de cloreto de benzalcônio. Neste método, as partículas ficarão sobre agitação constante nessa solução, por 3 horas para promover interações entre os materiais. A dopagem ocorre através de mecanismos de absorção, adsorção e ainda troca iônica. Após transcorrido esse período, a solução será filtrada e elevada a estufa por 50°C por 24 horas.

### **Síntese e caracterização do scaffold contendo nanopartículas de $\beta$ -TCP dopada com agentes antimicrobianos**

Materiais a poli ( $\epsilon$ -caprolactona) (PCL, Mw = 80,000) será adquirida pela LACTEL Absorbable Polymers (Birmingham, AL, EUA). Gelatina tipo B de pele bovina (~225 defloração, Mw=50000), 1,1,1,3,3,3-hexafluoro-2-propanol (HFP) e clorexidina,  $\beta$ tcp e cloreto de benzalcônio serão comprados da Sigma-Aldrich (St. Louis, MO, EUA).

Serão preparadas duas soluções de polímeros diferentes dissolvendo PCL (poli  $\epsilon$ -caprolactona) ou PCL / gel (PCL / GEL, razão de 1: 1, p / p) em HFP para produzir soluções de 10% em peso (100 mg mL<sup>-1</sup>), as soluções serão agitadas durante noite. A solução PCL será então carregada com concentrações distintas (0, 5, 10, e 15% em peso, em relação ao peso total de polímero) das nanopartículas de  $\beta$ -TCP carregadas com agentes antimicrobianos;

Considerando que a solução PCL/GEL será carregada com apenas 15% em peso de nanopartículas (para investigar o efeito de hidrofilia/hidrofobia da atividade antibacteriana). As misturas serão agitadas para 24 h e sonicadas por 90 minutos desse uso para melhorar a dispersão das nanopartículas dentro da solução de polímero, e depois a solução será dispensada usando um sistema de eletrospinning de alta tensão (ES50P-10W/DAM, Gamma High-Voltage Research Inc., Ormond Beach, FL, EUA).

Para a dispersão da solução será utilizada uma bomba de seringa (Legato 200, KD Scientific Inc., Holliston, MA, EUA) e um tambor coletor de aço inoxidável na terra do colectador da bomba para agitar a solução mecânicamente a uma velocidade (BDC6015, Cafrafo Limited, Georgian Bluffs, ON, CA) (BOTTINO et al., 2013; GADELLE et al., 2003). As soluções serão individualmente carregadas em uma seringa de plástico (Becton, Dickinson and Company, Franklin Lakes, NJ, EUA) equipado com uma ponta sem corte metálica 27G (CML Supply, Lexington, KY, EUA) e *electrospin* à temperatura ambiente, usando os seguintes parâmetros: uma distância de rotação fixa de 18 cm, mandril rotativo com 120 rpm de velocidade, taxa de fluxo de 1,5 mL / h e variando tensões elétricas de acordo com a solução. As esteiras obtidas (matrizes) serão então secas sob vácuo por pelo menos 48 horas para remover completamente qualquer solvente restante.

### **Caracterização da morfologia e composição das fibras eletrofiadas**

A morfologia e a arquitetura geral das fibras eletrofiadas serão avaliadas utilizando um microscópio eletrônico de varredura de emissão de campo (FE-SEM, modelo JSM-6701F, JEOL, Tóquio, Japão). As amostras tiradas de cada matriz serão montadas em um suporte de alumínio, revestidas com polipropileno como ouro-paládio e imagens a 5-7 kV serão obtidas. O diâmetro das fibras será calculado usando o software Image J (National Institutes of Health, Bethesda, MD, EUA) e medindo 50 fibras simples por cada imagem obtida (3 imagens / grupo) na mesma ampliação ( $5.000\times$ ). A espectroscopia de raios X de dispersão de energia (EDS) será realizada sob FE-SEM para analisar semi-quantitativamente a composição química das fibras.

A incorporação das nanopartículas nas fibras de polímero será investigada usando microscopia eletrônica de transmissão (TEM, modelo JEM-2010, JEOL). As características químicas e a incorporação das nanopartículas de todas as matrizes também serão avaliadas por espectroscopia de infravermelho transformado de Fourier (FTIR) no modo de reflexão total atenuado (ATR /FTIR-4100, JASCO Analytical Instruments, Easton, MD, EUA), na faixa de 700-4000 cm<sup>-1</sup> com uma resolução de 4 cm<sup>-1</sup>.

### **Ângulo de contato (AC)**

As soluções serão montadas em o mandril rotativo ( $n = 10$ ). Os parâmetros de electrospinning serão os mesmos que acima mencionados. O AC das matrizes fibrosas será medido usando um goniômetro (Modelo PG-2, Gardco, Paul N. Gardner Company Incorporated, Pompano Beach, FL, EUA) deixando cair três gotas consecutivas de água destilada (~ 5 µL) por amostra. A medida dos ângulos será então calculada em média.

### **Propriedades mecânicas**

As propriedades mecânicas (Resistência à tração, módulo de Young e alongamento ao intervalo) de todas as matrizes obtidas serão avaliadas por teste de tração uni-axial. Amostras retangulares (15 × 3 mm<sup>2</sup>) serão testadas ( $n = 8$ ) secas (teste imediato sem armazenamento) ou molhadas (teste depois de armazenamento em solução de PBS durante 24h) utilizando uma velocidade de 1 mm/min<sup>-1</sup>. A espessura da amostra será determinada com um paquímetro medindo em cinco diferentes locais da amostra. Os dados mecânicos serão obtidos das curvas de estresse e deformação de cada espécime e os resultados serão relatados com a média ± desvio padrão.

### **Propriedades antimicrobianas**

#### **Teste de difusão em ágar**

A eficácia antimicrobiana das nanofibras será avaliada através da incubação das nanofibras em meio de cultura contendo as seguintes espécies bacterianas: *Actinomyces eschweilii* (ATCC 43143; American Type Culture Collection, Manassas, VA), *Enterococcus faecalis* (ATCC 29212), *Aggregatibacter actinomycetemcomitans* (ATCC 33384) e *Fusobacterium*

*nucleatum* (ATCC 25586) através do ensaio de difusão em ágar (Bottino et al., 2014).

As amostras em forma de disco ( $f=5\text{mm}$ ) serão opesadas desinfetadas por luz ultravioleta (30 minutos de cada caldo). *E. faecalis* e *A. actinomycetemcomitans* serão cultivados anaerobicamente durante 24 horas em 5 ml de infusão de cérebro e coração suplementada com Levedura de 5 g / L e 5% de volume de vitamina K + hemin. *E. faecalis* e *A. actinomycetemcomitans* serão cultivados aerobicamente durante 24 horas em 5 ml de caldo de sojatríptico. Cem microlitros de cada caldo serão colocados em placas de ágar sangue para formar um gramado bacteriano que será dividido em 3 zonas: 10mL 0,12% de clorexidina (controle positivo), 10 ml de água destilada (controle negativo) e as amostras de fibra em forma de disco (PALASUK et al., 2014; KAMOCKI, NOR and BOTTINO, 2015). Após 2 dias de incubação, as zonas de inibição de crescimento serão medidas (emmm).

Para as salíquatas, as amostras serão cortadas com formato quadrado (15/15mm) ( $n=3$ ), desinfetadas e enxaguado. Cada amostra será colocada num frasco de vidro individual com PBS estéril (5mL a 37°C); as salíquatas de 500mL serão extraídas nos dias 1, 7, 14 e 21 e substituídas por uma quantidade equivalente de PBS fresco. As amostras de núcleo serão armazenadas a 20 °C até a utilização. As placas bacterianas serão preparadas e cultivadas como acima mencionado, e após 2 dias de incubação aeróbica ou anaeróbica, os diâmetros (emmm) das zonas claras de inibição do crescimento serão medidos (PALASUK et al., 2014; BOTTINO et al., 2014). As unidades formadoras de colônias por mililitro e *E. faecalis* serão selecionadas especificamente com base na sua associação com a necrose pulpar induzida por trauma imaturo (NAGATA et al., 2014).

As amostras de eletrosping ( $n=6$ ) serão cortadas, desinfetadas, fixadas em um suporte de amostra de plástico (CellCrown; Scaffdex Ltd, Tampere, Finlândia) e colocadas individualmente em placas de 24 poços. *E. faecalis* e *A. actinomycetemcomitans* serão cultivados aerobicamente durante a noite em 50mL de sobrinhatripticae 2mL de caldo inoculado serão colocados em copos para serem incubados aerobicamente durante 3 dias (BOTTINO et al., 2014). As

amostras serão removidas, enxaguadas com solução salina e colocadas em frascos de 3 mL com PBS ( $n = 4$  / grupo / espécie), que serão submetidos a sondagem e submetidos a vórtice para remover as bactérias não aderidas ao biofilme. Será preparada uma diluição salina 1: 100; a solução de 100 mL de película de película dissolvida será colocada em espiral em placas de ágar sangue, que serão incubadas com atividade ( $37^{\circ}\text{C}$  durante 24 horas) e contadas. Dois grupos de amostras serão fixados em solução de glutaraldeído 2,5% tamponada (Sigma Aldrich) e desidratado sem soluções de etanol descendentes antes da análise de microscopia eletrônica de varredura (MEV).

#### **Teste de contato direto modificado**

Cepas de *Enterococcus faecalis* armazenadas a  $-80^{\circ}\text{C}$  serão reativadas, sendo transferidos 100  $\mu\text{l}$  do inóculo bacteriano para um tubo estéril contendo 9 mL de BHI + 1 mL de glicose, e incubados por 18 h em estufa de CO<sub>2</sub>. Após este período, 10  $\mu\text{L}$  da mistura serão transferidos para uma placa contendo ágar sangue e será realizado um streak do caldo no ágar. A placa será incubada por 24 h em estufa de CO<sub>2</sub> e a parte iridocrescente registrada na placa, serão coletadas colônias isoladas, estas serão transferidas para um tubo estéril com 9 mL de BHI + 1 mL de glicose (starter) e incubadas por 18 h em estufa de CO<sub>2</sub>.

Discos de 6 mm de diâmetro e 1 mm de espessura ( $n=3$ ), serão confeccionados. Todos os grupos experimentais serão avaliados, incluindo os grupos controle. O experimento será realizado em diferentes momentos, sendo 1, 12 e 24 horas; 3, 5 e 7 dias; 1, 2, 3 e 4 meses.

O tempo de duração da atividade antibacteriana será avaliado após períodos de armazenamento da amostra em água destilada à  $37^{\circ}\text{C}$ . Os discos serão esterilizados por radiação UV e alocados individualmente nos poços das placas de cultura de 24 poços com 20  $\mu\text{l}$  de suspensão bacteriana, que posteriormente serão incubados a  $37^{\circ}\text{C}$ . Após esse período será acrescentado 180  $\mu\text{L}$  de BHI, para uma adequada homogeneização e será levado ao shaker por 5 min e em seguida, realizada a diluição seriada, finalizando com o plaqueamento em meio BHI de 20  $\mu\text{l}$  de cada uma das diluições realizadas utilizando a técnica da gota. Finalmente as placas serão incubadas por 24 h a  $37^{\circ}\text{C}$ . Após esse período, será realizada a contagem das unidades formadoras de colônia (UFC) e calculadas. O teste será realizado em triplicata (Ll et al., 2009).

## **Modelodeformação de biofilme demicrocosmos**

Discos de hidroxiapatita (HA) (n=4/grupo) estéreis serão usados como substrato para o crescimento dos biofilmes. Os discos de HA serão revestidos durante a noite à 4°C com colágeno de origem bovina tipo I (10 mg / mL decolágeno em HC1 de 0,012-M em água; Coesão, Palo Alto, Califórnia, EUA).

Aplacasubgingivalserácoletadadeumvoluntárioadultosaudávelesuspensoemcald o de infusão de cérebro-coração (BHI; Becton Dickinson, Sparks, Okla., EUA). A densidade celular será ajustada em um espectrofotômetro a 405 nm(modelon.º3350;Bio-

RadLaboratories,Richmond,Va.,EUA)aumadensidadedeaproximadamente7,5por 10unidadesformadorasdecolôniaspormililitroemBHI caldo. Os discos serão incubados em BHI em cultura celular de 24 poçosplacas,comassuspensõesdaplacaemcondiçõesesanaeróbicasusandoumsaco anaeróbioemindicadoranaeróbico(AnaeroGen,OXOID,Hampshire,Winchester, Reino Unido) a 37°C. Cada poço irá conter 1,8 mL de caldo de BHlestérile0,2mLnínculo,emqueasamostrasseraõmantidassubmersas.OmeioBHI serásubstituídoporumeioBHInovoumavezporsemanasemadiçãodenovosmicro organismos.

### **Ensaiodeviabilidadebacteriananobiofilme.**

Umacamadafinadecadamaterial(0,1g)serácuidadosamentecolocadanobi filmesdetrêssemanas.Osespécimesserãoentãocolocadosnaincubadoraporperíodo experimentaisde7e30dias(n=3).Omaterialemcadaum dos discos será lavado suavemente três vezes com uma solução salinatamponadacomfosfato (PBS).

UmKitdeviabilidade bacteriana(Viver/KitdeViabilidadeBacterianaBacLight Mortal L-7012) e ensaios quantitativos (Molecular Probes, Eugene,Ore., EUA) para microscopia será utilizado para colorir o biofilme e marcar ascélulasvivas emortasatravés daanálisedemicroscopiaconfocal.

As imagens microscópicas de varredura a laser confocal de 512 por 512pixels serão capturados usando uma câmera EZ-C1 3.40 e construídos usando o software 691 (Nikon Corp., Tóquio, Japão). Cinco áreas serão selecionadas aleatoriamente na superfície do disco de cada espécime para ser escaneadas(1,2 mm por 1,2 mm para cada área) pelo CLSM (Confocal laser scanning microscope) e análise de reconstrução tridimensional. Três espécimes serão avaliados, totalizando 15 medidas por grupo e período de tempo. Cinco varreduras separadas, 20-p.m. profundo (tamanho da etapa de 0,5 milhas, 40 fatias / pilha), de cada amostra serão realizadas para padronizar a área e o volume do biofilme.

Os índices vivo/morto de discos HA serão analisados usando o software elmaris 7.2 (Bitplane Inc., St. Paul, Minn., EUA). O volume relação entre fluorescência vermelha e fluorescência verde e vermelha indicará a proporção de células mortas. As proporções de mortos volume de células após exposição a diferentes scaffolds serão submetidas a análise de variância e testes de Tukey usando SPSS Software 17.0 (SPSS Inc., Chicago, IL, EUA).

### **Citocompatibilidade**

As amostras serão esterilizadas com luz ultravioleta e serão individualmente colocadas nos poços de placas de 24 poços contendo 5 mL de meio de Eagle modificado com alfa esterilizado (Gibco Invitrogen Corporation, Grand Island, NY), suplementado com 10% de soro fetal bovino (FBS) (Atlanta Biologicals Inc, Flowery Branch, GA) e incubada a 37 °C. Serão coletadas alíquotas (500 mL) a 1, 7, 14, 21 e 28 dias para avaliar a toxicidade celular ao longo do tempo (23). As células-tronco de polpa dental humana (DPSCs) (Lonza, Walkersville, MD) obtidas de terceiros molares permanentes serão cultivadas em meio de Eagle modificado com Dulbecco's modified Eagle medium (DMEM) com 10% de FBS e 1% de penicilina-estreptomicina (Sigma-Aldrich) em uma incubadora umidificada a 37 °C com 5 % de CO<sub>2</sub>. As células serão semeadas em placas de cultura de tecidos de 96 poços. Após 4 horas de incubação, o meio será removido e substituído pelas alíquotas recolhidas (100 mL) que serão ajustadas para 10% de FBS e 1% de penicilina-estreptomicina. Após a incubação, será acrescentado 40 mL de CellTiter 96 AQueous One Solution Reagent (Promega Corporation, Madison, WI) para reagir com a solução durante 2 horas antes de leitura a absorção em 490 nm em um leitor de placas (BioTek).

nstruments Inc, Winooski, VT) contrapõe o sem branco. Os DPSCs cultivados com ameaí serão utilizados como o controle positivo (23).

### **Ensaios de proliferação (WST-1)**

As HDPSCs serão colhidas por tripsinização, contados e semeados em lamelas de cultura de células tratadas de 13 mm (Thermanox, Thermo Fisher Scientific Inc, Rochester, NY, EUA) em placas de 24 poços com uma densidade de 104/poço (1500 µL de meio de cultura). Enquanto isso, os scaffolds (15 × 15 mm<sup>2</sup>, n = 6 / grupo) serão montados em CellCrown™ (Scaffdex, Tampere, Finlândia), desinfetados em etanol a 70% durante 30 min e enxaguados duas vezes em PBS estéril (Sigma).

Após um período de incubação de 4h para permitir a ligação celular, os CellCrowns com os scaffolds serão introduzidos nos poços. Uma distância de 2 mm entre as células e os scaffolds será padronizada usando anéis de plástico. As colunas de controle (em branco) serão preparadas em meio sem células e em meio com células mas sem scaffolds (100% de sobrevivência). Uma solução saturada (50 mg / mL) de CIP em DMEM será preparada por agitação durante 4h, à TA, seguido de centrifugação (3000 rpm) durante 15 min. O sobrenadante será esterilizado por filtração usando um filtro de seringa de 0,22 µm.

O ensaio WST-1 (Roche Diagnostics, Mannheim, Alemanha) será utilizado para avaliar os efeitos dos scaffolds contendo CIP na proliferação de HDPSC até 7 dias de exposição de célula / andame (Bottino et al. 2013). Após 3, 5 e 7 dias, o CellCrown com scaffolds serão removidos. Uma quantidade de 500 µL de DMEM será deixada em cada poço. Em seguida, o reagente de WST-1 será adicionado na proporção de 10:1 (isto é, 50 µL) em cada poço. Após 2 h de incubação em 5% de CO<sub>2</sub> numa atmosfera umidificada a 37°C, será transferido 100 µL do volume total presente em cada poço para placas de 96 poços (BOTTINO et al., 2013). O meio completo com células sem exposição ao suporte e meio completo sem células será atribuído como controles positivos e negativos, respectivamente. A densidade óptica (OD) do corante incorporado será determinada lendo a absorbância a 450 nm num leitor de microplacas contra uma coluna em branco (BOTTINO et al., 2013). A proliferação será calculada como uma razão de OD do valor experimental para o controlo positivo; ambos serão subtraídos pelo controlo negativo (BOTTINO et al., 2013).

## **Modelo Animal com Ratos**

O projeto será submetido ao Comitê de Ética em Experimentação Animal(CEEA) da Universidade Federal de Pelotas (UFPel). Todos os procedimentos serão realizados de acordo com as diretrizes institucionais para cuidado e uso dos animais. As reações teciduais ósseas dos diferentes grupos experimentais serão avaliadas, após 3 períodos experimentais (7, 14 e 28 dias; n=5 por período).

O número de grupos experimentais e grupos controle será definido de acordo com o desempenho dos materiais durante os testes físico-químicos, antimicrobianos e de biocompatibilidade. Para a seleção dos animais será realizada uma randomização dos mesmos e, após, a cauda dos animais será marcada individualmente para a identificação dos mesmos e cegamento dos investigadores. Os ratos Wistar ficarão em gaiolas plásticas (dois por gaiola) localizados em racks ventilados a 22°C com ciclo de luz de 12 horas (luzes acesas das 7:00 até às 19:00 horas). Durante a realização dos experimentos, será fornecida uma dieta padrão de comida (gavagem) e água filtrada ad libitum.

### **Intervenção**

A metodologia será adaptada de Assmann et al. (2015). Os animais serão anestesiados com 80mg/kg de quetamina (Virbac do Brasil Indústria e Comércio Ltda, São Paulo, SP, Brasil) e 10mg/kg de xilazina. O fêmur direito será usado para intervenção. A tricotomia será realizada e a área será desinfetada com solução de álcool iodado. Uma incisão de 5cm de comprimento será feita na pele, os tecidos serão separados por camadas e o periôsteo será incisionado com bisturi. Três cavidades de 2mm de diâmetro serão preparadas na superfície cortical do fêmur, separadas aproximadamente 6mm entre si, com uma demão de baixa velocidade e umbrocade a coredondan número 6 (KGSorenson, peça

São Paulo, São Paulo, Brasil) sob irrigação constante com solução salina e aspiração.

A broca será posicionada perpendicularmente ao fêmur e desencadeada ateatingir a medula óssea. A cavidade cirúrgica será designada a leitorialmente para grupos experimentais e controle negativo (cavidade vazia). Os scaffoldss serão inseridos imediatamente na cavidade. Será suturada a ferida em camadas (Vicryl Ethicon, Johnson & Johnson, São José dos Campos, SP, Brasil).

Após procedimentos experimentais, os animais serão colocados em gaiolas individuais até sua recuperação da anestesia. Será injetado intramuscularmente uma Igéicoopióide (50mg/kg) (Tramal 50, Pfizer Indústria Farmacêutica, Guarulhos, Brasil).

#### Eutanásia

Os animais serão sacrificados aos 7, 14 e 28 dias após a intervenção (n=5/grupo em cada ponto de tempo). Eles serão eutanasiados com sobredose de anestésico Isoflurano (Virbac do Brasil Indústria e Comércio LTDA, Brasil), por via inalatória. A perna operada será desarticulada e dissecada para isolar o fêmur. Em seguida, com um disco de diamante de baixa velocidade (KG Sorensen, São Paulo, Brasil), o osso será seccionado transversalmente para separar a região com as cavidades cirúrgicas. Cada fragmento será armazenado individualmente em formalina com tampão neutro a 10% durante 48 horas.

#### Processamento histológico

Após fixação, as amostras serão enxaguadas sem solução salina tamponada com fosfato durante 20 min e então descalcificadas com ácido nítrico a 10% (Sigma Aldrich, St. Louis, EUA), que será agitada à temperatura ambiente durante 3-4 semanas. As amostras serão colocadas em blocos de parafina e processadas para análise histológica. Secções com 5mm de espessura serão cortadas transversalmente e o eixo longo do fêmur, montadas em lâminas, e

coradas com hematoxilina-eosina (H & E). As fatias serão analisadas com microscópio de luz (RM2235, Leica, São Paulo, Brasil), utilizando aumentos de 40, 100, 200 e 400X. O processo de reparo será analisado de acordo com características histológicas por um patologista previamente calibrado. O Kappa ponderado intra-examinador será calculado para a presença de células inflamatórias, fibras e formação de barreira de tecido duro.

O setor celular será condensação de fibras e será analisado qualitativamente de acordo com os critérios descritos por Tavares et al. (2013). O componente inflamatório celular será determinado pela presença de neutrófilos, linfócitos, eosinófilos, macrófago e células gigantes. A formação de barreira de tecido duro será modificada a partir das diretrizes de Assman et al. (2014), como:

1. Ausência: não há deposição de tecido duro na cavidade;
2. Formação de tecido ósseo imaturo, iniciando o processo de fechamento linear de feito experimental;
3. Parcial: fechamento parcial da cavidade por deposição de tecido duro;
4. Completa: fechamento total da cavidade por deposição de tecido duro.

## Análises Estatísticas

Para a realização da análise estatística, o método estatístico será escolhido com base na heterogeneidade dos dados e distribuição normal ou não normal. Para todos os testes será considerado o valor  $p < 0,05$  como estatisticamente significante. Para a realização da análise estatística, será utilizado o programa estatístico SPSS.

## Orçamento

Descrição	Custo total R\$
Kit dedupla pigmentação para células vivas/mortas	4,408,00
Kit I de proliferação celular (MTT)	2,088,00
Meio de Eagle modificado de Dulbecco (DMEM)–altaglicose	255,00
CaldodeInfusão decérebro e coração	213,00
Meio agar de infusão decérebro e coração	979,00
Clorexidina	745,00
CloretodeBanzalcônio	2,089,00
100 Placas de 24 poços	550,00
200 Placas de petri	400,00
Eppendorfs	100,00
Ponteiras amarelas	150,00
FastGreen FCF (Verde rápido corante)	1,350,00
<b>TOTAL</b>	<b>13,327,00</b>

## Cronograma

Semestre/Ano							
<b>Mar.a Ago./2017</b>							
<b>Ago.aDez./2017</b>			X				
<b>Jan.aJun/2018</b>		X	X				
<b>Jul.aDez./2018</b>			X	X			
<b>Jan.ajun./2019</b>	X	X					
<b>Jul.aDez./2019</b>			X				
<b>Jan.aMar./2020</b>	X	X	X	X			
		X					
		X					

## Apêndice

### Esquemadasmetodologias

#### Fase1 –Aquisição dosmateriaise preparodaspárticulas

Dopagem das nanopartículas de  $\beta$ TCP com agentes antimicrobianos

Caracterização da dopagem com MEVeMET

No CDC– bio

NaFurg

#### Fase2–Obtençãodos scaffoldse caracterizaçãofísico-química

Síntese e caracterização do scaffold contendo nanopartículas de  $\beta$ -TCPdopada com agentes antimicrobianos; Ângulodecontato(AC);

Universidade de Michigan sob Orientação do professor Marco Bottino.

#### Fase3-AvaliaçãodasPropriedadesantimicrobianas

Testededifusãoemágar

Universidade de Michigan sob Orientação do professor Marco Bottino.

Testedecontatodiretomodificado

Modelodeformação debiofilmedemicocosmos

Laboratório demicrobiologi aUFPel

Ensaiodeviabilidadebacteriananobiofilme



Laboratório daURGS(Confocal)

### Fase3-Avaliação do desempenho biológico dos scaffolds

Citocompatibilidade  
Ensaios de proliferação (WST-1)

Universidade de Michigan sob Orientação  
do professor Marco Bottino.

Modelo Animal com Ratos



UFPel

### **3. RELATÓRIO DE TRABALHO DE CAMPO**

Durante o desenvolvimento do projeto, as nanofibras foram espinadas e caracterizadas, no entanto, durante a avaliação de biocompatibilidade foi observado que as nanofibras de  $\beta$ -tcp dopadas com CHX se mostraram tóxicas as células HDPSCs e SHEDS em um modelo testado *in vitro*. O passo seguinte da pesquisa seria a redução das concentrações de  $\beta$ -tcp e CHX na formulação final das nanofibras. No entanto, devido a situação mundial originada a partir da pandemia COVID-19, o projeto inicialmente proposto em 2018 não pode ser realizado.

Durante o período de Doutorado Sanduíche, tive a oportunidade de desenvolver vários projetos secundários ao projeto de tese inicial. Dentre estes, um projeto muito especial foi o: "*Injectable MMP-responsive Nanotube-modified Gelatin Hydrogel for Dental Infection Ablation*". Pode-se dizer que este projeto compreende uma síntese de tudo que aprendi durante todos os anos no laboratório. Ele abrange toda a caracterização de um material em várias vertentes, caracterização química, física, mecânica, microbiológica e biocompatibilidade.

O objetivo principal do projeto foi desenvolver um hidrogel antimicrobiano para ser usado na desinfecção de dentes durante a revascularização. Durante o desenvolvimento deste hidrogel, ao realizarmos a caracterização antimicrobiana, não foi observado ação antimicrobiana. Nesse momento, não sabíamos o porquê de um hidrogel contendo clorexidina não apresentava ação antimicrobiana. Então esse projeto ficou paralisado por um tempo. Enquanto isso, durante o desenvolvimento de outros projetos, foi possível observar que o GelMA foi sensível a colagenases que têm um papel importante na formação das lesões perirradiculares, adicionalmente, após a eliminação da doença, os níveis de colagenase caem para normalidade. Sendo então o GelMA sensível a colagenase, durante as periapicopatias, esse hidrogel vai ser degradado mais rapidamente cessando a infecção reduzindo a taxa de degradação do GelMA. Diante disso, pudemos entender que a entrega dos fármacos ocorre pela degradação do hidrogel principalmente pela degradação do GelMA mediada pela ação das colagenases.

Em virtude disto, diante do cenário de pandemia e para que eu pudesse assumir o concurso para professor substituto da UFPel, foi optado para esta defesa, a utilização destes projetos secundários desenvolvidos durante o período de estágio de doutorado sanduíche na Universidade de Michigan.

### **4. ARTIGO1**

O presente artigo foi publicado na revista ACS Applied Materials & Interfaces- *Fator de impacto: 8.758 (2019) Qualis A1* edesenvolvido em cooperação interinstitucional e internacional sobre orientação do professor Rafael Guerra Lund e coorientação do prof. Evandro Piva, e sob a supervisão estrangeira do prof. Marco Cicero Bottino.

## **Injectable MMP-responsive Nanotube-modified Gelatin Hydrogel for Dental Infection Ablation**

Juliana S. Ribeiro<sup>†,§</sup>, Ester A. F. Bordini<sup>†,¶</sup>, Jessica A. Ferreira<sup>†</sup>, LingMei<sup>‡</sup>,  
Nileshkumar Dubey<sup>†</sup>, J. Christopher Fenno<sup>¶</sup>, Evandro Piva<sup>§</sup>,  
Rafael G. Lund<sup>§</sup>, Anna Schwendeman<sup>†</sup>, and Marco C. Bottino<sup>†,\*</sup>

<sup>†</sup>Department of Cariology, Restorative Sciences and Endodontics, School of Dentistry, University of Michigan, Ann Arbor, Michigan, United States.

<sup>§</sup>Department of Restorative Dentistry, School of Dentistry, Federal University of Pelotas, Pelotas, RS, Brazil.

<sup>¶</sup>Department of Dental Materials and Prosthodontics, School of Dentistry, São Paulo State University, Araraquara, São Paulo, Brazil.

<sup>‡</sup>Department of Pharmaceutical Sciences, College of Pharmacy and Biointerfaces Institute, University of Michigan, Ann Arbor, Michigan, United States.

<sup>¶</sup>Department of Biologic and Materials Sciences & Prosthodontics, School of Dentistry, University of Michigan, Ann Arbor, Michigan, United States.

### **\*Corresponding author:**

Marco C. Bottino, DDS, PhD

University of Michigan School of Dentistry

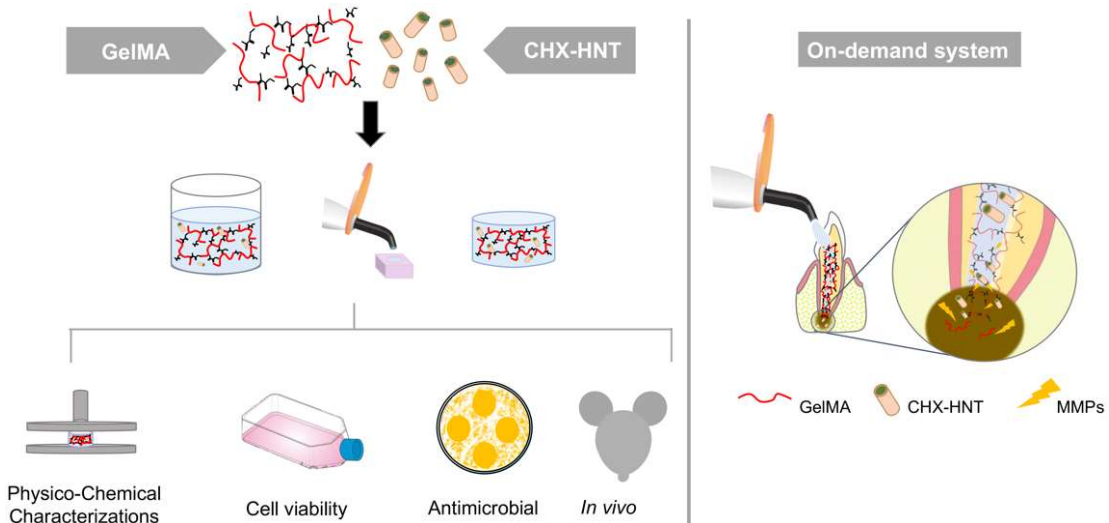
Department of Cariology, Restorative Sciences and Endodontics

1011 N. University (Room 5223), Ann Arbor, MI - 48109, USA.

Tel: +1-734.763.2206 Fax: +1-734.936.1597.

[mbottino@umich.edu](mailto:mbottino@umich.edu)

## Graphical Abstract



**ABSTRACT:** Photocrosslinkable gelatin methacryloyl (GelMA) hydrogel has been widely examined in regenerative engineering, because of its good cell-tissue affinity and degradability in the presence of matrix metalloproteinases. Halloysite aluminosilicate nanotube (HNT) is a known reservoir for the loading and sustained delivery of therapeutics. Here we formulate injectable chlorhexidine (CHX)-loaded nanotube-modified GelMA hydrogel that is cytocompatible, biodegradable, provides sustained release of CHX for infection ablation while displaying good biocompatibility. The effects of HNTs and CHX on hydrogels' degradability and mechanical properties, as well as on the kinetics of CHX release, and on the antimicrobial efficacy against oral pathogens were systematically assessed. Cytocompatibility in stem cells from human exfoliated deciduous teeth and inflammatory response *in vivo* using a subcutaneous rat model were determined. Our hydrogel system (CHX loaded nanotube-modified GelMA) showed minimum localized inflammatory responses, supporting its ability for drug delivery applications. Moreover, we showed that the incorporation of CHX-loaded nanotubes reduces the mechanical properties, increases the swelling ratio, and diminishes the degradation rate of the hydrogels. Importantly, the presence of CHX-loaded nanotubes inhibits bacterial growth with minimal cell toxicity. Our findings provide a new strategy to modify GelMA hydrogel with chlorhexidine-loaded nanotubes for clinical use as an injectable drug delivery strategy for dental infection ablation.

**KEYWORDS:** *drug delivery, hydrogel, infection, endodontics, dentistry, matrix metalloproteinases*

## ■ INTRODUCTION

Dental caries is the most common chronic disease among children and young adults age 6 to 19 years.<sup>1</sup> Etiologically speaking, caries is a time-dependent multifactorial infectious disease, which, if not properly managed, may lead to pulp tissue necrosis and consequential endodontic therapy.<sup>2</sup> Appraisals from the American Association of Endodontists indicate that ~ 16 million patients undergo root canal treatment every year in a procedure that involves surgical removal of the necrotic pulp tissue, followed by disinfection, mechanical instrumentation of the root canal, and final sealing with a thermoplastic material prior to tooth restoration.<sup>3</sup>

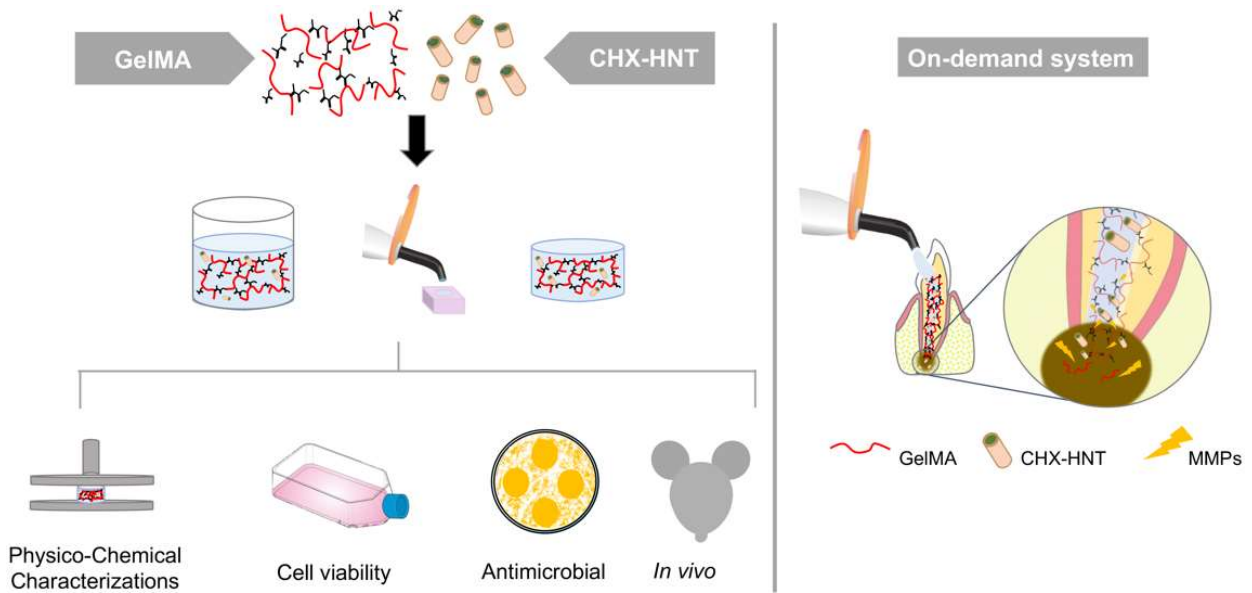
The microbial population in endodontic infections changes as the infection progresses. First, the infection is characterized mostly by the presence of facultative microbes.<sup>4-5</sup> Over time, an environment favoring anaerobic growth is established, both with the decline in oxygen levels due to bacterial metabolism and the lessening of blood flow due to tissue necrosis.<sup>6</sup> For example, *P. gingivalis*, an obligatory anaerobic Gram-negative microbe has been linked with endodontic infections, especially in apical periodontitis.<sup>6</sup> Of note, in addition to the most common virulence factors such as lipopolysaccharides, *P. gingivalis* proteinases (collagenases) have shown to play a key role in its pathogenesis mechanism.<sup>7-8</sup>

Clinically speaking, the root canal anatomy is highly complex, and thus the mechanical removal of tissue remnants, biofilm, and infected dentin cannot always guarantee a bacteria-free niche.<sup>9</sup> As a result, infected tissues can be left behind, where microorganisms can grow and proliferate.<sup>10</sup> Collectively, the anatomical challenges as well as the presence of clinical signs/symptoms, strongly support the indication of a multiple-visit therapy and employment of intracanal medications.<sup>11</sup> Although calcium hydroxide [Ca(OH)<sub>2</sub>] has been used clinically as an interappointment medication, research shows that it may not be entirely effective against *E. faecalis* and *C. albicans*. Instead, chlorhexidine digluconate (CHX) has been suggested based on its ability to ablate periapical inflammation.<sup>12-13</sup> Unfortunately, a growing body of research

suggests dose-dependent toxicity<sup>14-15</sup>; thus, underscoring the need to develop a delivery system to promote the controllable release of low, yet potent, antimicrobial doses of CHX. In this way, advances in the use of aluminosilicate clay nanotubes (Halloysite<sup>®</sup>) as a reservoir for the loading and sustained delivery of therapeutics reported by our group<sup>16,17</sup> and others<sup>18,19</sup>, present new prospects in designing injectable and degradable nanotube-modified hydrogels aimed at ablating endodontic infection with minimal or no adverse reactions. In detail, as previously reported, the modification of polymeric fibers with tetracycline (TCH)-loaded nanotubes led to sustained and controlled release, as opposed to the burst liberation observed when TCH was directly added into the fibers.<sup>20</sup>

Gelatin methacryloyl (GelMA) is a biocompatible and biodegradable photopolymerizable hydrogel that originated from the modification of amine-containing side groups of gelatin (Gel) with methacrylamide and methacrylate groups.<sup>21,22</sup> Gelatin, a natural polymer that can be obtained by denaturing collagen, has shown almost identical composition and biological properties to those of collagen while retaining both cell binding and MMP-responsive degradation sites.<sup>23</sup> Similar to other reported hydrogels, when considering its use in drug delivery, GelMA can be efficiently mixed with a wide array of additives, such as, but not limited to nanotubes and biomolecules.<sup>24</sup> Of note and highly relevant to the proposed work, during periapical pathology development, after endodontic therapy, persistent infections have been associated with increased levels of matrix metalloproteinases (MMP-1, MMP-2, MMP-8, and MMP-9) in the periapical area.<sup>25,26</sup> Thus, we postulate that a photopolymerizable GelMA could be successfully tuned to function as an on-demand depot of CHX that would be triggered by the hydrogel exposure to high levels of MMPs, and thus releasing the therapeutic agent once apical periodontitis is established. The present study is the first to report on the synthesis and clinical potential of an on-demand (MMP-responsive) injectable, biodegradable and biocompatible nanotube-modified GelMA hydrogel system for delivering CHX intracanal as a suitable strategy for dental infection ablation (Scheme 1).

**Scheme 1. Schematic Illustration of the Formulation and Evaluation of the Proposed Hydrogel**



## ■ RESULTS AND DISCUSSION

Our findings suggest an on-demand (MMP-responsive) system for delivering CHX intracanal from an injectable, biodegradable and biocompatible nanotube-modified hydrogel. A delivery mechanism, primarily based on GelMA degradation successfully mediated by MMP presentation, and subsequent liberation of antimicrobially potent and cytocompatible CHX concentration is demonstrated.

**Halloysite Nanotubes Modification.** The morphological details (length 321-806 nm and diameter 50.2-108 nm) of the nanotubes are presented in Figure 1a-b. Of note, TEM micrographs clearly display the lumen, which allowed the loading of CHX. Halloysite spectrum showed characteristics peaks at  $\sim 3696 \text{ cm}^{-1}$  associated with the  $\text{Al}_2\text{-OH}$  stretching. Additional peaks at  $\sim 1017$  associated with the Si–O stretching and at  $\sim 911$  associated with the  $\text{Al}_2\text{-OH}$  bending can be seen (Figure 1c and Table). The spectra of H-C10% and H-C20% are derived from the modification with CHX. Peaks at  $1643 \text{ cm}^{-1}$  and  $1581 \text{ cm}^{-1}$  are related to C=N

stretching vibration. The peak at  $\sim 1529\text{ cm}^{-1}$  corresponds to the nitrogen hydrogen bond in CHX supporting the HNT-CHX interaction.

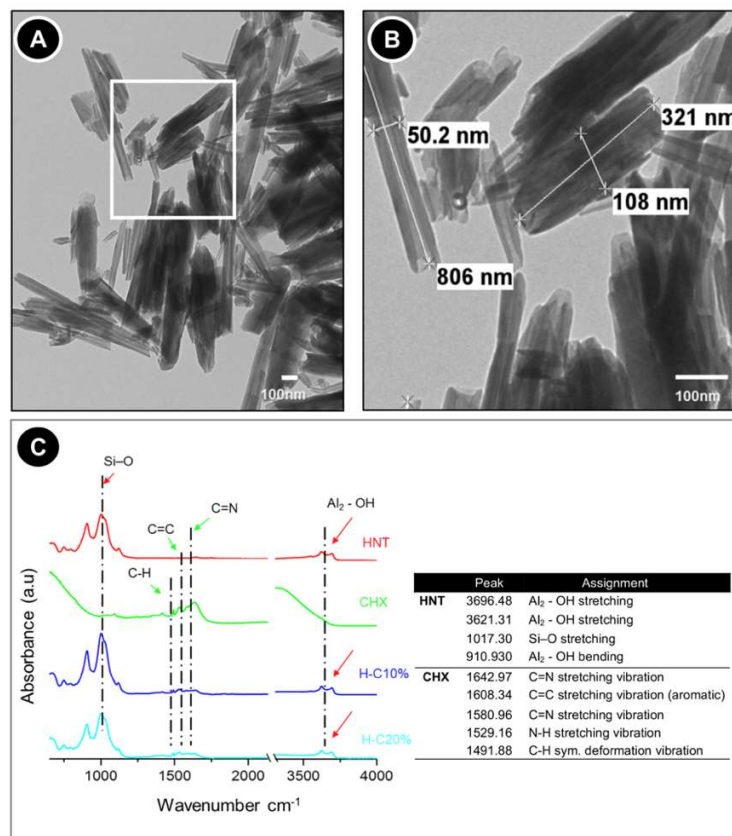


**Figure 1.** Morphological and chemical analyses of the nanotubes (HNTs, Halloysite<sup>®</sup>, Dragonite HP) with and without CHX.(a) Representative TEM micrograph of the as-received HNTs. (b) Inset high magnification TEM micrograph showing the uniform rod-like tubular structure, the hollow nature, and the morphological aspect of the tubes (scale bar = 100 nm). (c) ATR-FTIR spectra for pristine HNTs, CHX, and CHX-loaded nanotubes.

**CHX-loaded Nanotube-modified GelMA Hydrogels.** To appreciate the morphological features of the formulated hydrogels, cross-section SEM micrographs were obtained. It is well-known that during freeze-drying, the porosity of the material can experience changes; thus, all samples were processed in the same fashion. A consistent porous structure with pore size ranging from 40 to 143  $\mu\text{m}$  was observed among all formulations (Figure 2a-b). Furthermore, energy dispersive spectroscopy (EDS) highlights the presence and homogeneous distribution of HNTs within the GelMA hydrogel matrix (Figure 2c-d). Elemental mapping based on BSE-EDS analysis further confirmed the chemical nature of the nanotubes by the presence of Si and Al (Figure 2e-h), the major components of the HNTs.<sup>27</sup> It is well established that a 3D architecture with highly interconnected pores provides an advantageous environment for tissue regeneration, playing an important role in cell adhesion, migration, and proliferation. The obtained microstructure creates a suitable environment for cell penetration, supporting the rate of diffusion of oxygen and the uniform nutrient and waste exchange inside the hydrogels, allowing and helping the deposition of extracellular matrix by the cells.<sup>28,29</sup>

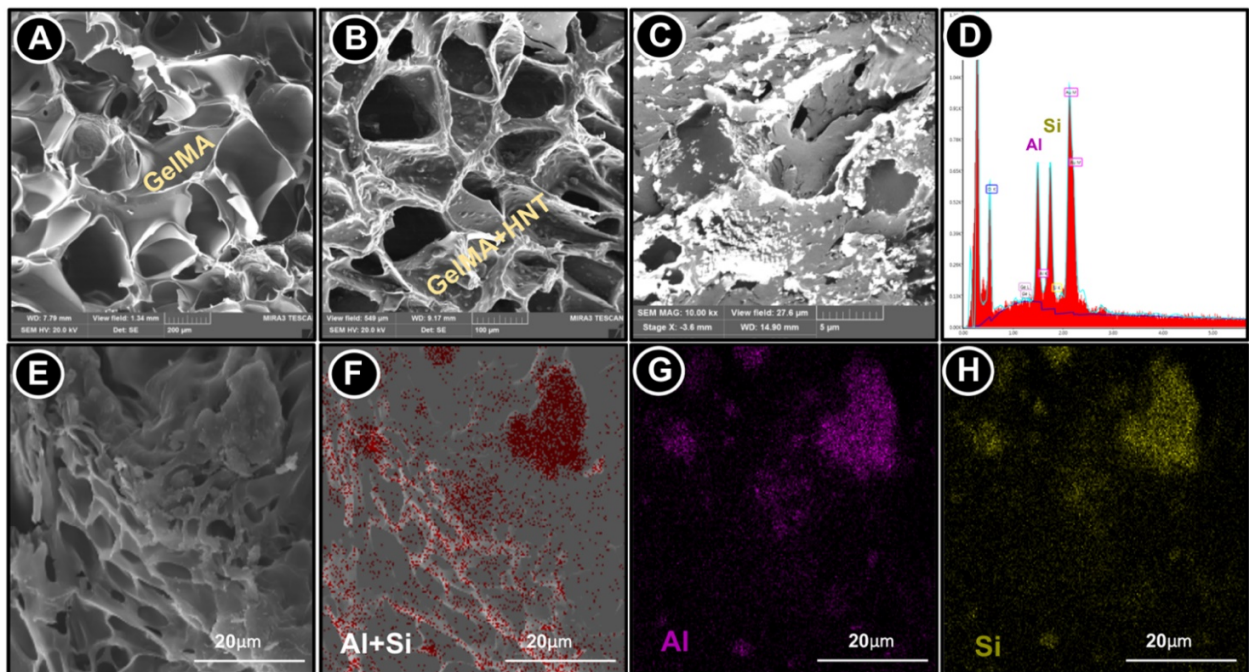


**Figure 2.** Morphological and chemical analyses of the nanotube-modified GelMA-based hydrogels.(a) SEM micrograph of a GelMA hydrogel cross-section. (b) SEM and (c) BSE-SEM micrographs of a cross-section of GelMA modified with CHX-loaded nanotubes (5%H-10%C). Note the presence of the aluminosilicate nanotubes based on the brightest areas throughout the microstructure (♦). (d) EDS results confirming the presence of Si and Al. (E-H) SEM micrographs combined with BSE/EDS elemental mapping of cross-section GelMA hydrogel modified with CHX-loaded nanotubes showing a uniform distribution of the nanotubes within the hydrogel matrix.

**Drug Release.** The release profiles of CHX from nanotube-modified GelMA hydrogels as a function of time are shown in Figure 3a-b. It is possible to observe a greater CHX release from H-C10% than H-C20%. It has been reported that sustained drug release may be due to the small size of HNTs, which confined drug diffusion. Noteworthy, although CHX-loaded HNTs were washed after loading, CHX can also be adsorbed on the external HNTs' surface. Within the first 24 h, the nanotube-modified hydrogels released between ~ 46% (1%H-C10%) and ~ 26% (2%H-C20%) of their total drug amount released over time. The mean drug amounts released from the 5%H-C10% and 5%H-C20% hydrogels were 6.5 µg/ml and 5.3 µg/ml, respectively after 24 h. The reported amounts promoted significant bacterial growth inhibition of the pathogens tested. Sustained drug release may prolong the contact time of the drug with the microorganism leading the amount of drug released into the medium reaching a level wherein the concentration could locally ablate the infection with minimal or no cell toxicity.<sup>30</sup>

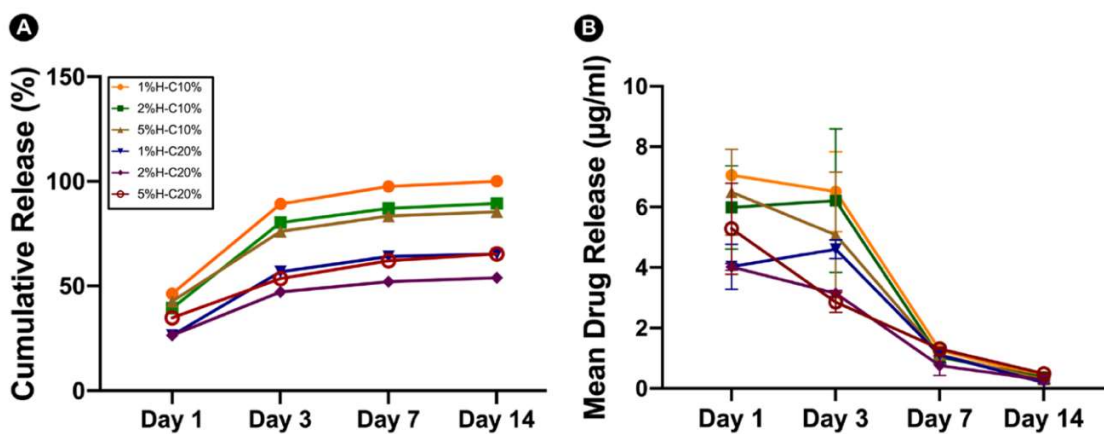


**Figure 3.** *In vitro* CHX release profiles from nanotube-modified GelMA loaded with distinct nanotubes (1, 2, and 5%) concentration and CHX solution concentration (10 and 20%) as a function of time. (a) Cumulative release (in %) and (b) Mean drug release (in µg/mL). The results are presented as mean ± SD (n=4).

**Swelling and Degradation.** The swelling ratio was investigated to determine the hygroscopicity of the nanotube-modified hydrogels. The results indicated that the addition of HNTs directly affected the swelling properties. The CHX-loaded nanotube incorporation into GelMA absorbs higher amounts of water into the material structure that slightly enhances its swelling ratio (Figure 4a). However, no significant differences were found between H-C10% and H-C20%. This higher swelling ratio typically indicates a network structure with larger pores and higher interstitial volume available, which improves the degradability of the materials due to fewer cross-links.<sup>31,32</sup> It is desirable for a hydrogel to maintain specific amounts of water in its structure since this property is related to the nutritional supply of cells.<sup>33</sup>

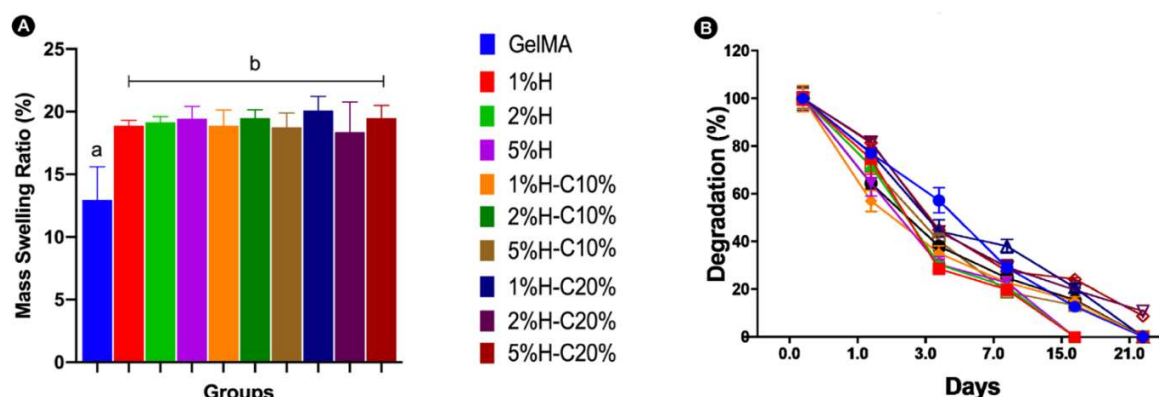


**Figure 4.** Swelling and enzymatic degradation (mass loss) of GelMA-based hydrogels. (a) The swelling ratio of GelMA and nanotube-modified GelMA-based hydrogels with and without CHX loading in DPBS at 37°C. (b) *In vitro* biodegradation of GelMA and nanotube-modified hydrogels in DPBS containing 1U/mL of collagenase type I at 37°C. The results are presented as mean ± SD (n=4).

Concerning the degradation profile of GelMA and the effect of the CHX loading via nanotube incorporation, we postulated that collagenase type I would mediate hydrogel degradation and thus CHX release. Knowing that GelMA hydrogels are MMP-sensitive, Figure 4b shows the complete degradation of the tested samples after 14 days. Statistical analysis revealed that HNT without CHX degraded faster than the groups modified with CHX-loaded nanotubes ( $p=0.05$ ). At 7 days, the degradation of the groups with no CHX addition was similar to groups modified with CHX at 10% and greater than the groups where CHX was added at 20%. On day 14, the non-CHX groups were completely degraded. At 21 days, no statistical differences were found among

the remaining groups. In general, the HNT-CHX incorporation significantly reduced the degradation rate of GelMA because of the presence of more chemical bonds formed among the hydrogel and the HNT-CHX, taking more time to be degraded by the MMP enzyme.<sup>34</sup> It has been related that the degradation speed of GelMA was inversely correlated with the degree of functionalization, the hydrogel concentration and the amount of enzyme present.<sup>35</sup> Nonetheless, despite the groups showing rapid *in vitro* degradation, the actual degradation within the root canal may be slower, as it is a closed environment.<sup>33</sup> Thus, the hydrogel would be trapped in the canal space and mainly subjected to MMPs action, such as in cases of recurrent apical periodontitis.<sup>13</sup>

**Biomechanical Properties.** Previous studies aimed at strengthening hydrogels using inorganic nanoparticles (e.g., hydroxyapatite, silicate, etc.) have reported the importance of optimizing particle concentration, since a threshold limit, in terms of reinforcement, appears to exist, primarily due to particle agglomeration, which can act as a microstructural defect.<sup>24</sup> For example, the incorporation of minute amounts (up to 0.5%) of nanosilicates in GelMA led to a significant enhancement in mechanical properties; however, it is worth mentioning that non-statistical differences were found between 0.05% and 0.5%. Hence, in the present work, the addition of HNTs (up to 5%) with or without loaded CHX did not promote significant biomechanical changes of GelMA (Figure 5a and 5b), except for 1%H-C10% and 1%H-C20%, which although statistically similar to unmodified GelMA, was not significant compared to most of the other nanotube-modified hydrogels. Taken together, the reported decrease in compressive modulus can be primarily attributed to the concentration of HNTs used.

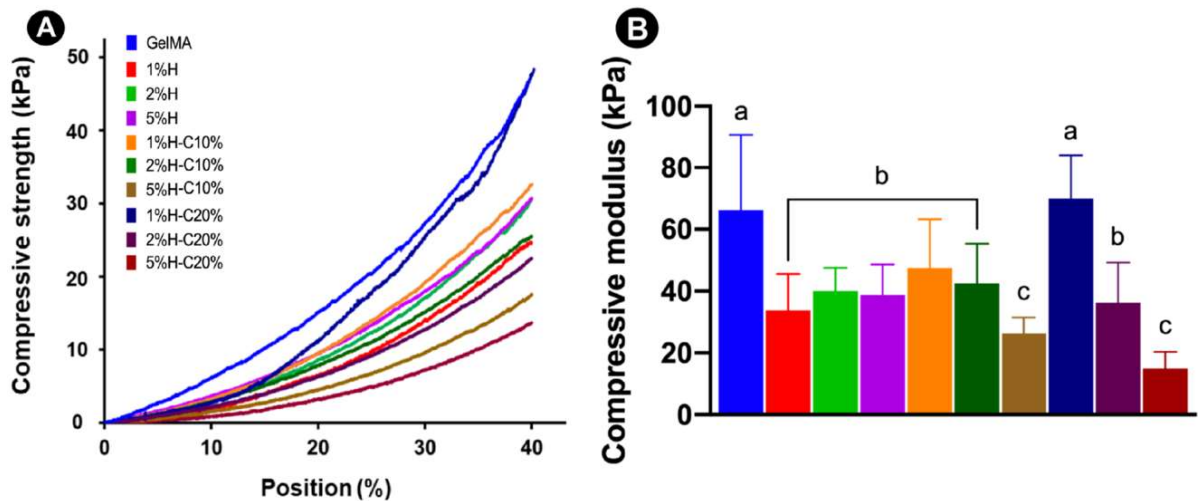


**Figure 5.** Biomechanical properties of GelMA-based hydrogels. (A) Representative stress-strain curves from nanotube-modified GelMA hydrogels loaded with different concentrations of nanotubes (1, 2, and 5%) and chlorhexidine solution concentration (CHX at 10 and 20%). (B) Compressive modulus (in kPa). The results are presented as mean  $\pm$  SD ( $n=10$ ).

**Cytotoxicity.** Determining the *in vitro* cytotoxicity of the proposed hydrogel system is key to validate its potential application as an on-demand intracanal drug delivery system for dental infection ablation. Here, we investigated the cytocompatibility of the hydrogels with human stem cells from exfoliated deciduous teeth (SHEDs). In comparison with the control (SHEDs cultured on the tissue culture plate), the number of surviving cells decreased after 24 h of exposure to the aliquots collected on day 3, for both concentrations (10% and 20%) of CHX-loaded nanotube-modified GelMA hydrogels (Figure 6). Nonetheless, the overall data showed an increase in cell viability above 70% to 80% for all groups when aliquots of 14, 21, and 28 days were tested. This might be explained by the fact that from day 3 a step-up in CHX release occurred, which agrees with the drug release data.

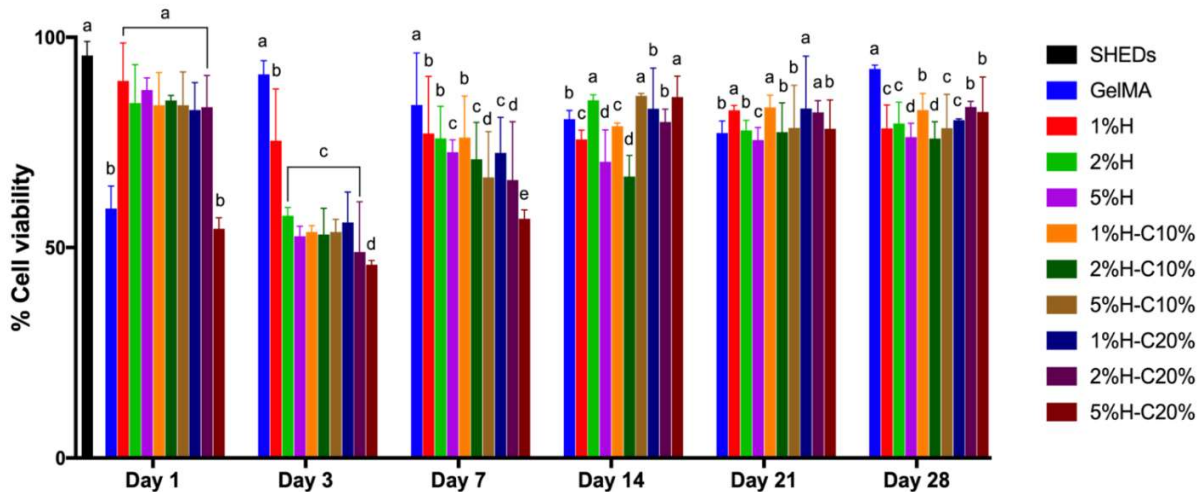


**Figure 6.** Cytotoxicity assay measured viability (%) of human exfoliated deciduous teeth stem cells (SHEDs) in response to aliquots at day 1, 3, 7, 14, 21, and 28 from GelMA-based hydrogels modified or not with 1%, 2% and 5% of halloysite nanotubes (H) and CHX-loaded nanotubes (H-C-10% and H-C-20%). Statistical analyses were compared with the same day. The percentage of cell viability was normalized by the mean absorbance of SHEDs cultured in the plate at day 1 (100%). Distinct letters indicate statistically significant differences between the groups when compared with the control (SHEDs cells). The results are presented as mean  $\pm$  SD (n=5).

**Screening CHX-loaded Nanotube-modified Hydrogels with the Best *In Vitro* Antimicrobial Properties.** Aiming to confirm the hypothesis that our proposed hydrogel possesses an on-demand drug delivery ability, agar diffusion assays were carried out with aliquots collected in 2 ways. Hydrogel samples of each group were placed in two different incubation media. As expected, for samples stored in PBS, the aliquots showed no bacterial inhibition for all groups in all-time points, thus supporting our hypothesis (MMP-responsive GelMA degradation). In the meantime, for aliquots obtained through incubation in the on-demand challenge (1 U/ml collagenase type A in sterile PBS) led to noticeable antimicrobial action over 21 days against four oral pathogens (Figure 7). Noteworthy, the incorporation of CHX-loaded nanotubes (CHX at 10 and 20%) at 5 wt.% led to greater inhibition zones against all microorganisms.

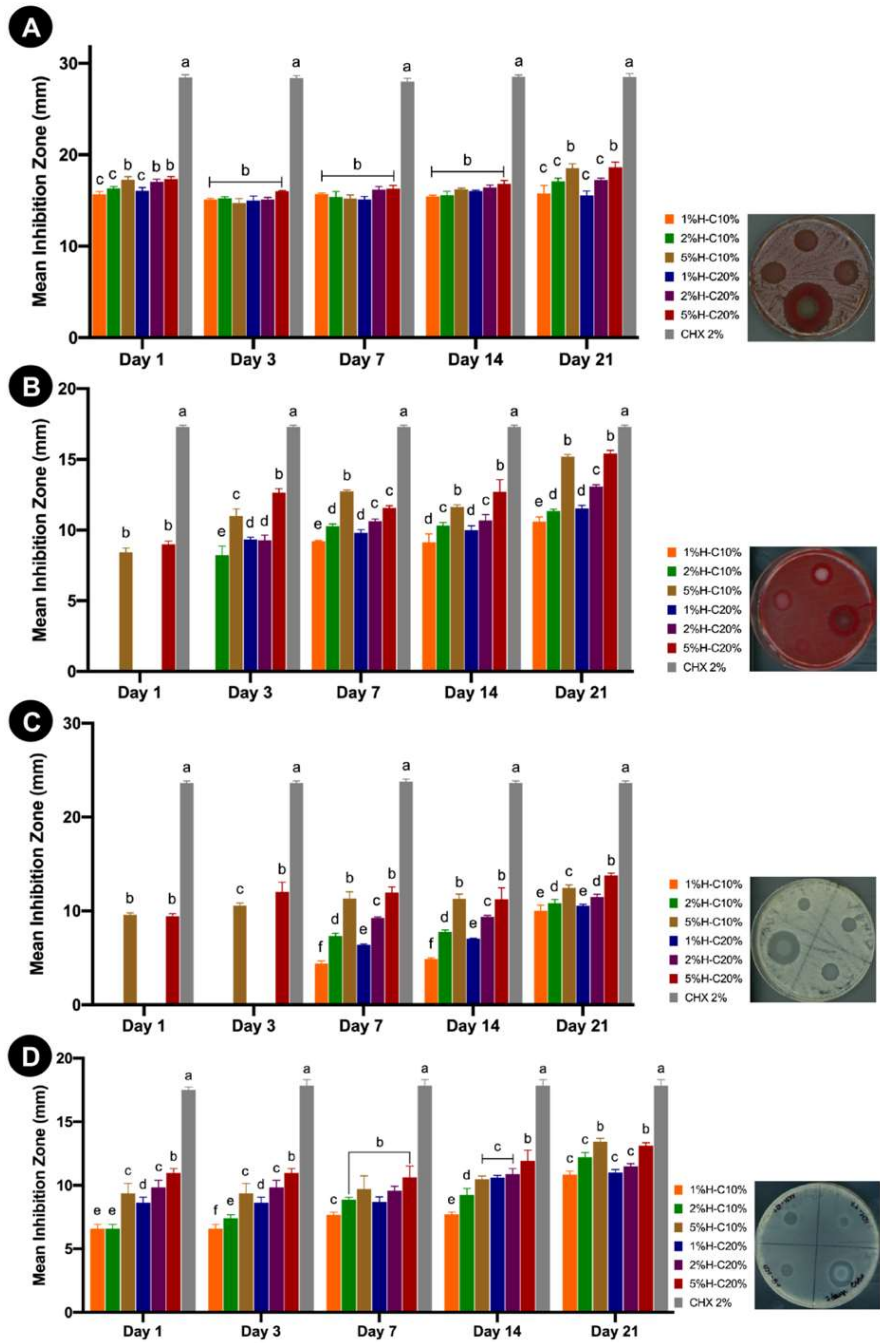


**Figure 7.** Results from agar diffusion assays are represented as a mean inhibition zone (in mm) against the different pathogens tested. (a) *A. naeslundii*; (b) *F. nucleatum*; (c) *C. albicans*, and (d) *E. faecalis* over time. Aliquots obtained through incubation in PBS only and incubated at the on-demand challenge (1 U/ml collagenase type A), over 21 days were tested. The same letters indicate an insignificant difference compared to the results of the same day of aliquots.

**Direct Contact.** *E. faecalis* are Gram-positive bacteria known to be associated with secondary endodontic infection, and its persistence is credited with its capacity to colonize the root canal and resist treatment.<sup>6</sup> *E. faecalis* can occur singly, in pairs, or as short chains. They are small enough to proficiently invade and live within dentinal tubules and have the capacity to endure prolonged periods of starvation until an adequate nutritional supply becomes available.<sup>36</sup> Once the bacteria become available in planktonic form inside dentinal tubules, it is critical to assess the antimicrobial effects of our GelMA-based hydrogels in a planktonic model. Taking into consideration the data collected in the agar diffusion assay, the following groups were tested, namely 5%H-10%C and 5%H-20%C, as well as Ca(OH)<sub>2</sub> and pristine GelMA as positive and negative controls, respectively. Significant differences were noticed among the CHX-loaded nanotube-modified hydrogels (5%H-10%C and 5%H-20%C) and Ca(OH)<sub>2</sub> when compared to unmodified/pristine GelMA (Figure 8a).

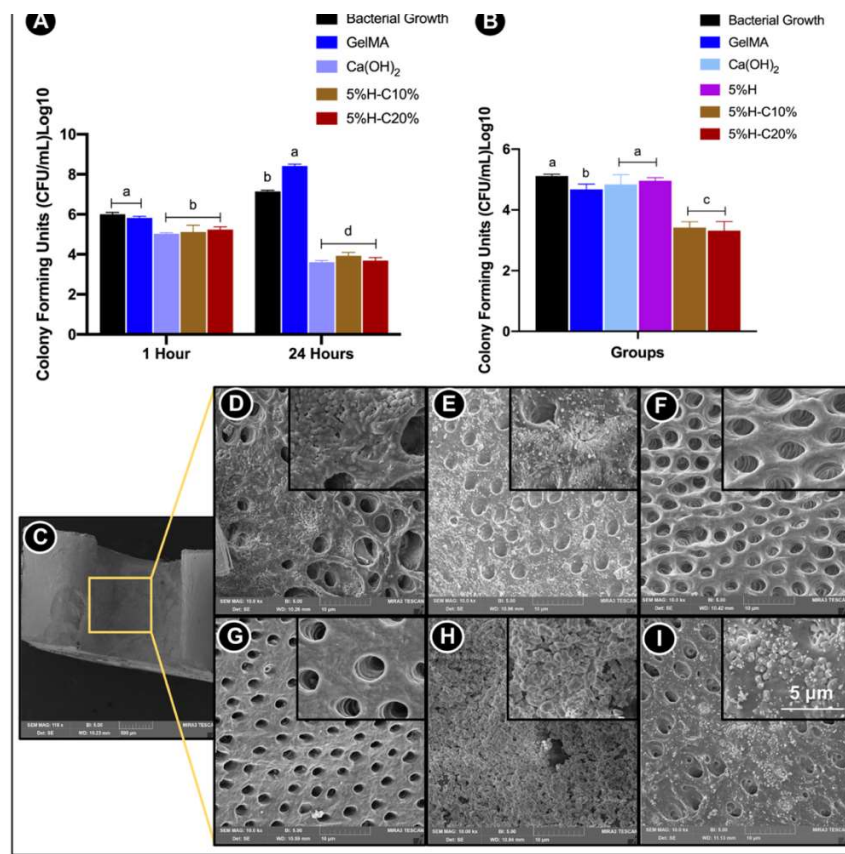


**Figure 8.** Antimicrobial properties of the formulated hydrogels.(a)Modified direct contact assay.Mean

counts of viable (CFU/mL) planktonic bacterial cells on GelMA-modified hydrogels. (b) Microcosmos biofilm model. CHX-loaded GelMA-based hydrogels (5%H-C10% and 5%H-C20%) significantly reduced bacterial numbers compared to all other groups. (c) SEM micrograph depicting the evaluated areas (inner root walls of dentin slices). (d-i) SEM micrographs of bacterial biofilm on the dentin surface of pristine GelMA (d), GelMA-5%H (e), GelMA-5%H-10%C (f), GelMA-5%H-20%C (g), Ca(OH)<sub>2</sub> (h) and bacterial growth, i.e., untreated dentin (I). Unmodified GelMA, CHX-free nanotube-modified GelMA groups demonstrate bacteria on dentin surfaces and inside dentinal tubules. CHX-loaded nanotube-modified GelMA hydrogels eliminated almost all bacteria on the dentin surface and inside dentinal tubules. Infected dentin slices treated with Ca(OH)<sub>2</sub> show bacterial presence within the calcium hydroxide paste. Note the abundant presence of biofilm on untreated dentin surfaces.

**Microcosmos Biofilm.** It is important to highlight that the direct contact test evaluated the action of the medication against the planktonic form of the bacteria. The physiological properties of the same bacteria in the culture medium are markedly different when compared to the bacterial cells in biofilms which are protected by the biofilm-specific extracellular matrix.<sup>37</sup> It is well known that root canal infections are biofilm mediated and according to the literature bacteria in biofilms maybe 1000 $\times$  times more resistant to antimicrobial agents and host defense mechanisms than their planktonic equivalents.<sup>38</sup> Therefore, to assess not only the antimicrobial activity against *E. faecalis* in a planktonic model but also the antimicrobial performance of our CHX-loaded nanotube-modified GelMA hydrogel in a more complex model, a microcosm biofilm model was used. As shown in Figure 8b, both the 5%H-C10% and 5%H-C20% groups led to the greatest biofilm inhibition, which was statistically different than the other groups. Notably, Ca(OH)<sub>2</sub> did not demonstrate significant action against the biofilm. In the SEM micrographs (Figure 8c-i), it is possible to note the presence of bacterial biofilm in the inner root walls of dentin slices of the unmodified GelMA, CHX-free nanotube-modified, and GelMA groups. However, in the CHX-loaded nanotube-modified GelMA hydrogels, a markedly absence of bacteria on dentin surface and inside dentinal tubules was noticed. Our data are in accordance with a previous study<sup>39</sup>, where the use of CHX in a drug delivery system was more effective against *E. faecalis* when compared to Ca(OH)<sub>2</sub>. However, it is important to emphasize that the efficacy of the Ca(OH)<sub>2</sub> paste is associated with prolonged disinfection periods, at least 7 days.<sup>40</sup> There has been increasing concern about the insufficient antimicrobial efficacy of Ca(OH)<sub>2</sub> against *E. faecalis*,

even after prolonged contact between the medication and root canal.<sup>40</sup> On the other hand, the most emblematic feature of CHX is that its positively charged molecules can be adsorbed by dentin preventing microbial colonization as a result of its substantive antimicrobial activity.<sup>41</sup>

**In Vivo Biocompatibility and Biodegradation.** As we know from the literature, in vitro and in vivo responses induced by biomaterials may be different in vitro and in vivo. Hence, subcutaneous implantation in rats was used for biocompatibility and biodegradation evaluation.<sup>42</sup> In this study, GelMA, 5%H, and 5%H-C10% hydrogels were evaluated after subcutaneous implantation in rats (Figure 9).

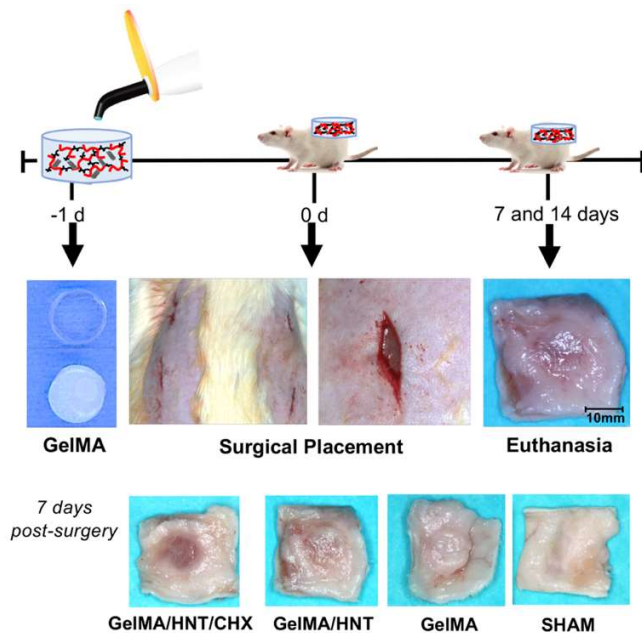


**Figure 9.** *In vivo* biocompatibility and biodegradation of the GelMA-based hydrogels. Schematic representation of the surgical implantation of GelMA, 5%H and 5%H-C10% hydrogels in a dorsal subcutaneous region of 6-week old Fischer 344 rats. The hydrogel samples were retrieved after 7 and 14 days. Representative macrophotographs of the explants 7 days post-implantation.

Representative images obtained after H&E staining of GelMA, 5%H and 5%H-C10% and SHAM explants after 7 and 14 days *in vivo* are shown in Figure 10. Overall, no signs of host inflammatory responses were observed. At days 7 and 14, 5%H and 5%H-C10% hydrogels revealed minimal inflammatory cell infiltration, mainly being restricted to the borders of the

hydrogels. The host cells that did infiltrate appear to be mononuclear cells (e.g., macrophages, monocytes), as evidenced by cellular morphology. Ingrowth of blood vessels was observed at sparse locations around the borders of both GelMA, 5%H and 5%H-C10% (yellow arrowheads) hydrogels at both time points indicating material compatibility with angiogenesis. Additionally, no foreign-body giant cells were found in any of the evaluated groups. These results demonstrate the low immunogenicity of GelMA, regardless of the presence of nanotubes or CHX. The findings of this work are in agreement with previous studies which has been shown GelMA hydrogels did not exert cytotoxicity.<sup>43</sup>

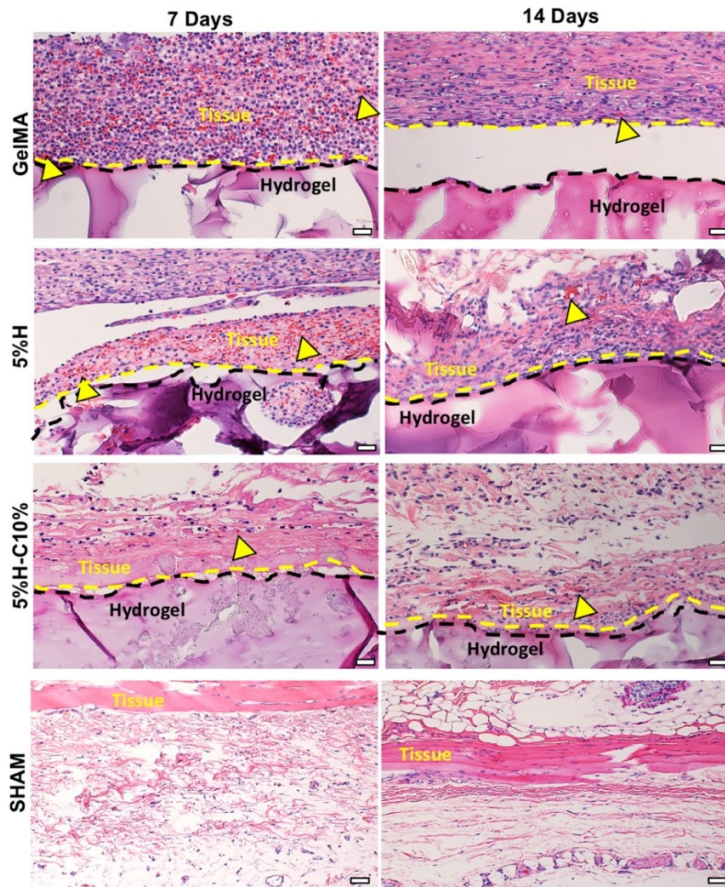


**Figure 10.** Histological analysis of the implanted hydrogels. Representative H&E staining images of of GelMA, 5%H and 5%H-C10% and SHAM explants (hydrogels with the surrounding tissue) after 7 and 14 days *in vivo* (scale bar = 200  $\mu$ m). Yellow arrowheads indicate the presence of numerous blood vessels containing murine erythrocytes.

Our histological data also illustrate specific details about hydrogels' degradation process *in vivo*. As depicted in Figure 11, GelMA hydrogel shows significant degradation at 7 days, with continuous resorption at 14 days. Meanwhile, the GelMA constructs were still present at the implantation site after 14 days.

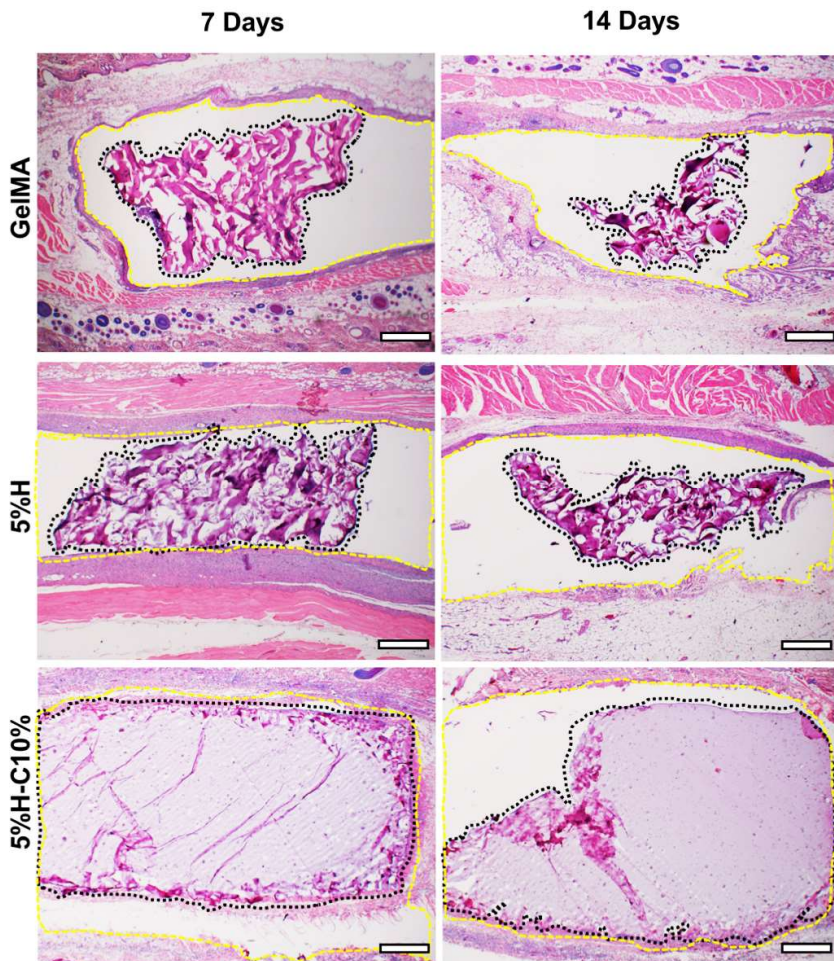


**Figure 11.** Histological analysis of the implanted GelMA hydrogels. Representative H&E staining images of GelMA, 5%H and 5%H-C10% and SHAM explants (hydrogels with the surrounding tissue) after 7 and 14 days *in vivo* (scale bar = 200  $\mu\text{m}$ ). The black dashed lines delineate the implanted hydrogels' border, highlighting the hydrogel degradation over time while the yellow dashed lines delineate the subcutaneous tissue surrounding the hydrogel.

In contrast, the 5%H-C10% showed a slower degradation profile on days 7 and 14 compared to GelMA and 5%H counterparts. Collectively, the *in vivo* biodegradation results correlate well with those obtained *in vitro*, whereby the GelMA hydrogel degraded rapidly, with almost half of

mass loss at day 14. Moreover, the data show that the presence of CHX-loaded nanotubes significantly reduced the degradation rate of GelMA, which can be attributed to the potential physical masking by HNTs of the sites of action for an enzymatic reaction. Our findings agree with similar work, where the presence of nanosilicates up to 0.5% (w/v) led to a significantly reduced degradation rate.

Results demonstrated that both *in vitro* and *in vivo* degradation rate of the formulated GelMA-based hydrogels were dependent on HNTs and CHX concentration. Overall, these results confirmed that composite hydrogels could be efficiently degraded *in vivo*, through the simultaneous action of multiple phagocytes and interrelated degradation pathways.<sup>44,45,46,47,48</sup> Neutrophils and monocytes might be able to initially shape degradation via the release of hydrolytic enzymes (serine proteases). These compounds can modulate the degradation process making it more or less vulnerable for the propagation of macrophage-driven degradation.<sup>59</sup> However, despite the groups show rapid *in vitro* and *in vivo* biodegradation, the actual degradation within the root canal may be slower as it is a closed environment. Nonetheless, although the site of implantation differed from the proposed clinical application, it is worth mentioning that the subcutaneous *in vivo* biocompatibility model performed herein had representative mechanisms and consequences of tissue-biomaterial interactions and is the most commonly used model able to provide an initial assessment of biomaterial compatibility with living tissues and degradation kinetics mediated by endogenous enzymatic mechanisms.

The main goal of the endodontic (root canal) treatment is to remove bacteria, virulence factors, and toxins in order to eradicate the inflammatory reaction in the apical area. Once the area is free of bacteria and its products, the inflammatory process and inflammatory cells slow down. Thus, we can infer that root canal treatment acts by reducing the active and latent forms of MMPs in root canal exudates and, in turn, the destruction of MMP-dependent inflammatory tissue.<sup>49</sup> Within this context, chlorhexidine has been used as an adjunct medication in periapical treatment<sup>50,39</sup> particularly in situations where the root is not completely formed (open apex). In

sum, we successfully engineer an on-demand intracanal drug delivery system based on the modification of GelMA with halloysite nanotubes loaded with chlorhexidine. Overall, we present strong evidence that our GelMA-based injectable drug delivery system would be clinically suitable for a number of therapeutic strategies aiming at ablating infection, particularly prior to regeneration in cases of endodontic and periodontal applications.

## ■ CONCLUSIONS

In this study, we formulate injectable chlorhexidine (CHX)-loaded nanotube-modified GelMA hydrogel that is cytocompatible, biodegradable, and provides sustained release of CHX for dental infection ablation. Taking into consideration the lack of dental stem cell toxicity of the designed (CHX)-loaded nanotube-modified hydrogel system in addition to good biocompatibility and minimum localized inflammatory responses as determined by *in vivo* experiments, we can envisage that the proposed injectable GelMA-based hydrogels can be used for sustained intracanal drug delivery applications in endodontics. Nonetheless, further *in vivo* studies (periapical disease model) based on this proof-of-concept research, should be performed in order to enable the translation of the proposed drug delivery strategy to the clinics.

## ■ MATERIALS AND METHODS

**Materials and Chemicals.** Aluminosilicate clay nanotubes (HNT, Halloysite<sup>®</sup>, Dragonite HP) were obtained as a gift from Applied Minerals Inc. (New York, NY, USA). TEM grid (Cu 200 mesh) was purchased from Structure Probe, Inc. (West Chester, PA, USA). Chlorhexidine digluconate(20%) aqueous solution, type-A gelatin (300 bloom) from porcine skin, methacrylic anhydride (MA), L-glutamine, Brain Heart Infusion Broth, and agar (BHI) were procured from Sigma-Aldrich (St. Louis, MO, USA). Dulbecco's phosphate-buffered saline (DPBS), alpha-modified Eagle's Medium ( $\alpha$ -MEM), fetal bovine serum (FBS), and penicillin-streptomycin were acquired from Gibco-Invitrogen (San Diego, CA, USA). Absolute-200 proof ethanol (Fisher

Scientific, Waltham, MA, USA), lithium phenyl-2,4,6-trimethylbenzoylphosphinate (LAP L0290, TCI America, Portland, OR, USA), ethylenediamine tetra-acetic acid (EDTA; Inter-Med, Inc., Racine, WI, USA), collagenase type I (Hoffman-La Roche Ltd., Basel, Switzerland), and CellTiter 96 AQueous One Solution Reagent (Promega Corporation, Madison, WI, USA) were obtained from their respective manufacturers.

**CHX Loading into Nanotubes.** To validate the morphological characteristics of Halloysite<sup>®</sup>, transmission electron microscopy (TEM JEM-2010, JEOL, Tokyo, Japan) was done. Briefly, 10 µL of an aqueous dispersion of sieved (<45 µm) HNTs was pipetted onto a holey carbon TEM grid, allowed to air-dry, and imaged at 100 kV.<sup>16</sup>

Chlorhexidine digluconate was used to prepare 10% and 20% CHX solutions (v/v) in distilled water for HNTs loading as previously established by our group.<sup>16</sup> 1.25 g of the sieved HNTs and 5 mL of the respective CHX solutions were centrifuged, vortexed for 20 s, and sonicated for 2 h. Then, the mixture was placed in a vacuum (25 in.Hg) chamber (Hi-Temp Vacuum, Thermo Scientific). After 1 h, the mixture was vortexed for 1 h and the vacuum was reapplied. Finally, the HNT+CHX solutions were washed and centrifuged (3000 rpm) for 10 min, then stored at 37°C for 7 days until completely dried. The dried mixture was once again sieved at 45 µm and dried prior to further use.<sup>18</sup> CHX-loaded HNTs were obtained (hereafter referred to as H-C10% and H-C20%, respectively). Fourier transform infrared spectroscopy in the attenuated total reflection mode (FTIR-ATR, Nicolet iS50, Thermo Fisher Scientific Inc.) was carried out to assess the presence of CHX. The spectra of pristine HNTs, CHX, as well as CHX-loaded nanotubes, were collected in the 400–4000 cm<sup>-1</sup> range with a resolution of 4 cm<sup>-1</sup> (64 scans).

**Gelatin Methacryloyl (GelMA).** GelMA synthesis was carried out as described previously.<sup>51,52</sup> Briefly, on a heating plate at 50°C, type-A gelatin (10% w/v) was solubilized into DPBS. Next, 8 mL of methacrylic anhydride (MA) was introduced dropwise into the Gel solution and allowed to react for 2 h under stirring conditions. To ensure the interruption of the reaction, an equal amount (8 mL) of DPBS was added at 40°C. Finally, in order to remove salts and unreacted

monomers, the mixture was dialyzed in DI water using 12-14 kDa dialyzes tubing at 45 ± 5°C for 1 week and the water was changed every 12 h. The prepared solution was frozen at -80°C overnight, lyophilized (LabconcoFreeZone 2.5L, Labconco Corporation, Kansas City, MO, USA) for 7 days, and stored at -80°C until further use.<sup>23</sup>

**CHX-loaded Nanotube-modified GelMA Formulation and Characterization.** To create GelMA-based hydrogels, 0.6 g of GelMA was dissolved in 4 mL of DPBS at 50°C. This was followed by the addition of 0.45 mg of the photoinitiator (LAP) at 50°C under stirring (240 rpm) conditions; thus, establishing the pure GelMA group (15% GelMA, control). CHX-loaded nanotubes (H-C10% and H-C20%) at specified amounts (1, 2, and 5% w/v; hereafter referred as 1%H, 2%H, and 5%H) were dispersed into the GelMA solutions. Analogously, CHX-free nanotubes in the aforementioned amounts were also added to GelMA. To fabricate the GelMA and GelMA-modified samples for the various analyses reported, predetermined volumes ranging from 100-150 µL of the prepared solutions, were placed in custom-made silicone molds (CutterSil Putty PLUS, Kulzer US, South Bend, IN, USA) and photocrosslinked for 15 s with a curing LED light (Bluephase, Ivoclar-Vivadent, Amherst, NY, USA) with a broadband spectrum of 385-515 nm. After crosslinking, the samples were removed from their molds.

The microstructures of GelMA and nanotube-modified GelMA hydrogels were evaluated by scanning electron microscopy (SEM, Tescan MIRA3 FEG-SEM, Tescan USA Inc., Warrendale, PA, USA). Pore morphology was analyzed in cylindrical-shaped (6-mm diameter × 10-mm thick) samples prepared as previously described. Prior to SEM imaging, samples (n=3/group) were freeze-dried, cross-sectioned, and sputter-coated with Au-Pd. Elemental mapping was carried out using energy-dispersive spectroscopy by electron backscattered diffraction (EBSD) and an EDAXHikariEBSD camera mounted on an SEM to determine the chemical constituents.

**Drug Release.** Ultra-performance liquid chromatography (UPLC) was used to investigate the release profile of CHX from the various CHX-loaded nanotube-modified GelMA hydrogels. The UPLC system consisted of an Acquity Quaternary Solvent Manager, Sample Manager-FTN,

Column Manager, and TUV Detector (Waters Corporation, Milford, MA, USA). Hydrogel samples (6-mm diameter × 2-mm thick) modified or not with CHX-loaded nanotubes were individually immersed into 5 mL DPBS containing 1U/mL of collagenase type I, followed by incubation at 37°C. At predetermined time intervals, 500 µL aliquots were drawn and the same amounts were added back to keep the extraction volume constant. The aliquots were filtered using a 0.22-µm nylon membrane under vacuum prior to analysis. Separation of the CHX was carried out with an AcquityUPLC-BEH C18 column (1.7 µm, 2.1 × 100 mm) at 40°C. The mobile phase was acetonitrile/buffer (1% triethylamine adjusted to pH 3.5 by acetic acid)/(35/65) at 0.5 mL/min with an injection volume of 10 µL. CHX concentration was detected by UV absorbance at 259 nm.

**Swelling and Enzymatic Degradation.** The swelling capacity of the GelMA-based hydrogels was determined by using the known hydration of the gels. Briefly, after incubation in DPBS at 37°C for 24 h, wet samples (6-mm diameter × 2-mm thick, n=3/group) were blot-dried using low-lint content tissue paper (Kimberly-Clark, Irving, TX, USA) and weighed on an analytical balance to obtain wet weights ( $W_w$ ). The dry weights ( $W_d$ ) were determined after the samples' lyophilization. The swelling rate (%) was calculated as  $(W_w - W_d)/W_d \times 100$ .<sup>22</sup>

For degradation analysis, identical cylindrical-shaped samples (n=4/group) were incubated in glass vials (VWR International, LLC, Radnor, PA, USA) with 5 mL DPBS containing 1U/mL collagenase type I at 37°C. At predetermined time intervals up to 21 days, each sample was removed from the solution and washed (2×) with sterile DI water, blot-dried, and weighed on an analytical balance. The collagenase-enriched solutions were replaced with fresh ones every 3 days to maintain constant enzyme activity. The degradation ratio of the hydrogel was calculated using the following equation:

Degradation ratio (%) =  $\frac{W_t}{W_0} \times 100$  (where  $W_t$  is the residual wet weight at different time points and  $W_0$  is the initial wet weight).

**Biomechanical Testing.** To evaluate the compressive modulus, cylindrical-shaped (8-mm diameter × 3-mm thick) samples were prepared. In detail, 150 µL of the GelMA-based hydrogels were dispensed into the mold followed by 15 s of photocrosslinking. The samples (n=5/group) were incubated in DPBS at 37°C. After 24 h, the samples were blot-dried and then subjected to unconfined compression at a strain rate of 2 mm/min (expert 5601, ADMET Inc., Norwood, MA, USA) at room temperature. The compressive modulus was calculated as the slope of the linear region of the stress-strain curves corresponding with 0-10% strain.<sup>24</sup>

**Cytotoxicity.** To examine whether modification of GelMA with CHX-loaded nanotubes would lead to cell toxicity, samples (6-mm diameter × 2-mm thick) were prepared for an *in vitro* assay in accordance with the International Standards Organization guidelines (ISO10993-5).<sup>21</sup> To that end, the samples (n=5/group) were first UV-treated for 30 min on each side for disinfection purposes and then individually placed in sterile glass vials containing 5 mL of α-MEM supplemented with 10% FBS, L-glutamine, 1% penicillin-streptomycin, and 1U/mL of collagenase type I. Next, the samples were incubated at 37°C at predetermined time points up to 28 days and 500 µL aliquots were collected to determine the cytotoxicity over time. Of note, equal amounts were added back to each vial to keep the extraction volume constant. Finally, the collected aliquots were filtered through a 0.22-µm membrane prior to cell exposure.

Stem cells from human exfoliated deciduous teeth (SHEDs), kindly donated by Dr. Jacques Nör (University of Michigan, School of Dentistry, Ann Arbor, MI, USA), were cultured in an incubator at 37°C, with 5% CO<sub>2</sub> in α-MEM supplemented with 10% FBS, 1% L-glutamine, and 1% penicillin-streptomycin.<sup>33</sup> Cells at passages 4-7 were used. SHEDs were seeded at a density of 2.5×10<sup>3</sup> cells/well and allowed to adhere to the wells of 96-well plates. After 24 h, the media was replaced by the collected extracts (100 µL) from the hydrogels and kept in contact with the cells for 24 h. Subsequently, 20 µL of CellTiter 96 AQueous One Solution Reagent was added to the test wells and allowed to react for 2 h at 37°C in a humidified 5% CO<sub>2</sub> atmosphere. The incorporated dye was measured by reading the absorbance at 490 nm (SpectraMax iD3,

Molecular Devices, LLC, San Jose, CA, USA) against a blank column. SHEDs cultured in complete α-MEM was used as positive control. Absorbance values were converted to a percentage and compared with the values obtained for the test groups.

**Determination of Antimicrobial Activities.** The antimicrobial properties of CHX-loaded nanotube-modified GelMA hydrogels were determined by means of an agar diffusion assay against *Actinomyces naeslundii* (*A. naeslundii*, ATCC 12104), *Candida albicans* (*C. albicans*, ATCC 90028), *Fusobacterium nucleatum* (*F. nucleatum*, ATCC 25586), and *Enterococcus faecalis* (*E. faecalis*, ATCC 19433). Cylindrical-shaped (6-mm diameter × 2-mm thick) samples were prepared and then disinfected as previously mentioned. The microorganisms were cultured for 24 h in 5 mL of BHI broth. Each bacterial suspension was spectrophotometrically adjusted to obtain  $3 \times 10^8$  CFU/mL. 100 μL of each broth was swabbed onto BHI agar plates to form a bacterial lawn.

To determine the sustained antimicrobial effects, and more importantly, the MMP-responsive on-demand nature of the hydrogels, samples (6-mm diameter × 2-mm thick) were prepared (n=3/group). Next, the samples were individually incubated in glass vials with 5 mL of sterile PBS (with and without 1U/mL of collagenase type I) at 37°C. At predetermined time intervals up to 21 days, 500 μL aliquots were drawn and replaced with an equivalent amount of fresh PBS. The retrieved aliquots were stored at -20°C until further use. Each bacterial plate was divided into 4 zones, namely 10 μL of 2% chlorhexidine digluconate (CHX; positive control), 10 μL of DI water (negative control), and 20 μL of the GelMA-based aliquots (2 zones/plate randomly assigned). After 24 h (*E. faecalis* and *C. albicans*) or 48 h (*F. nucleatum* and *A. naeslundii*) of incubation, the diameters (in mm) of the clear zones of growth inhibition were measured.

**Direct contact test.** The direct contact test was performed to investigate the antimicrobial effects of the CHX-loaded nanotube-modified hydrogels in a planktonic mode.<sup>54</sup> Samples (6-mm diameter × 2-mm thick) were disinfected by UV-irradiation and then placed on the wells of 96-well plates (n=6/group). *E. faecalis* were grown overnight in BHI broth in aerobic conditions at

37°C. 20 µL of the bacterial suspension ( $3 \times 10^8$  CFU/mL) was added to each well. The samples were incubated for 1 h and 24 h at 37°C. The same volume of bacterial suspension without test samples was also incubated as a control (bacterial growth). After, 1 h or 24 h, 180 µL of BHI was added in each well and soaked for 10 min. 100 µL from each well was transferred to centrifuge tubes containing 900 µL of saline solution for serial dilution. The serial dilutions were carried out in BHI agar plates. Each plate received 3×20 µL drops per dilution. The plates were incubated at 37°C for 24 h and CFU/mL counted.

**Microcosmos Biofilm.** To determine the antibiofilm properties, the hydrogels that displayed a good relationship between cell viability and antimicrobial activity (over time assays) were selected for testing. Thirty-six recently extracted and caries-free single root human teeth collected based on a local (University of Michigan, Ann Arbor, MI, USA) Institutional Review Board (HUM-00154490) were cleaned and stored in 0.1% thymol.<sup>35</sup> The teeth were cut to obtain 2-mm thick dentin slices. Briefly, the crowns were sectioned 2 mm above the cementum enamel junction, and a cut was then performed along the buccolingual plane. The specimens were wet-finished with SiC papers (600-1200 grit). The dentin slices were immersed in 2.5% NaOCl and 17% ethylenediaminetetraacetic acid solutions for 3 min each in an ultrasonic bath, rinsed in sterile saline solution for 10 min, and then autoclaved at 121°C for 20 min.<sup>36</sup> A supragingival plaque was collected from a healthy adult volunteer based on a local Institutional Review Board (HUM-00164678) and suspended in BHI broth. This suspension was incubated in an anaerobic chamber for 24 h. Then the bacterial cell amount was adjusted to  $\sim 7.5 \times 10^7$  CFU/mL in BHI broth.

The dentin slices were allocated in 24-well plates containing 1.8 ml of BHI and 0.2 mL of the inoculum and then incubated in an anaerobic chamber for 7 days to allow for biofilm formation. The broth was changed every 2 days. Infected dentin slices (n=6/group) were randomly divided into 6 groups: GelMA, 5%H, 5%H-C10%, 5%H-C20%, Ca(OH)<sub>2</sub> paste (positive control), and an untreated 7-day-old biofilm (negative control). After 7 days, the non-adherent bacteria were

removed from the samples by gently rinsing them in PBS. Then, 50  $\mu$ L of each hydrogel formulation was placed above the biofilm/dentin samples and photocrosslinked for 15 s. The samples were incubated for 7 days in the anaerobic chamber. Next, the samples were allocated to determine CFU/mL (n=4) and for SEM imaging (n=2).

For CFU/mL, the samples were carefully removed from the wells and placed in centrifuge tubes containing 1000  $\mu$ L of saline solution for serial dilution. The dilutions were carried out in BHI agar plates. The plates were incubated at 37°C for 24 h in an anaerobic chamber and the CFU/mL counted. For SEM evaluation, the samples were removed from the wells, and gently washed in PBS, and fixed overnight in 2.5% glutaraldehyde. The samples were then dehydrated in increasing concentrations of alcohol solution. After dehydration, the samples were placed in increasing concentrations of HMDS solutions. The dentin slices were then coated with Au-Pd prior to SEM imaging.<sup>56</sup>

**In vivo Biocompatibility and Biodegradation.** All animal procedures followed the ARRIVE guidelines for reporting animal research and were in accordance with the procedures of the local Institutional Animal Care and Use Committee (PRO00008502). Eight (8) 6-week-old male Fischer 344 rats (300-320 g) were allocated for the experiments (Envigo RMS, Inc., Oxford, MI, USA). All surgical procedures were performed under general anesthesia induced with inhalation isoflurane (Piramal, Pennsylvania, PA, USA) (4-5%) for induction and maintained with isoflurane (1-3%). After anesthesia, small separated subcutaneous pockets were bluntly created through short dorsal skin incisions (10-mm in length) and cylindrical-shaped samples (8-mm diameter x 3-mm thick) of GelMA, 5%H and 5%H-C10% hydrogels were implanted (n=4/group). Sham was used as a control. After wound closure, the animals were allowed to recover from anesthesia. At 7 or 14 days post-implantation, the animals were euthanized by CO<sub>2</sub> inhalation, and the implanted hydrogels were retrieved together with the surrounding peri-implantation tissue and fixed in 10% buffered formalin overnight. The fixed explanted samples were then embedded in paraffin, cut in 6  $\mu$ m-thick sections, and stained with hematoxylin and eosin (H&E) to investigate

under light microscopy the presence of luminal structures containing red blood and inflammatory cells while also assessing hydrogel degradation (Nikon E800, Shinagawa, Tokyo, Japan).<sup>44</sup>

**Statistics.** Statistical analysis was performed by one-way analysis of variance (ANOVA) and a p-value of less than 0.05 was considered to be statistically significant.

## ■ AUTHOR INFORMATION

### Corresponding Author

\*E-mail: [mbottino@umich.edu](mailto:mbottino@umich.edu)

### Notes

The authors declare no competing financial interest.

## ACKNOWLEDGMENTS

M.C.B. acknowledges the National Institutes of Health (NIH)/National Institute of Dental and Craniofacial Research (NIDCR) (Grants K08DE023552 and R01DE026578). The content is solely the responsibility of the authors and does not necessarily represent the official views of the National Institutes of Health. J.S.R. was supported in part by a scholarship from CAPES Foundation (Brazil).

## REFERENCES

- (1) N. Center for Health Statistics, NCHS Data Brief, Number 307, July 2018, 2015 2015-2016.  
[https://www.cdc.gov/nchs/data/databriefs/db307\\_table.pdf#1](https://www.cdc.gov/nchs/data/databriefs/db307_table.pdf#1).
- (2) Eramo, S.; Natali, A.; Pinna, R.; Milia, E. Dental Pulpregeneration via CellHoming. *Int. Endod. J.* 2018, 51, 405–419.
- (3) Eklund, S. A. Trends in Dental Treatment, 1992 to 2007. *J. Am. Dent. Assoc.* 2010, 141, 391–399.
- (4) Qian, W.; Ma, T.; Ye, M.; Li, Z.; Liu, Y.; Hao, P. Microbiota in the Apical Root Canal System of Tooth with Apical Periodontitis. *BMC Genomics* 2019, 20 (Suppl 2): 189.
- (5) Antunes, H. S.; Rocas, I. N.; Alves, F. R. F.; Siqueira, J. F. J. Total and Specific Bacterial Levels in the Apical Root Canal System of Teeth with Post-treatment Apical Periodontitis. *J. Endod.* 2015, 41, 1037–1042.

- (6) Narayanan, L. L.; Vaishnavi, C. Endodontic Microbiology. *J. Conserv. Dent.* 2010, 13, 233–239.
- (7) D.J. Harrington, Bacterial Collagenases and Collagen-degrading Enzymes and their Potential Role in Human Disease. *Infect. Immun.* 1996, 64, 1885–1891.
- (8) Sorsa, T.; Ingman, T.; Suomalainen, K.; Haapasalo, M.; Konttinen, Y.T.; Lindy, O.; Saari, H.; Uitto, V.J. Identification of Proteases from Periodontopathogenic Bacteria as Activators of Latent Human Neutrophil and Fibroblast-type Interstitial Collagenases. *Infect. Immun.* 1992, 60, 4491–4495.
- (9) De-Deus, G.; Barino, B.; Zamolyi, R. Q.; Souza, E.; Fonseca, A. Jr.; Fidel S.; Fidel, R. A. Suboptimal Debridement Quality Produced by the Single-file F2 Protaper Technique in Oval-shaped Canals. *J. Endod.* 2010, 36, 1897–1900.
- (10) Gomes, B. P. F. A.; Vianna, M. E.; Zaia, A. A.; Almeida, J. F. A.; Souza-Filho, F. J.; Ferraz, C. C. Chlorhexidine in Endodontics. *Braz. Dent. J.* 2013, 24, 89–102.
- (11) Marwah, N.; Dutta, S.; Singla, R. Single Visit versus Multiple Visit Root Canal Therapy. *Int. J. Clin. Pediatr. Dent.* 2008, 1, 17–24.
- (12) Mohammadi, Z. Chlorhexidine Gluconate, its Properties and Applications in Endodontics. *Iran. Endod. J.* 2008, 2, 113–25.
- (13) Barbosa-Ribeiro, M.; Arruda-Vasconcelos, R.; de-Jesus-Soares, A.; Zaia, A. A.; Ferraz, C. C. R.; de Almeida, J. F. A.; Gomes, B. P. F. A. EffectivenessofCalciumHydroxide-based Intracanal Medicationon Infectious/inflammatory Contents in Teeth with Post-treatment Apical Periodontitis. *Clin. Oral Investig.* 2019, 23, 2759–2766.
- (14) Pereira, M. S. S.; Faria, G.; Bezerra Da Silva, L. A.; Tanomaru-Filho, M.; Kuga, M. C. Rossi, M. A. Response of Mice Connective Tissue to Intracanal Dressings Containing Chlorhexidine. *Microsc. Res. Tech.* 2012, 75, 1653–1658.
- (15) Lessa, F. C. R.; Aranha, A. M. F.; Nogueira, I.; Giro, E. M. A.; Hebling, J.; Costa, C. A. S. Toxicity of Chlorhexidine on Odontoblast-like Cells. *J. Appl. Oral Sci.* 2010, 18, 50–8.
- (16) Feitosa, S. A.; Palasuk, J.; Geraldeli, S.; Windsor, L. J.; Bottino, M. C. Physicochemical and Biological Properties of Novel Chlorhexidine-loaded Nanotube-modified Dentin Adhesive. *J. Biomed. Mater. Res. B. Appl. Biomater.* 2019, 107, 868–875.
- (17) Palasuk, J.; Windsor, L. J.; Platt, J. A.; Lvov, Y.; Geraldeli, S.; Bottino, M. C. Doxycycline-loaded

Nanotube-modified Adhesives Inhibit MMP in a Dose-dependent Fashion. *Clin. Oral Investig.* 2018, 22, 1243–1252.

(18) Abdullayev, E.; Lvov, Y. Halloysite Clay Nanotubes as a Ceramic “Skeleton” for Functional Biopolymer Composites with Sustained Drug Release. *J. Mater. Chem. B*. 2013, 1, 2894–2903.

(19) Wei, W.; Minullina, R.; Abdullayev, E.; Fakhrullin, R.; Mills, D.; Lvov, Y. Enhanced Efficiency of antiseptics with Sustained Release from Clay Nanotubes. *RSC Adv.* 2014, 4, 488–494.

(20) Qi, R.; Guo, R.; Shen, M.; Cao, X.; Zhang, L.; Xu, J.; Yu, J.; Shi, X. Electrospun Poly(lactic-co-glycolic acid)/halloysite Nanotube Composite Nanofibers for Drug Encapsulation and Sustained Release. *J. Mater. Chem.* 2010, 20, 10622–10629.

(21) Rahali, K.; Ben Messaoud, G.; Kahn, C. J. F.; Sanchez-Gonzalez, L.; Kaci, M.; Cleymand, F.; Fleutot, S.; Linder, M.; Desobry, S.; Arab-Tehrany, E. Synthesis and Characterization of Nanofunctionalized Gelatin Methacrylate Hydrogels. *Int. J. Mol. Sci.* 2017, 18, E2675.

(22) Nichol, J. W.; Koshy, S. T.; Bae, H.; Hwang, C. M.; Yamanlar, S.; Khademhosseini, A. Cell-laden

Microengineered Gelatin Methacrylate Hydrogels. *Biomaterials*. 2010, 31, 5536–5544.

(23) Monteiro, N.; Thrivikraman, G.; Athirasala, A.; Tahayeri, A.; França, C. M.; Ferracane, J. L.; Bertassoni, L.E. Photopolymerization of Cell-laden Gelatin Methacryloyl Hydrogels Using a Dental Curing Light for Regenerative Dentistry. *Dent. Mater.* 2018, 34, 389–399.

(24) Paul, A.; Manoharan, V.; Krafft, D.; Assmann, A.; Uquillas, J. A.; Shin, S. R.; Hasan, A.; Hussain, M. A.; Memic, A.; Gaharwar, A. K.; Khademhosseini, A. Nanoengineered Biomimetic Hydrogels for Guiding Human Stem Cell Osteogenesis in Three Dimensional Microenvironments. *J. Mater. Chem. B*. 2016, 4, 3544–3554.

(25) Paula-Silva, F. W. G.; da Silva, L. A. B.; Kapila, Y. L. Matrix Metalloproteinase Expression in Teeth with Apical Periodontitis is Differentially Modulated by the Modality of Root Canal Treatment. *J. Endod.* 2010, 36, 231–237.

(26) Jain, A.; Bahuguna, R. Role of Matrix Metalloproteinases in Dental Caries, Pulp and Periapical Inflammation: An Overview. *J. Oral Biol. Craniofacial Res.* 2015, 5, 212–218.

- (27) Abdullayev, E.; Lvov, Y. Halloysite Clay Nanotubes for Controlled Release of Protective Agents Delivered by Ingenta, 2011, 11, 10007–10026.
- (28) Gupte, M.J.; Ma, P. X. Nanofibrous Scaffolds for Dental and Craniofacial Applications. *J. Dent. Res.* 2012, 91, 227–234.
- (29) Zhu, Y.; Zhang, Q.; Shi, X.; Han, D. Hierarchical Hydrogel Composite Interfaces with Robust Mechanical Properties for Biomedical Applications. *Adv. Mater.* 2019, 31, e1804950.
- (30) Raso, E. M. G.; Cortes, M. E.; Teixeira, K. I.; Franco, M. B.; Mohallem, N. D. S.; Sinisterra, R. D. A New Controlled Release System of Chlorhexidine and Chlorhexidine:  $\beta$ cd Inclusion Compounds Based on Porous Silica. *J. Incl. Phenom. Macrocycl. Chem.* 2010, 67, 159–168.
- (31) Sun, J.; Iakunkov, A.; Rebrikova, A. T.; Talyzin, A.V. Exactly Matched Pore Size for the Intercalation of Electrolyte Ions Determined Using the Tunable Swelling of Graphite Oxide in Supercapacitor Electrodes. *Nanoscale.* 2018, 10, 21386–21395.
- (32) Kirsch, M.; Birnstein, L.; Pepelanova, I.; Handke, W.; Rach, J.; Seltsam, A.; Schepers, T.; Lavrentieva, A. Gelatin-Methacryloyl (GelMA) Formulated with Human Platelet Lysate Supports Mesenchymal Stem Cell Proliferation and Differentiation and Enhances the Hydrogel's Mechanical Properties. *Bioeng. (Basel, Switzerland)*. 2019, 6, X.
- (33) Huang, K.; Ou, Q.; Xie, Y.; Chen, X.; Fang, Y.; Huang, C.; Wang, Y.; Gu, Z.; Wu, J. Halloysite Nanotube Based Scaffold for Enhanced Bone Regeneration. *ACS Biomater. Sci. Eng.* 2019, 5, 4037–4047.
- (34) Modaresifar, K.; Hadjizadeh, A.; Niknejad, H. Design and Fabrication of GelMA/chitosan Nanoparticles Composite Hydrogel for Angiogenic Growth Factor Delivery. *Artif. Cells, Nanomedicine Biotechnol.* 2018, 35–46, 1799–1808.
- (35) Pepelanova, I.; Kruppa, K.; Schepers, T.; Lavrentieva, A. Gelatin-Methacryloyl (GelMA) Hydrogels with Defined Degree of Functionalization as a Versatile Toolkit for 3D Cell Culture and Extrusion Bioprinting. *Bioeng. (Basel, Switzerland)*. 2018, 5.
- (36) Kayaoglu, G.; Orstavik, D. Virulence Factors of *Enterococcus faecalis*: Relationship to Endodontic Disease. *Crit. Rev. Oral Biol. Med.* 2004, 15, 308–320.
- (37) Neelakantan, P.; Romero, M.; Vera, J.; Daood, U.; Khan, A. U.; Yan, A.; Cheung, G. S. P. Biofilms in Endodontics—Current Status and Future Directions. *Int. J. Mol. Sci.* 2017, 18, E1748.

- (38) Devaraj, S.; Jagannathan, N.; Neelakantan, P. Antibiofilm Efficacy of Photoactivated Curcumin, Triple and Double Antibiotic Paste, 2% Chlorhexidine and Calcium Hydroxide Against Enterococcus faecalis In Vitro. *Sci. Rep.* 2016, 6, 24797.
- (39) Stuart, C. H.; Schwartz, S. A.; Beeson, T. J.; Owatz, C. B. Enterococcus faecalis: Its Role in Root Canal Treatment Failure and Current Concepts in Retreatment. *J. Endod.* 2006, 32, 93–98.
- (40) Sjogren, U.; Figdor, D.; Spangberg, L.; Sundqvist, G. The Antimicrobial Effect of Calcium Hydroxide as a Short-term Intracanal Dressing. *Int. Endod. J.* 1991, 24, 119–125.
- (41) Segura-Egea, J. J.; Gould, K.; Sen, B. H.; Jonasson, P.; Cotti, E.; Mazzoni, A.; Sunay, H.; Tjäderhane L, DummerPMH. European Society of Endodontontology Position Statement: The Use of Antibiotics in Endodontics. *Int. Endod. J.* 2018, 51, 20–25.
- (42) Yang, G.; Xiao, Z.; Long, H.; Ma, K.; Zhang, J.; Ren, X.; Zhang, J. Assessment of the Characteristics and Biocompatibility of Gelatin Sponge Scaffolds Prepared by Various Crosslinking Methods. *Sci. Rep.* 2018, 8, 1616.
- (43) Assmann, A.; Vegh, A.; Ghasemi-Rad, M.; Bagherifard, , S.; Cheng, G.; Sani, E. S.; Ruiz-Esparza, G. U.; Noshadi, I.; Lassaletta, A. D.; Gangadharan, S.; Tamayol, A.; Khademhosseini, A.; Annabi, A. A Highly Adhesive and Naturally Derived Sealant., *Biomaterials*. 2017, 140, 115–127.
- (44) Chen, Y. C.; Lin, R. Z.; Qi, H.; Yang, Y.; Bae, H.; Melero-Martin, J. M.; Khademhosseini, A. Functional Human Vascular Network Generated in Photocrosslinkable Gelatin Methacrylate Hydrogels. *Adv. Funct. Mater.* 2012, 22, 2027–2039.
- (45) Labow, R. S.; Tang, Y.; McCloskey, C.B.; Santerre, J.P. The Effect of Oxidation on the Enzyme-catalyzed Hydrolytic Biodegradation of Poly(urethane)s. *J. Biomater. Sci. Polym. Ed.* 2002, 13, 651–665.
- (46) McBane, J. E.; Santerre, J. P.; Labow, R. Role of Protein Kinase C in the Monocyte-derived Macrophage-mediated Biodegradation of Polycarbonate-based Polyurethanes. *J. Biomed. Mater. Res. A*. 2005, 74, 1–112.
- (47) McBane, J. E.; Santerre, J. P.; Labow, R. Effect of Phorbol Esters on the Macrophage-mediated Biodegradation of Polyurethanes via Protein Kinase C Activation and other Pathways. *J. Biomater. Sci. Polym. Ed.* 2009, 20, 437–453.

- (48) Annabi, N.; Rana, D.; Shirzaei Sani, E.; Portillo-Lara, R.; Gifford, J.L.; Fares, M. M.; Mithieux, S. M.; Weiss, A. S. Engineering a Sprayable and Elastic Hydrogel Adhesive with Antimicrobial Properties for Wound Healing. *Biomaterials*. 2017, 139, 229–243.
- (49) Sambandam, V.; Neelakantan, P. Matrix Metalloproteinases (mmp) in Restorative Dentistry and Endodontics. *J. Clin. Pediatr. Dent.* 2014, 39, 57–59.
- (50) Sakko, M.; Tjäderhane, L.; Rautemaa-Richardson, R. Microbiology of Root Canal Infections. *Prim Dent J.* 2016, 5, 84-89.
- (51) Xiao, W.; He, J.; Nichol, J. W.; Wang, L.; Hutson, C. B.; Wang, B.; Du, Y.; Fan, H.; Khademhosseini, A. Synthesis and Characterization of Photocrosslinkable Gelatin and Silk Fibroin Interpenetrating Polymer Network Hydrogels. *Acta Biomater.* 2011, 7, 2384–2393.
- (52) Van Den Bulcke; A. I.; Bogdanov, B.; De Rooze, N.; Schacht, E. H.; Cornelissen, M.; Berghmans, H. Structural and Rheological Properties of Methacrylamide Modified Gelatin hydrogels. *Biomacromolecules*. 2000, 1, 31–38.
- (53) Rosa, V.; Zhang, Z.; Grande, R.H.M.; Nör, J. E. Dental Pulp Tissue Engineering in Full-length Human Root Canals. *J. Dent. Res.* 2013, 92, 970–975.
- (54) Correa, C. F.; Santana, L.R.; Silva, R.M.; Noremburg, B.S.; Lund, R.G.; Ribeiro, J.S.; Motta, F. v.; Bomio, M. R. D.; Nascimento, R. M.; Carreño, N. L. V. Antimicrobial Activity from Polymeric Composites-based Polydimethylsiloxane/TiO<sub>2</sub>/GO: Evaluation of Filler Synthesis and Surface Morphology. *Polym. Bull.* 2017, 74, 2379–2390.
- (55) Bottino, M. C.; Albuquerque, M. T. P.; Azabi, A.; Münchow, E. A.; Spolnik, K. J.; Nör, J. E.; Edwards, P. C. A Novel Patient-specific Three-dimensional Drug Delivery Construct for Regenerative Endodontics. *J. Biomed. Mater. Res. B. Appl. Biomater.* 2019, 107, 1576–1586.
- (56) Albuquerque, M. T.; Valera, M. C.; Moreira, C. S.; Bresciani, E.; de Melo, R. M.; Bottino, M. C. Effects of Ciprofloxacin-containing Scaffolds on Enterococcus faecalis Biofilms. *J. Endod.* 2015, 41, 710–714.

## **5. ARTIGO 2**

O seguinte artigo foi formatado e será submetido à apreciação pelo periódico *Dental Materials -Fator de impacto: 4.495 (2019) Qualis A1*. Assim como o estudo anterior, ele foi desenvolvido através da cooperação internacional UFPel-UMICH, sob a orientação do professor brasileiro, Rafael Guerra Lund, e a co-supervisão estrangeira do prof. Marco Cicero Bottino.

### **GELATIN-METHACRYLATE HYDROGEL AS A DRUG-DELIVERY SYSTEM FOR CHLORHEXIDINE IN ROOT CANAL DISINFECTION**

#### **Highlights**

- Chlorhexidine-based hydrogel showed a good spectrum of action against endodontic pathogens.
- Injectable antimicrobial hydrogel for tissue engineering applications.
- Chlorhexidine-loaded methacrylate gelatin hydrogel for root canal disinfection.

#### **Abstract**

#### **Objectives**

The present study sought to synthesize a novel chlorhexidine-based hydrogel which possesses a good spectrum of action against endodontic pathogens and cell-friendly drug delivery systems for regenerative endodontics.

#### **Methods**

The CHX- modified GelMA was successfully synthesized using CHX concentrations between 0.12 and 5%. Hydrogel microstructure was evaluated by scanning electron microscopy (SEM). Swelling and Enzymatic Degradation was assessed to determine microenvironmental conditions. A compression test was performed to evaluate the influence of CHX at GelMA hydrogel mechanical properties. The antimicrobial effect and the antibiofilm effect were assessed using an agar diffusion method and a microcosms model, respectively. The biocompatibility was

evaluated by applying the extracts of the samples collected overtime on a culture of Stem Cells from Human Exfoliated Deciduous Teeth (SHEDs). Data were analyzed using One- and Two-way ANOVA, and Tukey ( $\alpha=0.05$ ).

## **Results**

The novel GelMA hydrogel with incorporation of CHX was successfully synthesized. The incorporation of CHX does not change the micromorphology of the hydrogel and swelling profiles of the sample at experimental and 15% GelMA group. Still, the CHX incorporation diminishes the degradation rate of the hydrogels and increases the compression modulus and material stiffness. Regarding antimicrobial tests, the incorporation of CHX showed a statically significant decrease in the number of bacteria colonies at 0.12 and 0.5% of concentration and completely inhibited the growth of biofilm at 1, 2 and 5% concentration. Regarding cell viability, the CHX addition at different concentrations do not lead to cytotoxic effects on SHED cells, having viability values approximately  $> 70\%$ .

## **Significance**

The addition of CHX into the GelMA showed great antimicrobial action with the potential to be used as an injectable drug-delivery system to be used in regenerative endodontics.

## Introduction

The traditional endodontic therapy involves debridement through mechanical instrumentation, disinfection of root canal, and the filling of the space, which results in apical sealing of teeth [1]. Despite the well-recognized clinical success in mature permanent teeth, the traditional endodontic treatment in immature permanent teeth is challenging for endodontics. In this case, the Calcium hydroxide ( $\text{Ca(OH)}_2$ ) or mineral trioxide aggregate (MTA) thought the apexification technique had been the most used [2]. These materials are used to treat these cases by inducing the formation of an apical barrier through the calcification of periapical tissues [3]. However, this technique is not able to induce a continuous root development, resulting in a thin dentin wall and a wide-open apice, which may lead to cervical fracture compromising the long-term integrity of the tooth [4].

In this context, regenerative endodontic therapy emerged intending to restore pulp function and the maturation of the roots of permanent immature teeth that suffered the interruption of root formation[5,6]. This technique relies on the combination of disinfection (with the use of antibiotic pastes e.g., triple antibiotic paste [TAP]) and intracanal stem cell recruitment approach thought the evoked bleeding from the periapical tissues. Nevertheless, recent studies showed these antibiotic mixtures to be cytotoxic to stem cells of apical papillae (SCAP) and Dental pulp stem cells (DPSCs) and are related to dentin discoloration, anti-angiogenic processes, and difficulty to manage[7]. Based on this, numerous *in vitro* and *in vivo* studies have been proposed to optimize the disinfection procedure during endodontic regeneration through the control drug delivery[5,7–10]. This optimization technique has been focused on maintaining the survivability and function of the SCAP and DPSCs in the periapical area, and at the same time have an efficient antimicrobial action.

Currently, CHX is considered the gold standard of antiseptics, is the most widely preventive agent researched in dentistry [11–13]. The CHX has been used in disinfection of the skin, wounds, and mucous membranes but also has been used in the areas of urology, gynecology, and otorhinolaryngology [14–16]. In dentistry, it has been widely used in the control of dental plaque and gingivitis [12]. Its use in the prevention and treatment of caries is highly consolidated[17–19]; In endodontics, it is used as an irrigating substance [20–22] and intracanal medication alone or in combination with other substances [22,23], among other uses. Although CHX is widely used, there are still some concerns about its use in endodontics and regenerative endodontics due to its controversial related cytotoxicity. To minimize this effect and better control antibiotics

release, many studies have been developing new strategies to deliver CHX into the infected site, among them nanoparticles and hydrogels[8].

Gelatin methacryloyl (GelMA) is a well-established semi-synthetic hydrogel that originated from the modification of amine-containing side groups of gelatins (Gel) with methacrylamide and methacrylate groups. GelMA has been used for tissue regeneration once it is pointed as biocompatible and useful in biological interactions [24]. The GelMA can be easily functionalized or mixed with a wide range of additives, such as antibiotics, nanotubes, and biomolecules [8,25,26]. An important feature of GelMA is the metalloproteinases (MMP) degradation sites [27]. Thus, during the periapical pathology, the higher levels of metalloproteinases will induce a faster degradation of the GelMA, leading to higher drug delivery [28,29]. However, without the presence of MMPs, the degradation of the hydrogel is lower, reducing the diffusion of the drug culminating in an on-demand delivery system.

Based on this, we synthesized a novel chlorhexidine-based hydrogel possessing a potential good spectrum of action against endodontic pathogens drug delivery systems for regenerative endodontics. We hypothesized that by combining the antimicrobial features of the CHX with the GelMA, the drug delivery would be controlled by the MMP presence.

## **2. Material and method**

### **2.1. Materials**

Chlorhexidine digluconate (20%) aqueous solution, type-A gelatin (300 bloom) from porcine skin, methacrylic anhydride (MA), Brain Heart Infusion Broth, and agar (BHI) were purchased from Sigma-Aldrich (St. Louis, MO, USA). L-glutamine, Dulbecco's phosphate-buffered saline (DPBS), alpha-modified Eagle's Medium ( $\alpha$ -MEM), fetal bovine serum (FBS), and penicillin-streptomycin were acquired from Gibco-Invitrogen (San Diego, CA, USA). Lithium phenyl-2,4,6-trimethyl-benzoyl phosphinate (LAP L0290, TCI America, Portland, OR, USA), ethylenediamine tetra-acetic acid (EDTA; Inter-Med, Inc., Racine, WI, USA), collagenase type I (Hoffman-La Roche Ltd., Basel, Switzerland), and CellTiter 96 Aqueous One Solution Reagent (Promega Corporation, Madison, WI, USA) were obtained from their respective manufacturers.

### **2.2. Gelatin Methacryloyl (GelMA) synthesis**

The GelMA synthesis was carried out, as described previously [25,27]. Type-A gelatin (10% w/v) was solubilized into DPBS, with the help of a heating plate at 50°C. Next, 8 mL of methacrylic anhydride (MA) was carefully dropped into the solution and left to react for 2 h under stirring

conditions. To interrupt the functionalization, 100ml of DPBS was added at 40°C. To remove the unreacted monomers, the solution was poured into 12-14 kDa dialysis tubing and dialyzed in DI water at 45 ± 5°C for 1 week. The water was changed twice a day. After 7 days, the solution was filtered, frozen and freeze-dried (LabconcoFreeZone 2.5L, Labconco Corporation, Kansas City, MO, USA) for 5 days, and stored at -20°C until further use.

### **2.3. GelMA with Chlorhexidine preparation**

Solutions at different concentrations (0.12, 0.5, 1, 2, and 5%) were prepared by dissolving 20% chlorhexidine digluconate solution in H<sub>2</sub>O (Lot #BCBM3595V, Sigma–Aldrich, St. Louis, MO). Then, the lyophilized GelMA was dissolved into these solutions at 15%(w/v). After dissolving, the photoinitiator (LAP) was added 0.05%(w/v) at 50°C under stirring (240 rpm) conditions; The pure GelMA was used as the control group (15% GelMA, control).

### **2.4. GelMA sample preparation**

Volumes ranging from 100-150 µL of the experimental solutions were placed in custom-made silicone molds (CutterSil Putty PLUS, Kulzer US, South Bend, IN, USA) and photocrosslinked for 15 s with curing LED light (Bluephase, Ivoclar-Vivadent, Amherst, NY, USA) with a broadband spectrum of 385-515 nm. After crosslinking, the samples were removed from their molds and stored at the fridge to be used later.

### **2.5. Chemical and Morphological characterization**

Fourier transform infrared spectroscopy in the attenuated total reflection mode (FTIR-ATR, Nicolet iS50, Thermo Fisher Scientific Inc.) was carried out to assess the presence of CHX into GelMA. The spectra of pristine CHX and GelMA as well as GelMA containing the different amounts of CHX, were collected in the 400-4000 cm<sup>-1</sup> range with a resolution of 4 cm<sup>-1</sup> (64 scans).

The micromorphology and pores size of GelMA hydrogels was evaluated by scanning electron microscopy (SEM, Tescan MIRA3 FEG-SEM, Tescan USA Inc., Warrendale, PA, USA). Cylindrical-shaped (6-mm diameter and 10-mm thick) samples of all groups were prepared, as previously described. Then, samples were freeze-dried, cross-sectioned, and coated with Au-Ps by sputtering. The images were obtained in a Tescan Rise microscope (Tescan Orsay Holding, Kohoutovice, CZ) with secondary electrons detector. The pores diameter was analyzed using software Image J (National Institute of Health NIH).

## **2.6. Swelling and Enzymatic Degradation**

The swelling capacity of GelMA-based hydrogels was performed as previously described in a recent study [8]. First, samples (6 mm in diameter  $\pm$  2 mm in thickness, n = 3 / group) of hydrogels were poured into distilled water at 37 ° C for 24 h. After this period, wet samples were dried using tissue paper with low fiber content (Kimberly-Clark, Irving, TX, USA) and weighed on an analytical balance to obtain the 'wet weight' (W<sub>w</sub>). The specimens were then freeze-dried to determine the 'dry weight' (W<sub>d</sub>). The swelling rate (%) was calculated as (W<sub>w</sub>-W<sub>d</sub>) / W<sub>d</sub> × 100. For the evaluation of the degradation rate, samples similar to those used in the swelling methodology (n = 4/group) were incubated in glass flasks (VWR International, LLC, Radnor, PA, USA) with 5 mL of distilled water containing 1U / mL of type I collagenase at 37 ° C. To ensure the enzymatic activity of collagenase, solutions enriched with collagenase were replaced with new ones every 3 days. At predetermined intervals of up to 28 days, the samples were removed from the collagenase water solution, slightly dried using low-content tissue paper fiber, and weighed on a digital analytical balance. The hydrogel degradation ratio was calculated using the following equation:

$$\text{Degradation ratio (\%)} = \frac{W_t}{W_0} \times 100$$

(where W<sub>t</sub> is the residual wet weight at different points in time, and W<sub>0</sub> is the initial wet weight × 100).

## **2.7. Biomechanical Testing**

Mechanical properties are fundamental parameters to consider when developing hydrogel for biomedical uses [30,31]. To evaluate the influence of CHX addition in the compressive modulus cylindrical-shaped samples (8 mm in diameter  $\pm$  3 mm in thickness) were made, and a group of 15 % GelMA hydrogel without CHX was used as a control. The samples (n=12/group) were incubated in distilled water for 24h at 37°C. Then, the samples were blot-dried and subjected to unconfined compression at room temperature. It used a strain rate of 2 mm/min (expert 5601, ADMET Inc., Norwood, MA, USA). The compressive modulus was calculated as the slope of the linear region of the stress-strain curves corresponding with 0-6% strain.

## **2.8. Cytotoxicity**

The evaluation of the CHX based hydrogels effect on cells was evaluated using MTT cell viability assay, following the International Standards Organization guidelines (ISO10993-5: Tests for Cytotoxicity—In Vitro Methods). Samples (6 mm in diameter  $\pm$  2 mm in thickness, n = 6 / group) were prepared and sterilized by a UV treatment (30 min on each side). Then, the samples were placed in sterile glass vials containing 5 mL of alpha minimum essential medium supplemented with 10% fetal bovine serum, L-glutamine, and 1% penicillin-streptomycin and incubated at 37°C. At predetermined time points up to 14 days, aliquots of 500 $\mu$ L were collected, and equal amounts were added back to each vial to keep the initial volume constant. The extracts were frozen to determine the cytotoxicity over time. Before using the extracts were filtered in a 0.22- $\mu$ m membrane.

SHEDs kindly donated by Dr. Jacques Nör (University of Michigan, School of Dentistry, Ann Arbor, MI, USA), were cultured in an incubator at 37°C, with 5% CO<sub>2</sub> in 96-well plates in the previously mentioned media. Cell passage number 5 was used. SHEDs were seeded at a density of 5x10<sup>3</sup> cells/well and allowed to adhere for 24 h. At 24 h, each well was washed with 100  $\mu$ L of PBS to remove the non-adhered and died cell. Then, the media was replaced by the collected extracts (100  $\mu$ L) from the hydrogels and kept in contact with the cells for 24 h. Subsequently, 20  $\mu$ L of CellTiter 96 Aqueous One Solution Reagent was added to the test wells and allowed to react for 4h at 37°C in a humidified 5% CO<sub>2</sub> atmosphere. The incorporated dye was measured by reading the absorbance at 490 nm (SpectraMax iD3, Molecular Devices, LLC, San Jose, CA, USA) against a blank column. SHEDs cultured in complete  $\alpha$ -MEM were used as a positive control. Absorbance values were converted to a percentage and compared with the values obtained for the test groups.

## 2.9. Antimicrobial effect

### 2.9.1. Disc diffusion Method

Chlorhexidine antimicrobial properties are well known, in this study to measure antimicrobial properties of the hydrogel as a function of the chlorhexidine concentration, two evaluations were made, direct contact – agar diffusion assay and Biofilm of microcosms with CFU.

For agar diffusion assay evaluation, 6 samples (Cylindrical-shaped 6-mm diameter, 2-mm thick) from each group were prepared, these were placed under UV light radiation for 30 min each side. The agar diffusion was tested against *Actinomyces naeslundii* (A.naeslundii, ATCC 12104), and *Enterococcus faecalis* (E. faecalis, ATCC 19433). The bacterial suspension was adjusted to obtain a 3  $\times$  10<sup>8</sup> colony-forming unit (CFU/mL). Then, 100  $\mu$ L of each bacteria broth was swabbed onto the agar plates to form a bacterial lawn. The agar plates containing the

microorganisms were divided into 4 zones, 3 of these the GelMA samples and in one zone, 10 µL of with 2% CHX in water (positive control). After the time point incubation for each bacterium, the diameters of the halos were measured in millimeters.

#### **2.9.2. Antibiofilm Assay (CFU/mL)**

A microcosm biofilm model was used to determine the antibiofilm effect of the formulations. In this assay, a supragingival plaque of healthy adults was collected and suspended in BHI Broth. This suspension was incubated for 24 h in an anaerobic chamber (10% CO<sub>2</sub>). The bacterial cell suspension was adjusted to ~ 7.5 × 10<sup>7</sup>CFU/mL in BHI broth, 300 ul were placed at a 24 well plate, and taken to the incubator at 37°C for 2h to allow the formation of a layer of biofilm adhered to the bottom of the plate. After 2h, samples (2 from each group) at transwell were placed, 1500 ul of sterile BHI was added, and samples were incubated for 24 h. After 24 hours, the samples and the transwell were carefully removed, and 100 ul of each well were taken and placed in an Eppendorf containing 900 ul of saline solution for serial dilution. The dilution was seeded in BHI agar plates and incubated at 37°C for 24 h in an anaerobic chamber. Lastly, the CFU/mL counted[32].

#### **2.10 Statistics**

Statistical analysis was performed by one-way analysis of variance (ANOVA) and a p-value of less than 0.05 was considered to be statistically significant.

### **3. Results**

#### **3.1. Chemical and Morphological characterization**

The morphological features of the experimental hydrogels were evaluated by SEM. Figure 1 shows a highly porous structure, with a honeycomb structure at all groups. At all samples, honeycomb morphology can be observed, with porous size ranges from 15 to 100 µm. No statistical differences were observed between the pore size and the pore distribution of the CHX concentration at GelMA hydrogel.

The FTIR spectra for CHX, GelMA and CHX-GelMA are presented in Figure2. All the hydrogel spectra (GelMA and GelMA with different concentrations of CHX) showed a similar spectrum. GelMA hydrogel is obtained from a modification of gelatin with methacrylate anhydride. Among

$1645\text{ cm}^{-1}$ , a significant peak related to amide I, primarily C=O stretching groups, appears. The band around  $1540\text{ cm}^{-1}$  corresponds to C–N–H and C–H  $1473\text{ cm}^{-1}$ [24,33].

### **3.2. Swelling and Enzymatic Degradation**

Figure 3 shows the mass loss through 28 days of the GelMA and GelMA/CHX hydrogels. The results indicated that the modification with CHX at GelMA hydrogel dramatically reduced its mass loss ratio. As can be observed, the degradation rate in the first 7 days is the statistical equivalent in all groups and degrades around 25% of the samples. After that, the 15% GelMA completely degrades at 28 days in a constant ratio, and the groups with CHX remain constant, showing a mass ranging from  $79.1 \pm 9.9$  to  $65.5 \pm 24.8$ , which is a significant difference ( $p < .05$ )—indicating a substantial increase of GelMA hydrogel stability with CHX presence without the dependency of concentration.

The swelling features of the experimental groups (Figure 4) were not statistically different from the control group (GelMA without modification), which is consistent with the pore size, distribution, and concentration SEM analysis. After 24 hours, the groups showed swelling rates ranging from  $11.7 \pm 0.8$  (control group) to  $9.7 \pm 0.6$  (2%CHX).

### **3.3. Biomechanical Testing**

They must be biocompatible as well as have enough strength to stay in place for a reasonable time. Figure 5, (a) showed a stress-strain curve where can be observed two distinct regimes; the first one an elastic region (0 - 6%) described as a linear response of the compressibility by applying external hydrostatic pressure. In this regime, it is possible to obtain the compressive modulus, and in the second regime there is a non-linear deformation regime. The Figure 5 (b) represents the compressive modulus of groups. The data shows an increase of modulus is related to the amount of CHX at samples; GelMA hydrogel with 5% CHX presents a compressive modulus 2.3 times larger than the bare GelMA. The increase of this modulus is associated with stiffness of the material, indicating that the presence of CHX improves GelMA hydrogel biomechanical properties.

### **3.4. Cytotoxicity**

Cytotoxicity assays are essential to evaluate and determine the cytocompatibility of biomaterial. The cytotoxicity of CHX hydrogel in contact with SHEDs by MTS assay was investigated after 24 hours of exposure to the aliquots collected on 1, 7, and 15 days for all concentrations. The results of cell viability (Figure 6) showed that different concentrations of the CHX analyzed had no cytotoxic effects on SHED cells, having viability values approximately > 70%. The day 15 aliquot of 0.12% CHX showed the higher cell viability in comparison to other CHX concentration, while 5% CHX at day 1 showed lowest cell viability percentage.

### **3.5. Antimicrobial effect**

As can be seen in Figure 7a and b, presents the antimicrobial data for agar diffusion essay. Overall, all CHX-containing demonstrated significant growth inhibition of *E. faecalis* and *A. naeslundii*). Importantly, the inhibition zones were more pronounced in the largest concentrations.

Regarding the biofilm results (Figure 7c), the groups of GelMA hydrogel at concentrations of 1, 2, and 5% completely inhibited the growth of the biofilm. Moreover, the experimental groups with a lower concentration of CHX also showed a significant decrease among colonies, and all groups containing CHX presented a statistic difference with Bacteria control and GelMA without CHX.

## **4. Discussion**

The present study sought to synthesize a novel chlorhexidine-based hydrogel which possesses a good spectrum of action against endodontic pathogens, is cell friendly and has on-demand intracanal drug delivery systems for regenerative endodontics. GelMA hydrogel physical properties such as morphology, porosity, swelling, degradation, and mechanical properties are influenced by a polymer crosslinking and are related with cell behavior[34].

Three-dimensional tissue scaffold used in tissue engineering must have an interconnected and porous structure with an acceptable range of porous size to provide the ideal environment for cell proliferation and nutrients diffusion [35,36]. It is possible to observe an interconnect porous structure(Figure3), similar to a honeycomb-like structure [8,27,34], ideal for cellular growth and proliferation, indicating that CHX inclusion did not affect the morphology of the samples. At chemical analysis, it was possible to identify peaks related to vibrational bands of GelMA, as

previously shown. Nevertheless, vibration bands of CHX were not easy to categorize. This can be explained due to (i) the overlapping peaks of GelMA and CHX, and (ii) for this study were used gluconate de chlorhexidine, as this administration form has high water concentration, it was possible to observe H-O band ( $3000\text{-}3400\text{ cm}^{-1}$ ) associated to water, at CHX and all GelMA with CHX spectrum. Another evidence of CHX incorporation at samples is the microbial results, which showed excellent properties.

These results can also be confirmed by swelling profile evaluation, where no difference was found between the experimental groups with and the GelMA group. Swelling is directly related to the network and porous structure, once the interstitial volume and pores size have intime correlation [37–39]. Further, the swelling profile evaluation of the scaffolds is essential as the maintenance of a specific amount of water in the scaffolds is directly related to the nutritional supply of the cells [40]. GelMA is well known for its excellent ability to be used as scaffold[8,35,41], and as in this study no statistical difference was found between the experimental groups and the GelMA group, indicating that the tested percentages used of CHX do not chance this important characteristic of GelMA.

Collagenases play an important role in the periapical tissue destruction during the development of periapical lesions. When the collagenase enzyme is added to the water, it cleaves the gelatin chains [22,23].MMPs are similar to collagenase in their ability to cleave gelatin. As a result, the GelMA are MMP-sensitive and, based on this; the collagenase type 1 was used for the degradation essay. The incorporation of CHX in the GelMA resulted in a dramatic decrease in the degradation rate when compared to the control group. The same pattern was observed in a previous study where the incorporation of nanotubes functionalized with CHX was added into GelMA solutions at different concentrations and significantly reduced the degradation rate of GelMA. The stability of hydrogels for these applications is important; as degradation time of the material increases, the drug delivery at the region will increase as well.

Taken together, the evaluation of themorphology, porosity, swelling, degradation, and mechanical properties give to usan idea if the addition of a particular subststation may impair or improve the properties of these material [30,42]. In the field of tissue engineering, mechanical properties play an essential role in cellular behavior; injectable hydrogels provide ultimate flexibility in targeted drug delivery and tissue engineering systems[30]. It was observed an increase in sample stiffness is correlated to CHX concentration. As can be seen in Figure 5 (b) we have a significant increase between the compression module between the group 2% CHX and 5% CHX compared to the increase of the bare GelMA until 2% CHX, suggesting that from 2% CHX is no longer doped and becomes part of the structure of the material, causing

significant changes in their mechanical properties. Analysis of our cell viability data for hydrogel with different CHX concentration in compliance with UNI EN ISO 10993 regulation for toxicity of biomaterial has shown that cells have viability close to or above 70%, deeming that hydrogel is safe for endodontic application. While this study has not examined the kinetics of drug release, increase viability of cells over time might be associated with the pattern of antibiotic release i.e burst release, followed by sustained release of the drug from the hydrogel.

The literature has already shown that the presence of the previous infection can negatively affect the pulp tissue regeneration process, damaging tissue-forming cells, as well as stem cells in periapical tissues [43]. The most prevalent bacteria in cases of persistent infection are *E. faecalis*[18]. They are small enough for proficiently invading and living within dentinal tubules as single, in pairs, or as short chains. They can endure prolonged periods of starvation until an adequate nutritional supply becomes available. The analysis of antimicrobial properties reveals that this material is highly efficient, significantly inhibiting *E. faecalis* and *A. naeslundii*, when in contact of all CHX-containing hydrogels in 24 hours. Our data are in accordance with a previous study, where the use of CHX in a drug delivery system was more effective against *E. faecalis* and *A. naeslundii* [8].

It is a concern that, when bacteria are in the form of microbial biofilms, they are highly resistant to antibiotics due to the intrinsic protection offered by extracellular polymeric substances. In order to provide an approach closer to the clinical reality and at the same time provide a more complex antimicrobial assessment. We also evaluated the antimicrobial action against a biofilm model (Figures 7c). After 1 week of treatment, an antimicrobial efficacy was evaluated by means of the colony forming unit assay.

Here we assess the antimicrobial activity against a monoculture *E. faecalis* biofilm once the root canal infections are biofilm mediated. Also, *E. faecalis* are highly associated with secondary endodontic infection and can colonize the root canal and resist the chemical mechanical instrumentation. In a more complex biofilm model, the 1, 2 and 5% CHX hydrogels completely inhibited the bacterial growth (Figure 7c).

We hypothesize that this system has promising features when compared to the conventional treatments the TAP paste and the Ca(OH)<sub>2</sub>. It is well known that the combination of antimicrobial agents can lead to an increase in the risk of adverse effects, antagonism, and bacterial resistance, and systemic allergic reaction[44,45]. Also, the components of the TAP paste into the root canal system may impair angiogenesis and, consequently, the result of

regenerative endodontics[46].Regarding calcium hydroxide, the literature has already shown that it has limited antimicrobial efficacy as an intracanal dressing [47]. Also, the Ca(OH)<sub>2</sub>, may have some effects of calcium hydroxide on the biological property of growth factors derived from the dentinal matrix that also need to be investigated in RET[48].

In this way, CHX has been pointed out as having good potential to be used as intracanal medication. The CHX has been related to possessing the ability to ablate periapical inflammation. However, this ability is directly related to the dose of this drug. Thus, our results suggest that it is further needed to better control the release of the CHX and maintain the antimicrobial effect.

## 5. Conclusion

In this study, a new GelMA hydrogel with CHX presence was investigated as a promising candidate for endodontic treatment of mature teeth. As an outstanding characteristic of this material application, the novel hydrogel presented a lower degradation rate prolonging the drug delivery in the area. The swelling profile was similar to GelMA and displayed the same mechanical behavior of GelMA, with an increase of stiffness associated with an increase of CHX, in addition to good antimicrobial properties and promising cytocompatibility.

## References

- [1] De Rossi A, Silva LAB, Leonardo MR, Rocha LB, Rossi MA. Effect of rotary or manual instrumentation, with or without a calcium hydroxide/1% chlorhexidine intracanal dressing, on the healing of experimentally induced chronic periapical lesions. *Oral Surgery, Oral Med Oral Pathol Oral Radiol Endodontology* 2005;99:628–36. <https://doi.org/10.1016/j.tripleo.2004.07.018>.
- [2] Diogenes A, Ruparel NB. *Regeneration in Endodontic Procedures: Clinical Outcomes*. Dent Clin NA 2019;61:111–25. <https://doi.org/10.1016/j.cden.2016.08.004>.
- [3] Damle SG, Bhattacharjee H, Loomba A. Apexification of anterior teeth. *J Clin Pediatr Dent* 2012;36:263–8. <https://doi.org/10.17796/jcpd.36.3.02354g044271t152>.
- [4] Cvek M. Prognosis of luxated non-vital maxillary incisors treated with calcium hydroxide and filled with gutta-percha. A retrospective clinical study. *Endod Dent Traumatol* 1992;8:45–55.
- [5] Albuquerque MTP, Valera MC, Nakashima M, Nör JE, Bottino MC. *Tissue-engineering-*

based strategies for regenerative endodontics. *J Dent Res* 2014;93:1222–31.  
<https://doi.org/10.1177/0022034514549809>.

[6] Ruparel NB, Teixeira FB, Ferraz CCR, Diogenes A. Direct effect of intracanal medicaments on survival of stem cells of the apical papilla. *J Endod* 2012;38:1372–5.  
<https://doi.org/10.1016/j.joen.2012.06.018>.

[7] Porter MLA, Münchow EA, Albuquerque MTP, Spolnik KJ, Hara AT, Bottino MC. Effects of Novel 3-dimensional Antibiotic-containing Electrospun Scaffolds on Dentin Discoloration. *J Endod* 2016;42:106–12. <https://doi.org/10.1016/j.joen.2015.09.013>.

[8] Ribeiro JS, Bordini EAF, Ferreira JA, Mei L, Dubey N, Fenno JC, et al. Injectable MMP-Responsive Nanotube-Modified Gelatin Hydrogel for Dental Infection Ablation. *ACS Appl Mater Interfaces* 2020;12:16006–17. <https://doi.org/10.1021/acsami.9b22964>.

[9] Bottino MC, Albuquerque MTP, Azabi A, Münchow EA, Spolnik KJ, Nör JE, et al. A novel patient-specific three-dimensional drug delivery construct for regenerative endodontics 2018;1–11. <https://doi.org/10.1002/jbm.b.34250>.

[10] Albuquerque MTP, Nagata J, Bottino MC. Antimicrobial Efficacy of Triple Antibiotic-eluting Polymer Nanofibers against Multispecies Biofilm. *J Endod* 2017;43:S51–6.  
<https://doi.org/10.1016/j.joen.2017.06.009>.

[11] Balagopal S, Arjunkumar R. Chlorhexidine: The gold standard antiplaque agent. *J Pharm Sci Res* 2013;5:270–4.

[12] Saleem HGM, Seers CA, Sabri AN, Reynolds EC. Dental plaque bacteria with reduced susceptibility to chlorhexidine are multidrug resistant. *BMC Microbiol* 2016;16:1–9.  
<https://doi.org/10.1186/s12866-016-0833-1>.

[13] Haseeb R, Lau M, Sheah M, Montagner F, Quiram G, Palmer K, et al. Synthesis and characterization of new chlorhexidine-containing nanoparticles for root canal disinfection. *Materials (Basel)* 2016;9. <https://doi.org/10.3390/ma9060452>.

[14] Dyer JE, Taktak SY, Parkes AW, Garcez T, Gall Z. Chlorhexidine-related anaphylaxis in urological practice. *J Clin Urol* 2019;12:32–8. <https://doi.org/10.1177/2051415818788244>.

[15] Stone J, Bianco A, Monro J, Overbey JR, Cadet J, Choi KH, et al. Study To Reduce Infection Prior to Elective Cesarean Deliveries (STRIPES): A randomized clinical trial of chlorhexidine. *Am J Obstet Gynecol* 2020. <https://doi.org/10.1016/j.ajog.2020.05.021>.

- [16] Lakshmanan V, M. K. G, Karnaker V, Aroor R, Kamath P. S, Bhat V, et al. Prospective study on sterilization of rigid endoscopes in various otolaryngology clinics. *Int J Otorhinolaryngol Head Neck Surg* 2017;3:376. <https://doi.org/10.18203/issn.2454-5929.ijohns20171196>.
- [17] Solderer A, Kaufmann M, Hofer D, Wiedemeier D, Attin T, Schmidlin PR. Efficacy of chlorhexidine rinses after periodontal or implant surgery: a systematic review. *Clin Oral Investig* 2019;23:21–32. <https://doi.org/10.1007/s00784-018-2761-y>.
- [18] Al-Maweri SA, Nassani MZ, Alaizari N, Kalakonda B, Al-Shamiri HM, Alhajj MN, et al. Efficacy of aloe vera mouthwash versus chlorhexidine on plaque and gingivitis: A systematic review. *Int J Dent Hyg* 2020;18:44–51. <https://doi.org/10.1111/idh.12393>.
- [19] McGrath C, Zhou N, Wong HM. A systematic review and meta-analysis of dental plaque control among children and adolescents with intellectual disabilities. *J Appl Res Intellect Disabil* 2019;32:522–32. <https://doi.org/10.1111/jar.12561>.
- [20] Ferraz CCR. In vitro assessment of the antimicrobial action and the mechanical ability of chlorhexidine gel as an endodontic irrigant. *J Endod* 2001;27:452–5. <https://doi.org/10.1097/00004770-200107000-00004>.
- [21] Tervit C, Paquette L, Torneck CD, Basrani B, Friedman S. Proportion of Healed Teeth With Apical Periodontitis Medicated With Two Percent Chlorhexidine Gluconate Liquid: A Case-Series Study. *J Endod* 2009;35:1182–5. <https://doi.org/10.1016/j.joen.2009.05.010>.
- [22] Gonc LS, Costa R, Rodrigues V, Vieira C, Junior A, Soares RG, et al. The Effect of Sodium Hypochlorite and Chlorhexidine as Irrigant Solutions for Root Canal Disinfection : A Systematic Review of Clinical Trials 2016;42:527–32. <https://doi.org/10.1016/j.joen.2015.12.021>.
- [23] Saatchi M, Shokraneh A, Navaei H, Maracy MR, Shojaei H. Antibacterial effect of calcium hydroxide combined with chlorhexidine on Enterococcus faecalis: A systematic review and meta-analysis. *J Appl Oral Sci* 2014;22:356–65. <https://doi.org/10.1590/1678-775720140032>.
- [24] Rahali K, Ben Messaoud G, Kahn CJF, Sanchez-Gonzalez L, Kaci M, Cleymand F, et al. Synthesis and characterization of nanofunctionalized gelatin methacrylate hydrogels. *Int J Mol Sci* 2017;18. <https://doi.org/10.3390/ijms18122675>.
- [25] Nichol JW, Koshy ST, Bae H, Hwang CM, Yamanlar S, Khademhosseini A. Cell-laden microengineered gelatin methacrylate hydrogels. *Biomaterials* 2010;31:5536–44.

<https://doi.org/10.1016/j.biomaterials.2010.03.064>.

[26] Tamayol A, Annabi N, Khademhosseini A. Biomaterials Synthesis , properties , and biomedical applications of gelatin methacryloyl ( GelMA ) hydrogels 2015;73:254–71.  
<https://doi.org/10.1016/j.biomaterials.2015.08.045>.

[27] Monteiro N, Thrivikraman G, Athirasala A, Tahayeri A, França CM, Ferracane JL, et al. Photopolymerization of cell-laden gelatin methacryloyl hydrogels using a dental curing light for regenerative dentistry. Dent Mater 2018;34:389–99.  
<https://doi.org/10.1016/j.dental.2017.11.020>.

[28] Paula-Silva FWG, da Silva LAB, Kapila YL. Matrix Metalloproteinase Expression in Teeth with Apical Periodontitis Is Differentially Modulated by the Modality of Root Canal Treatment. J Endod 2010;36:231–7. <https://doi.org/10.1016/j.joen.2009.10.030>.

[29] Jain A, Bahuguna R. Role of matrix metalloproteinases in dental caries, pulp and periapical inflammation: An overview. J Oral Biol Craniofacial Res 2015;5:212–8.  
<https://doi.org/10.1016/j.jobcr.2015.06.015>.

[30] Vedadghavami A, Minooei F, Mohammadi MH, Khetani S, Rezaei Kolahchi A, Mashayekhan S, et al. Manufacturing of hydrogel biomaterials with controlled mechanical properties for tissue engineering applications. Acta Biomater 2017;62:42–63.  
<https://doi.org/10.1016/j.actbio.2017.07.028>.

[31] Oyen ML. Mechanical characterisation of hydrogel materials. Int Mater Rev 2014;59:44–59. <https://doi.org/10.1179/1743280413Y.0000000022>.

[32] Moon C-Y, Nam OH, Kim M, Lee H-S, Kaushik SN, Cruz Walma DA, et al. Effects of the nitric oxide releasing biomimetic nanomatrix gel on pulp-dentin regeneration: Pilot study. PLoS One 2018;13:e0205534. <https://doi.org/10.1371/journal.pone.0205534>.

[33] Sadeghi M, Heidari B. Crosslinked graft copolymer of methacrylic acid and gelatin as a novel hydrogel with ph-responsiveness properties. Materials (Basel) 2010;4:543–52.  
<https://doi.org/10.3390/ma4030543>.

[34] Athirasala A, Lins F, Tahayeri A, Hinds M, Smith AJ, Sedgley C, et al. A Novel Strategy to Engineer Pre-Vascularized Full-Length Dental Pulp-like Tissue Constructs. Sci Rep 2017;7:1–11. <https://doi.org/10.1038/s41598-017-02532-3>.

[35] Kutlusoy T, Oktay B, Apohan NK, Süleymanoğlu M, Kuruca SE. Chitosan-co-Hyaluronic

acid porous cryogels and their application in tissue engineering. *Int J Biol Macromol* 2017;103:366–78. <https://doi.org/10.1016/j.ijbiomac.2017.05.067>.

[36] Kathuria N, Tripathi A, Kar KK, Kumar A. Synthesis and characterization of elastic and macroporous chitosan-gelatin cryogels for tissue engineering. *Acta Biomater* 2009;5:406–18. <https://doi.org/10.1016/j.actbio.2008.07.009>.

[37] Nicodemus GD, Bryant SJ. Cell encapsulation in biodegradable hydrogels for tissue engineering applications. *Tissue Eng - Part B Rev* 2008;14:149–65. <https://doi.org/10.1089/ten.teb.2007.0332>.

[38] Wahid F, Hu XH, Chu LQ, Jia SR, Xie YY, Zhong C. Development of bacterial cellulose/chitosan based semi-interpenetrating hydrogels with improved mechanical and antibacterial properties. *Int J Biol Macromol* 2019;122:380–7. <https://doi.org/10.1016/j.ijbiomac.2018.10.105>.

[39] Guo B, Finne-Wistrand A, Albertsson AC. Facile synthesis of degradable and electrically conductive polysaccharide hydrogels. *Biomacromolecules* 2011;12:2601–9. <https://doi.org/10.1021/bm200389t>.

[40] Huang K, Ou Q, Xie Y, Chen X, Fang Y, Huang C, et al. Halloysite Nanotube Based Scaffold for Enhanced Bone Regeneration. *ACS Biomater Sci Eng* 2019;5:4037–47. <https://doi.org/10.1021/acsbiomaterials.9b00277>.

[41] Ha M, Athirasala A, Tahayeri A, Menezes PP, Bertassoni LE. Micropatterned hydrogels and cell alignment enhance the odontogenic potential of stem cells from apical papilla in-vitro. *Dent Mater* 2020;36:88–96. <https://doi.org/10.1016/j.dental.2019.10.013>.

[42] Sun M, Sun X, Wang Z, Guo S, Yu G, Yang H. Synthesis and properties of gelatin methacryloyl (GelMA) hydrogels and their recent applications in load-bearing tissue. *Polymers (Basel)* 2018;10. <https://doi.org/10.3390/POLYM10111290>.

[43] Kim SG. Infection and Pulp Regeneration 2016. <https://doi.org/10.3390/dj4010004>.

[44] Barnes GW, Langeland K. Antibody Formation in Primates Following Introduction of Antigens into the Root Canal. *J Dent Res* 1966;45:1111–4. <https://doi.org/10.1177/00220345660450041501>.

[45] Rybak MJ, McGrath BJ. Combination antimicrobial therapy for bacterial infections. Guidelines for the clinician. *Drugs* 1996;52:390–405. <https://doi.org/10.2165/00003495-000000000-00000>

199652030-00005.

- [46] Dubey N, Xu J, Zhang Z, Nör JE, Bottino MC. Comparative Evaluation of the Cytotoxic and Angiogenic Effects of Minocycline and Clindamycin: An In Vitro Study. *J Endod* 2019;45:882–9. <https://doi.org/10.1016/j.joen.2019.04.007>.
- [47] Sathorn C, Parashos P, Messer H. Antibacterial efficacy of calcium hydroxide intracanal dressing : a systematic review and 2007:2–10. <https://doi.org/10.1111/j.1365-2591.2006.01197.x>.
- [48] Bose R, Nummikoski P, Hargreaves K. A Retrospective Evaluation of Radiographic Outcomes in Immature Teeth With Necrotic Root Canal Systems Treated With Regenerative Endodontic Procedures. *J Endod* 2009;35:1343–9. <https://doi.org/10.1016/j.joen.2009.06.021>.

## List of figures

### Graphical Abstract

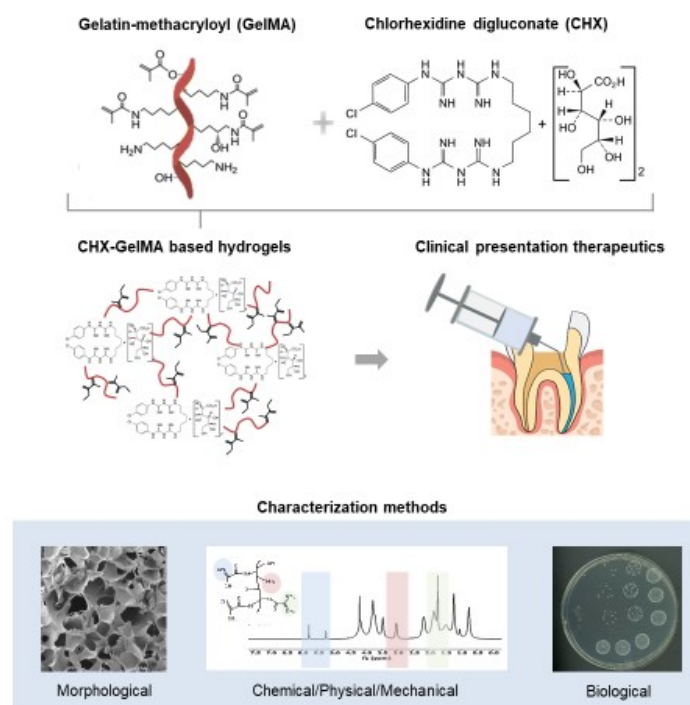


**Figure 1**

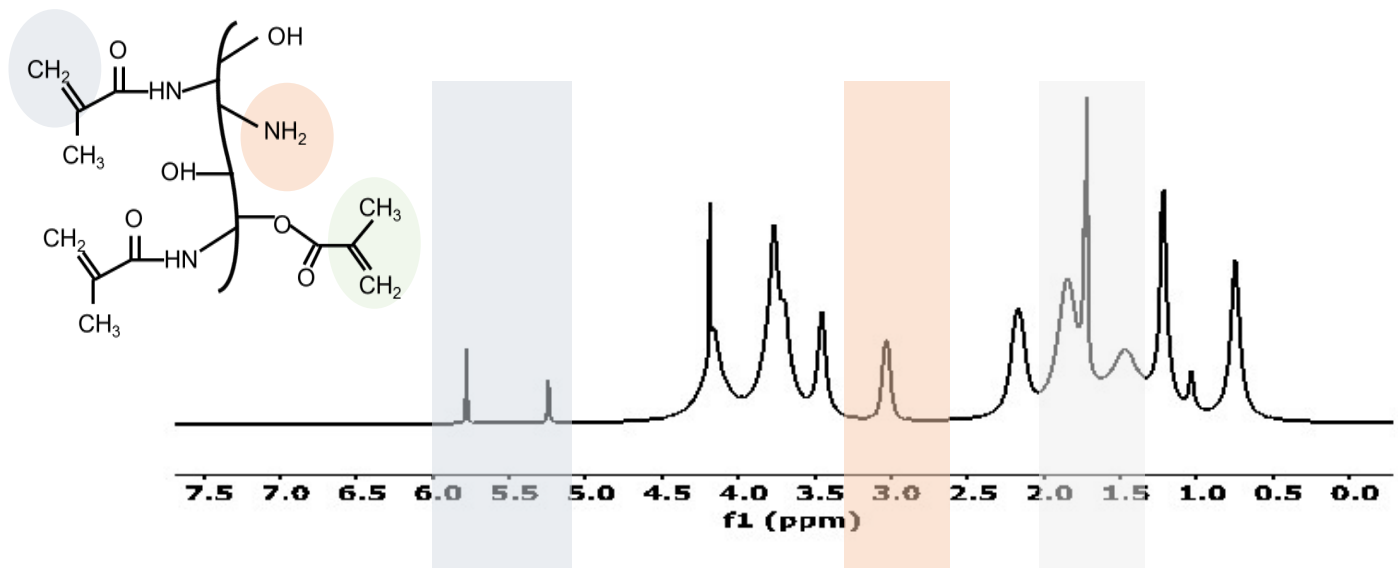


Figure 1. A)  $^1\text{H}$  NMR spectra of GelMA shows the areas of interest between 5.3 and 5.6 ppm and between 1.5 and 2 ppm of the methacryloyl groups incorporated into the gelatin. The signal at 3 ppm is due to the lysine methylene from gelatin.  $^1\text{H}$  NMR: proton nuclear magnetic resonance; GelMA: gelatin methacryloyl.

**Figure 2**

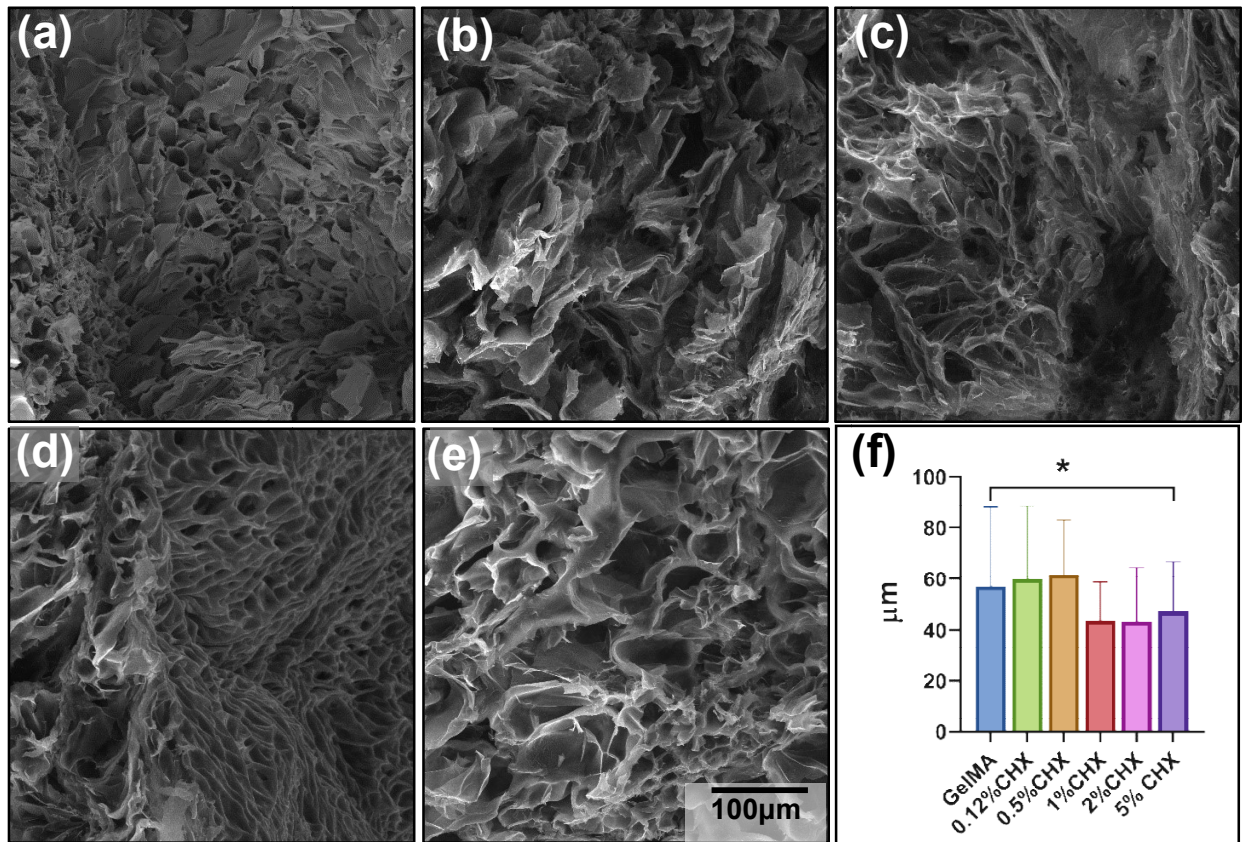


Figure 2: Morphology evaluation of the CHX based hydrogels. SEM micrograph of the GelMA and CHX based hydrogels cross-sectioned. (a) GelMA Hydrogel; (b) 0.5% CHX; (c) 1% CHX; (d) 2% CHX and (e) 5% CHX; (f) Porous size measurement; Asterisks (\*) indicates no statistical difference between the groups.

**Figure 3**

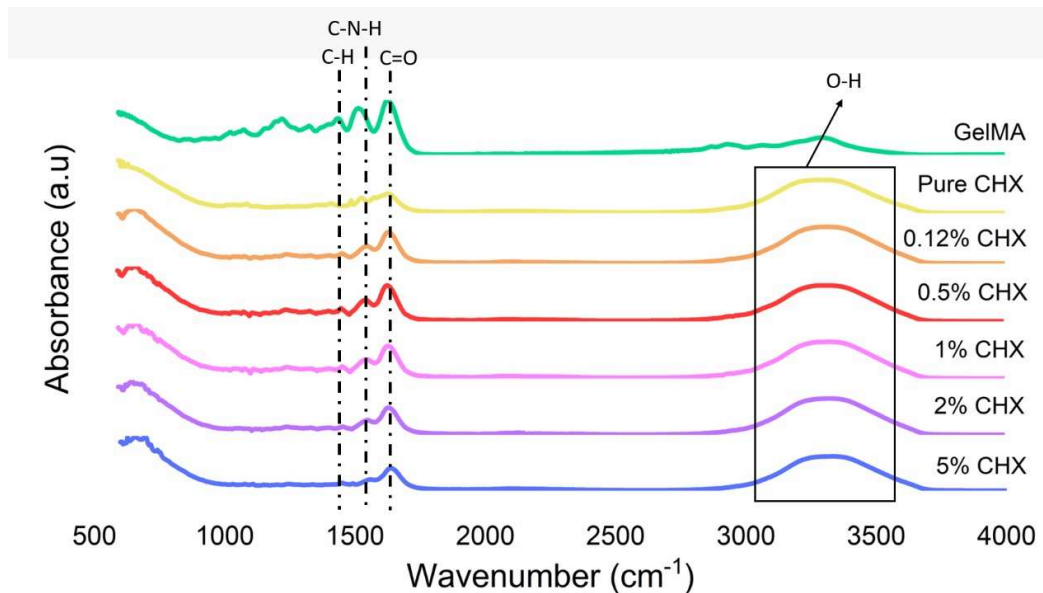


Figure 3: FTIR spectra of pristine GelMA and CHX and GelMA with the different concentrations of CHX.

**Figure 4**

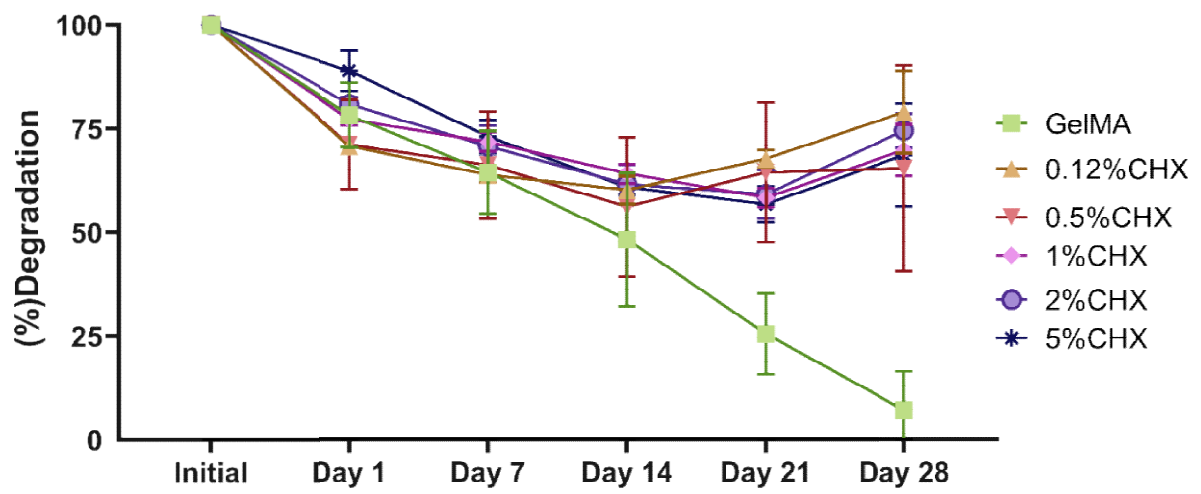


Figure 4: Mass loss of GelMA and CHX based hydrogels in the enzymatic degradation along 28 days. In vitro biodegradation of all groups in DI water containing 1U/mL of collagenase type I at 37°C. The results are presented as mean  $\pm$  SD (n=4).

**Figure 5**

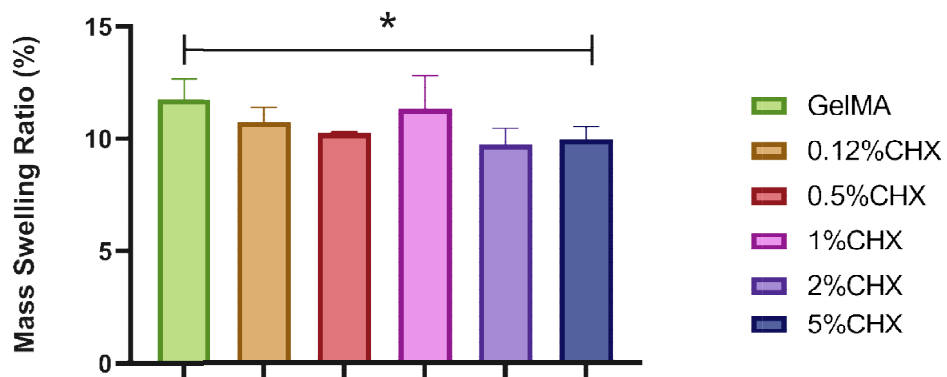


Figure 5: Swelling profile of CHX based hydrogels. Swelling ratio (%) reveals the amount of water absorbed in 24h at 37°C of all tested groups. The results are presented as mean  $\pm$  SD ( $n=4$ ).

**Figure 6**

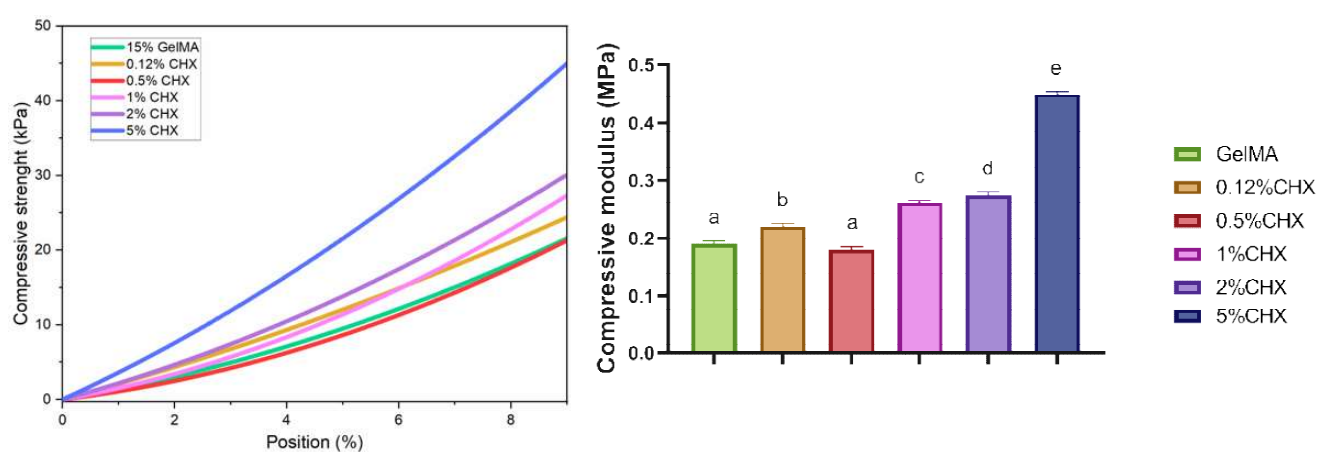


Figure 6: Biomechanical properties of 15% GelMA hydrogel with CHX incorporation. (a) Representative stress-strain of GelMA hydrogel with CHX (0.12, 0.5, 1, 2, and 5%). (b) Compressive modulus (MPa). The results are presented as mean  $\pm$  SD (n=5).

**Figure 7**

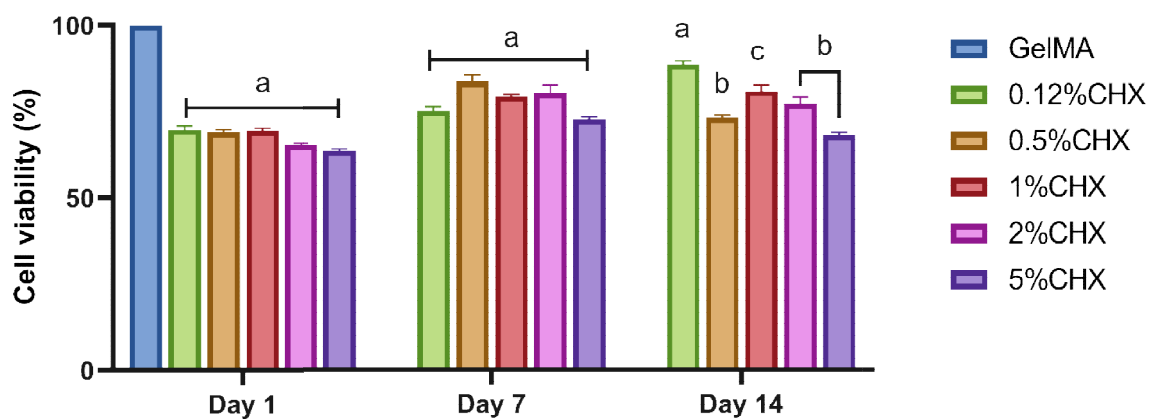


Figure 7: Cytotoxicity assay measured viability (%) of in response to aliquots at day 1, 7 and 14 from CHX-based hydrogels and GelMA without CHX. The percentage of cell viability was normalized by the mean absorbance of GelMA at day 1 (100%).

**Figure 8 a-c)**

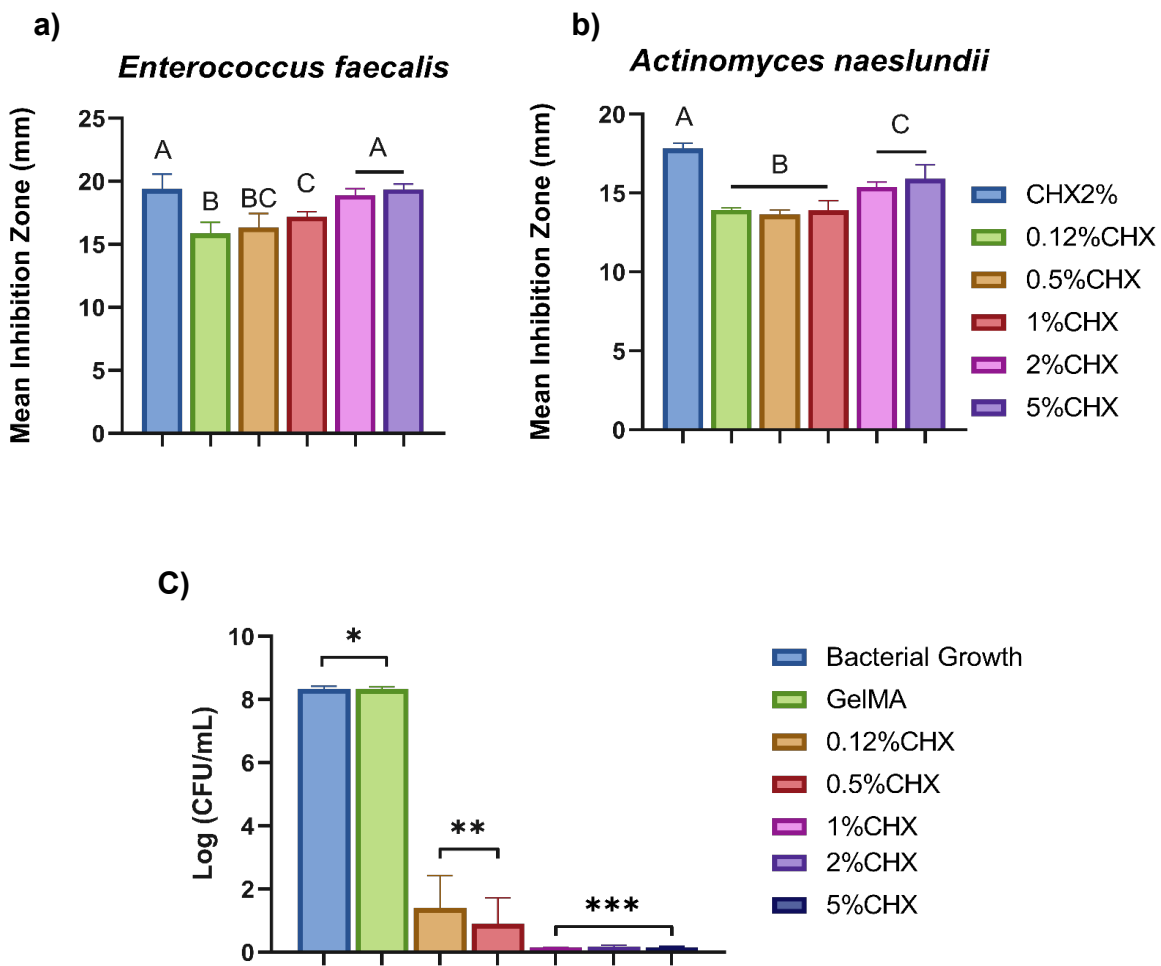


Figure 8a-b: (a) Mean and standard deviation of inhibition zone (mm) for the CHX-GelMA hydrogels against (a) *E. faecalis* and (b) *A. naeslundii*. Different uppercase letters indicate a statistically significant difference between the evaluated groups ( $p < 0.05$ ).

(6c): Antibiofilm properties of the CHX based GelMA hydrogels. The Microcosmos biofilm model was cultured. All CHX based hydrogels significantly reduced the Colony Forming Units numbers compared to the bacterial growth and GelMA groups. The results are presented as mean  $\pm$  SD ( $n=4$ ). Different asterisks indicate a statistically significant difference between the evaluated groups ( $p < 0.05$ ).

## **6. Considerações finais**

Neste trabalho, projetamos com sucesso hidrogéis injetáveis carregados com clorexidina degradáveis na presença de infecção periapical. Foi evidenciado ação antimicrobiana eficaz com citotoxicidade reduzida, mostrando alto potencial clínico em terapia de polpa vital e endodôntica regenerativa. Estudos adicionais para investigar a atividade antimicrobiana em um modelo mais complexo de biofilme assim como mais estudos de modelo animal e estudos in vivo em dentes imaturos de ratos são necessários para determinar o potencial do método de entrega de drogas sugerido a ser implementado nas clínicas.

## REFERENCIAS

- ABDULLAYEV, E.; LVOV, Y. Halloysite Clay Nanotubes for Controlled Release of Protective Agents Delivered by Ingenta. [s. l.], v. 11, n. 11, p. 10007–10026, 2011.
- ABDULLAYEV, E.; LVOV, Y. Halloysite clay nanotubes as a ceramic “skeleton” for functional biopolymer composites with sustained drug release. **Journal of Materials Chemistry B**, [s. l.], v. 1, n. 23, p. 2894–2903, 2013.
- ALBUQUERQUE, M. T. P. et al. Effects of Ciprofloxacin-containing Scaffolds on Enterococcus faecalisBiofilms. **JOURNAL OF ENDODONTICS**, [s. l.], v. 41, n. 5, p. 710–714, 2015.
- ANNABI, N. et al. Engineering a sprayable and elastic hydrogel adhesive with antimicrobial properties for wound healing. **Biomaterials**, Netherlands, v. 139, p. 229–243, 2017.
- ANTUNES, H. S. et al. Total and Specific Bacterial Levels in the Apical Root Canal System of Teeth with Post-treatment Apical Periodontitis. **Journal of endodontics**, United States, v. 41, n. 7, p. 1037–1042, 2015.
- ASSMANN, A. et al. A highly adhesive and naturally derived sealant. **Biomaterials**, Netherlands, v. 140, p. 115–127, 2017.
- BARBOSA-RIBEIRO, M. et al. Effectiveness of calcium hydroxide-based intracanal medication on infectious/inflammatory contents in teeth with post-treatment apical periodontitis. **Clinical Oral Investigations**, [s. l.], v. 23, n. 6, p. 2759–2766, 2019.
- BOTTINO, M. C. et al. Advanced Scaffolds for Dental Pulp and Periodontal Regeneration. **Dental clinics of North America**, United States, v. 61, n. 4, p. 689–711, 2017. Disponível em: <<http://www.embase.com/search/results?subaction=viewrecord&from=export&id=L622916070>>
- BOTTINO, M. C. et al. A novel patient-speci fi c three-dimensional drug delivery construct for regenerative endodontics. [s. l.], p. 1576–1586, 2018.
- CENTER FOR HEALTH STATISTICS, N. NCHS Data Brief, Number 307, April 2018. [s. l.], n. 307, p. 2015–2016, 2015. Disponível em: <[https://www.cdc.gov/nchs/data/databriefs/db307\\_table.pdf#1](https://www.cdc.gov/nchs/data/databriefs/db307_table.pdf#1)>
- CHEN, Y.-C. et al. Functional Human Vascular Network Generated in Photocrosslinkable Gelatin Methacrylate Hydrogels. **Advanced functional materials**, Germany, v. 22, n. 10, p. 2027–2039, 2012.
- CONDE, M. C. M. et al. A scoping review of root canal revascularization: relevant aspects for clinical success and tissue formation. **International Endodontic Journal**, Post-Graduate Program in Dentistry, School of Dentistry, Federal University of Pelotas, Pelotas, Brazil, v. 50, n. 9, p. 860–874, 2017. Disponível em: <<https://www.scopus.com/inward/record.uri?eid=2-s2.0-85006106952&doi=10.1111%2Fiej.12711&partnerID=40&md5=0c14ed97eb02997f6b276d4a096987c8>>
- CORREA, C. F. et al. Antimicrobial activity from polymeric composites-based polydimethylsiloxane/TiO<sub>2</sub>/GO: evaluation of filler synthesis and surface morphology. **Polymer Bulletin**, [s. l.], v. 74, n. 6, p. 2379–2390, 2017.
- DE-DEUS, G. et al. Suboptimal debridement quality produced by the single-file F2 protaper technique in oval-shaped canals. **Journal of Endodontics**, [s. l.], v. 36, n. 11, p. 1897–1900,

2010.

DEVARAJ, S.; JAGANNATHAN, N.; NEELAKANTAN, P. Antibiofilm efficacy of photoactivated curcumin, triple and double antibiotic paste, 2% chlorhexidine and calcium hydroxide against *Enterococcus faecalis* in vitro. **Scientific reports**, England, v. 6, p. 24797, 2016.

DIOGENES, A.; RUPAREL, N. B. Regenerative Endodontic Procedures: Clinical Outcomes. **Dental Clinics of North America**, Department of Endodontics, University of Texas Health Science Center at San Antonio, 7703 Floyd Curl Drive, San Antonio, TX 78229, United States, v. 61, n. 1, p. 111–125, 2017. Disponível em: <<https://www.scopus.com/inward/record.uri?eid=2-s2.0-84999026189&doi=10.1016%2Fj.cden.2016.08.004&partnerID=40&md5=bc1018493e776267972cef6119ad9947>>

DUBEY, N. et al. Comparative Evaluation of the Cytotoxic and Angiogenic Effects of Minocycline and Clindamycin: An In Vitro Study. **Journal of endodontics**, United States, 2019.

DUQUE, C. et al. In vitro and in vivo evaluations of glass-ionomer cement containing chlorhexidine for atraumatic restorative treatment. **Journal of Applied Oral Science**, [s. l.], v. 25, n. 5, p. 541–550, 2017.

EKLUND, S. A. Trends in dental treatment, 1992 to 2007. **Journal of the American Dental Association**, [s. l.], v. 141, n. 4, p. 391–399, 2010. Disponível em: <<http://dx.doi.org/10.14219/jada.archive.2010.0191>>

ERAMO, S. et al. Dental pulp regeneration via cell homing. **International endodontic journal**, England, v. 51, n. 4, p. 405–419, 2018.

FEITOSA, S. A. et al. Physicochemical and biological properties of novel chlorhexidine-loaded nanotube-modified dentin adhesive. **Journal of Biomedical Materials Research - Part B Applied Biomaterials**, [s. l.], v. 107, n. 3, p. 868–875, 2019.

GOMES, B. P. et al. In vitro antimicrobial activity of several concentrations of sodium hypochlorite and chlorhexidine gluconate in the elimination of *Enterococcus faecalis*. **International endodontic journal**, England, v. 34, n. 6, p. 424–428, 2001.

GOMES, B. P. F. A. et al. Chlorhexidine in endodontics. **Brazilian dental journal**, Brazil, v. 24, n. 2, p. 89–102, 2013. a.

GOMES, B. P. F. A. et al. Chlorhexidine in Endodontics. **Brazilian Dental Journal**, [s. l.], v. 24, n. 2, p. 89–102, 2013. b. Disponível em: <[http://www.scielo.br/scielo.php?script=sci\\_arttext&pid=S0103-64402013000200089&lng=en&tlng=en](http://www.scielo.br/scielo.php?script=sci_arttext&pid=S0103-64402013000200089&lng=en&tlng=en)>. Acesso em: 10 dez. 2018.

GOMES, B. P. F. de A.; HERRERA, D. R. Etiologic role of root canal infection in apical periodontitis and its relationship with clinical symptomatology. **Brazilian oral research**, Brazil, v. 32, n. suppl 1, p. e69, 2018.

GUPTE, M. J.; MA, P. X. Nanofibrous scaffolds for dental and craniofacial applications. **Journal of dental research**, United States, v. 91, n. 3, p. 227–234, 2012.

HARLAMB, S. C.; S.C., H. Management of incompletely developed teeth requiring root canal treatment. **Australian Dental Journal**, Private Practice, Burwood, NSW, Australia, v. 61, p. 95–106, 2016. Disponível em: <<http://www.embase.com/search/results?subaction=viewrecord&from=export&id=L611426852>>

HARRINGTON, D. J. Bacterial collagenases and collagen-degrading enzymes and their potential role in human disease. **Infection and immunity**, United States, v. 64, n. 6, p. 1885–1891, 1996.

HUANG, K. et al. Halloysite Nanotube Based Scaffold for Enhanced Bone Regeneration. **ACS Biomaterials Science & Engineering**, [s. l.], v. 5, n. 8, p. 4037–4047, 2019.

JACOBS, J. C. et al. Antibacterial Effects of Antimicrobials Used in Regenerative Endodontics against Biofilm Bacteria Obtained from Mature and Immature Teeth with Necrotic Pulps. **Journal of Endodontics**, Department of Endodontics, Indiana University School of Dentistry, Indianapolis, Indiana, United States, v. 43, n. 4, p. 575–579, 2017. Disponível em: <<https://www.scopus.com/inward/record.uri?eid=2-s2.0-85012914896&doi=10.1016%2Fj.joen.2016.12.014&partnerID=40&md5=eccb6aeb52c8e9dc9a29643f5a90efdb>>

JAIN, A.; BAHUGUNA, R. Role of matrix metalloproteinases in dental caries, pulp and periapical inflammation: An overview. **Journal of oral biology and craniofacial research**, Netherlands, v. 5, n. 3, p. 212–218, 2015. a.

JAIN, A.; BAHUGUNA, R. Role of matrix metalloproteinases in dental caries, pulp and periapical inflammation: An overview. **Journal of Oral Biology and Craniofacial Research**, [s. l.], v. 5, n. 3, p. 212–218, 2015. b. Disponível em: <<http://dx.doi.org/10.1016/j.jobcr.2015.06.015>>

KAYAOGLU, G.; ORSTAVIK, D. Virulence factors of Enterococcus faecalis: relationship to endodontic disease. **Critical reviews in oral biology and medicine : an official publication of the American Association of Oral Biologists**, United States, v. 15, n. 5, p. 308–320, 2004.

KIM, S. G. et al. Regenerative endodontics: a comprehensive review. **INTERNATIONAL ENDODONTIC JOURNAL**, [s. l.], v. 51, n. 12, p. 1367–1388, 2018.

KIRSCH, M. et al. Gelatin-Methacryloyl (GelMA) Formulated with Human Platelet Lysate Supports Mesenchymal Stem Cell Proliferation and Differentiation and Enhances the Hydrogel's Mechanical Properties. **Bioengineering (Basel, Switzerland)**, Switzerland, v. 6, n. 3, 2019.

LABOW, R. S. et al. The effect of oxidation on the enzyme-catalyzed hydrolytic biodegradation of poly(urethane)s. **Journal of biomaterials science. Polymer edition**, England, v. 13, n. 6, p. 651–665, 2002.

LESSA, F. C. R. et al. Toxicity of chlorhexidine on odontoblast-like cells. **Journal of applied oral science : revista FOB**, [s. l.], v. 18, n. 1, p. 50–8, 2010. Disponível em: <<http://www.ncbi.nlm.nih.gov/pubmed/20379682>> <<http://www.ncbi.nlm.nih.gov/pmc/articles/PMC5349028/>>

MARWAH, N.; DUTTA, S.; SINGLA, R. Single Visit versus Multiple Visit Root Canal Therapy. **International Journal of Clinical Pediatric Dentistry**, [s. l.], v. 1, n. 1, p. 17–24, 2008.

MCBANE, J. E.; SANTERRE, J. P.; LABOW, R. Effect of phorbol esters on the macrophage-mediated biodegradation of polyurethanes via protein kinase C activation and other pathways. **Journal of biomaterials science. Polymer edition**, England, v. 20, n. 4, p. 437–453, 2009.

MCBANE, J.; SANTERRE, P.; LABOW, R. Role of protein kinase C in the monocyte-derived macrophage-mediated biodegradation of polycarbonate-based polyurethanes. **Journal of biomedical materials research. Part A**, United States, v. 74, n. 1, p. 1–12, 2005.

MODARESIFAR, K.; HADJIZADEH, A.; NIKNEJAD, H. Design and fabrication of GelMA/chitosan nanoparticles composite hydrogel for angiogenic growth factor delivery.

**Artificial Cells, Nanomedicine and Biotechnology**, [s. l.], v. 46, n. 8, p. 1799–1808, 2018.

MOHAMMADI, Z. Chlorhexidine gluconate, its properties and applications in endodontics.

**Iranian endodontic journal**, [s. l.], v. 2, n. 4, p. 113–25, 2008. a. Disponível em:

<<http://www.ncbi.nlm.nih.gov/pubmed/24265633>%0A<http://www.ncbi.nlm.nih.gov/pmc/articles/PMC3834637/>>

MOHAMMADI, Z. Chlorhexidine gluconate, its properties and applications in endodontics.

**Iranian endodontic journal**, Iran, v. 2, n. 4, p. 113–125, 2008. b.

MOHAMMADI, Z.; SHALAVI, S. Is chlorhexidine an ideal vehicle for calcium hydroxide? A microbiologic review. **Iranian Endodontic Journal**, [s. l.], v. 7, n. 3, p. 115–122, 2012.

MONTEIRO, N. et al. Photopolymerization of cell-laden gelatin methacryloyl hydrogels using dental curing light for regenerative dentistry. **DENTAL MATERIALS**, [s. l.], v. 34, n. 3, p. 389–399, 2018. a.

MONTEIRO, N. et al. Photopolymerization of cell-laden gelatin methacryloyl hydrogels using a dental curing light for regenerative dentistry. **Dental Materials**, [s. l.], v. 34, n. 3, p. 389–399, 2018. b.

MURRAY, P. E. et al. Regenerative Endodontics: A Review of Current Status and a Call for Action. **Journal of Endodontics**, P.E. Murray, Department of Endodontics, College of Dental Medicine, Nova Southeastern University, Fort Lauderdale, FL, United States, United States, v. 33, n. 4, p. 377–390, 2007. Disponível em:

<<http://www.embase.com/search/results?subaction=viewrecord&from=export&id=L46412435>>

NARAYANAN, L. L.; VAISHNAVI, C. Endodontic microbiology. **Journal of Conservative Dentistry : JCD**, [s. l.], v. 13, n. 4, p. 233–239, 2010.

NAZZAL, H. et al. Regenerative endodontic therapy for managing immature non-vital teeth: A national survey of UK paediatric dental specialists and trainees. **British Dental Journal, Paediatric Dentistry**, University of Leeds, Clarendon Way, Leeds, WF14JN, United Kingdom, v. 224, n. 4, p. 247–254, 2018. Disponível em: <<https://www.scopus.com/inward/record.uri?eid=2-s2.0-85042600151&doi=10.1038%2Fsj.bdj.2018.122&partnerID=40&md5=b6dc403477ab191d580d077d3618571a>>

NEELAKANTAN, P. et al. Biofilms in Endodontics—Current status and future directions. **International Journal of Molecular Sciences**, [s. l.], v. 18, n. 8, 2017.

NICHOL, J. W. et al. Cell-laden microengineered gelatin methacrylate hydrogels. **Biomaterials**, Netherlands, v. 31, n. 21, p. 5536–5544, 2010. a.

NICHOL, J. W. et al. Cell-laden microengineered gelatin methacrylate hydrogels. **Biomaterials**, [s. l.], v. 31, n. 21, p. 5536–5544, 2010. b.

PALASUK, J. et al. Doxycycline-loaded nanotube-modified adhesives inhibit MMP in a dose-dependent fashion. **Clinical Oral Investigations**, Department of Restorative Dentistry, Faculty of Dentistry, Naresuan University, Phitsanulok, 65000, Thailand, v. 22, n. 3, p. 1243–1252, 2018. Disponível em: <<https://www.scopus.com/inward/record.uri?eid=2-s2.0-85030173807&doi=10.1007%2Fs00784-017-2215-y&partnerID=40&md5=7166142bd1d76d8043c5277c88b6d66e>>

PAUL, A. et al. Nanoengineered biomimetic hydrogels for guiding human stem cell osteogenesis in three dimensional microenvironments. **Journal of materials chemistry. B**, England, v. 4, n.

20, p. 3544–3554, 2016.

PAULA-SILVA, F. W. G.; DA SILVA, L. A. B.; KAPILA, Y. L. Matrix metalloproteinase expression in teeth with apical periodontitis is differentially modulated by the modality of root canal treatment. **Journal of endodontics**, United States, v. 36, n. 2, p. 231–237, 2010.

PEPEANOVA, I. et al. Gelatin-Methacryloyl (GelMA) Hydrogels with Defined Degree of Functionalization as a Versatile Toolkit for 3D Cell Culture and Extrusion Bioprinting. **Bioengineering (Basel, Switzerland)**, Switzerland, v. 5, n. 3, 2018.

PEREIRA, M. S. S. et al. Response of mice connective tissue to intracanal dressings containing chlorhexidine. **Microscopy Research and Technique**, [s. l.], v. 75, n. 12, p. 1653–1658, 2012.

QIAN, W. et al. Microbiota in the apical root canal system of tooth with apical periodontitis. **BMC Genomics**, [s. l.], v. 20, n. Suppl 2, 2019.

RAHALI, K. et al. Synthesis and characterization of nanofunctionalized gelatin methacrylate hydrogels. **International Journal of Molecular Sciences**, [s. l.], v. 18, n. 12, 2017.

RASO, E. M. G. et al. A new controlled release system of chlorhexidine and chlorhexidine: βcd inclusion compounds based on porous silica. **Journal of Inclusion Phenomena and Macrocyclic Chemistry**, [s. l.], v. 67, n. 1–2, p. 159–168, 2010.

RIAZ, A. et al. Comparison Of Two Intracanal Medicaments In Resolution Of Apical Radiolucency. **Journal of Ayub Medical College, Abbottabad : JAMC**, [s. l.], v. 30, n. 3, p. 320–324, 2018. Disponível em: <<http://www.ncbi.nlm.nih.gov/pubmed/30465358>>

ROSA, V. et al. Dental pulp tissue engineering in full-length human root canals. **Journal of dental research**, United States, v. 92, n. 11, p. 970–975, 2013.

SACHDEVA, G. S. et al. Regenerative endodontic treatment of an immature tooth with a necrotic pulp and apical periodontitis using platelet-rich plasma (PRP) and mineral trioxide aggregate (MTA): A case report. **International Endodontic Journal**, Department of Conservative Dentistry and Endodontics, Himachal Dental College and Hospital, Sundernagar, India, v. 48, n. 9, p. 902–910, 2015. Disponível em: <<https://www.scopus.com/inward/record.uri?eid=2-s2.0-84937730024&doi=10.1111%2Fiej.12407&partnerID=40&md5=4bf16f3ff88831172cad53f7b2b8f2b9>>

SJOGREN, U. et al. The antimicrobial effect of calcium hydroxide as a short-term intracanal dressing. **International endodontic journal**, England, v. 24, n. 3, p. 119–125, 1991.

SORSA, T. et al. Identification of proteases from periodontopathogenic bacteria as activators of latent human neutrophil and fibroblast-type interstitial collagenases. **Infection and immunity**, United States, v. 60, n. 11, p. 4491–4495, 1992.

STAMBOLSKY, C. et al. Histologic characterization of regenerated tissues after pulp revascularization of immature dog teeth with apical periodontitis using tri-antibiotic paste and platelet-rich plasma. **Archives of Oral Biology**, Department of Stomatology, School of Dentistry, University of Sevilla, C/Avicena s/n, Sevilla, 41009, Spain, v. 71, p. 122–128, 2016. Disponível em: <<https://www.scopus.com/inward/record.uri?eid=2-s2.0-84979938921&doi=10.1016%2Fj.archoralbio.2016.07.007&partnerID=40&md5=ca59b07de7be2a80686d709962df244a>>

STUART, C. H. et al. Enterococcus faecalis: its role in root canal treatment failure and current concepts in retreatment. **Journal of endodontics**, United States, v. 32, n. 2, p. 93–98, 2006.

SUN, J. et al. Exactly matched pore size for the intercalation of electrolyte ions determined using the tunable swelling of graphite oxide in supercapacitor electrodes. **Nanoscale**, England, v. 10, n. 45, p. 21386–21395, 2018.

TORABINEJAD, M. et al. Histologic Examinations of Teeth Treated with 2 Scaffolds: A PilotAnimal Investigation. **JOURNAL OF ENDODONTICS**, [s. l.], v. 40, n. 4, p. 515–520, 2014.

TORABINEJAD, M. et al. Regenerative Endodontic Treatment or Mineral Trioxide Aggregate Apical Plug in Teeth with Necrotic Pulps and Open Apices: A Systematic Review and Meta-analysis. **Journal of Endodontics**, Advanced Specialty Education Program in Endodontics, School of Dentistry, Loma Linda University, Loma Linda, California, United States, v. 43, n. 11, p. 1806–1820, 2017. Disponível em: <<https://www.scopus.com/inward/record.uri?eid=2-s2.0-85027417637&doi=10.1016%2Fj.joen.2017.06.029&partnerID=40&md5=0f74eb35da09afe97fc1f12a837ca66d>>

VAN DEN BULCKE, A. I. et al. Structural and rheological properties of methacrylamide modified gelatin hydrogels. **Biomacromolecules**, United States, v. 1, n. 1, p. 31–38, 2000.

WEI, W. et al. Enhanced efficiency of antiseptics with sustained release from clay nanotubes. **RSC Advances**, [s. l.], v. 4, n. 1, p. 488–494, 2014.

WHITING, D. et al. Characterization of the Cellular Responses of Dental Mesenchymal Stem Cells to the Immune System. **Journal of Endodontics**, Department of Endodontics, University of Washington, Seattle, Washington, United States, v. 44, n. 7, p. 1126–1131, 2018. Disponível em: <<https://www.scopus.com/inward/record.uri?eid=2-s2.0-85047923689&doi=10.1016%2Fj.joen.2018.03.018&partnerID=40&md5=38d1b93324323fd441a44b93846c3c35>>

WIDBILLER, M. et al. Cell Homing for Pulp Tissue Engineering with Endogenous Dentin Matrix Proteins. **Journal of Endodontics**, Department of Conservative Dentistry and Periodontology, University Hospital Regensburg, Regensburg, Germany, v. 44, n. 6, p. 956–962.e2, 2018. Disponível em: <<https://www.scopus.com/inward/record.uri?eid=2-s2.0-85044513792&doi=10.1016%2Fj.joen.2018.02.011&partnerID=40&md5=d05d3328b629837894f8a2a53b04d858>>

XIAO, W. et al. Synthesis and characterization of photocrosslinkable gelatin and silk fibroin interpenetrating polymer network hydrogels. **Acta Biomaterialia**, [s. l.], v. 7, n. 6, p. 2384–2393, 2011.

YANG, G. et al. Assessment of the characteristics and biocompatibility of gelatin sponge scaffolds prepared by various crosslinking methods. **Scientific reports**, England, v. 8, n. 1, p. 1616, 2018.

ZHU, Y. et al. Hierarchical Hydrogel Composite Interfaces with Robust Mechanical Properties for Biomedical Applications. **Advanced materials (Deerfield Beach, Fla.)**, Germany, v. 31, n. 45, p. e1804950, 2019.